Fabrication, Testing, and Adhesive Bonding of Hybrid Polymer Matrix Composite Reinforced with Sisal Fiber, E-Glass, and SiC

Gemechu Regasa Gemeda

A Thesis Submitted to the Department of Mechanical Engineering
School of Mechanical, Chemical, and Material Engineering

Presented in Partial Fulfillment of the Requirement for the Degree of Master's in Manufacturing Engineering

Office of The Graduate Studies
Adama Science and Technology University

June, 2024
Adama, Ethiopia

Fabrication, Testing, and Adhesive Bonding of Hybrid Polymer Matrix Composite Reinforced with Sisal Fiber, E-Glass, and SiC

Gemechu Regasa Gemeda

Advisor: Dr. Moera Gutu Jiru (Associate Professor)

A Thesis Submitted to the Department of Mechanical Engineering
School of Mechanical, Chemical, and Material Engineering

Presented in Partial Fulfillment of the Requirement for the Degree of Master's in Manufacturing Engineering

Office of The Graduate Studies
Adama Science and Technology University

June, 2024
Adama, Ethiopia

DECLARATION

I hereby declare that this Master Thesis entitled **"Fabrication, Testing, and Adhesive Bonding of Hybrid Polymer Matrix Composite Reinforced with Sisal Fiber, E-Glass, and SiC"** is my original work. That is, it has not been submitted for the award of any academic degree, diploma, or certificate in any other university. All sources of materials that are used for this thesis have been duly acknowledged through citation.

Gemechu Regasa Gemeda _____ _____

Name of student Signature Date

RECOMMENDATION OF ADVISOR

I/we, the advisor(s) of this thesis, hereby certify that I/we have read the revised version of the thesis entitled **"Fabrication, Testing, and Adhesive Bonding of Hybrid Polymer Matrix Composite Reinforced with Sisal Fiber, E-Glass, and SiC"** prepared under my/our guidance by Gemechu Regasa submitted in partial fulfillment of the requirements for the degree of Master of Science in Manufacturing Engineering.

Therefore, I/we recommend the submission of a revised version of the thesis to the department, following the applicable procedures.

_____	_____	_____
Main Advisor	Signature	Date

APPROVAL PAGE

I/we, the advisors of the thesis entitled **"Fabrication, Testing, and Adhesive Bonding of Hybrid Polymer Matrix Composite Reinforced with Sisal Fiber, E-Glass, and SiC"** and developed by Gemechu Regasa, hereby certify that the recommendations and suggestions made by the board of examiners are appropriately incorporated into the final version of the thesis.

Dr. Moera Gutu Jiru _____ _____

Main Advisor/Supervisor Signature Date

We, the undersigned, members of the Board of Examiners of the thesis by Gemechu Regasa, have read and evaluated the thesis entitled **"Fabrication, Testing, and Adhesive Bonding of Hybrid Polymer Matrix Composite Reinforced with Sisal Fiber, E-Glass, and SiC"** and examined the candidate during an open defense. This is, therefore, to certify that the thesis is accepted for partial fulfillment of the requirement of the degree of Master of Science in Manufacturing Engineering.

_____ _____ _____

Chairperson Signature Date

_____ _____ _____

Internal Examiner Signature Date

_____ _____ _____

External Examiner Signature Date

Finally, approval and acceptance of the thesis is contingent upon the submission of its final copy to the Office of Postgraduate Studies (OPGS) through the Department Graduate Council (DGC) and School Graduate Committee (SGC).

_____ _____ _____

Department Head Signature Date

_____ _____ _____

School Dean Signature Date

_____ _____ _____

Office of Postgraduate Studies, Dean Signature Date

ACKNOWLEDGMENT

First and foremost, I offer my heartfelt thanks to my Almighty God for granting me patience, strength, and inspiration throughout this research endeavor.

I would like to express my deepest gratitude to my esteemed advisor, Dr. Moera Gutu associate professor in the mechanical engineering department for his exceptional guidance, mentorship, and invaluable insights. His expertise and dedication have been instrumental in shaping the outcome of this research.

I would like to sincerely thank Mr. Sintayehu Legesse, the head of the mechanical engineering department, for his guidance, advice, and cooperation in helping me by providing a support letter required to different departments and organizations. I am very grateful to Dr. Sayeed Ahmed for purchasing and giving me research material from India and, to Mr. Birhanu Nigatu, the laboratory technician at the Ethiopian Defense University, for his help in carrying out the mechanical property tests.

I am also grateful to Abraham Dereje (PhD candidate), Olifan Abebe, and my friends for their unwavering support and encouragement. Your presence, and words of encouragement have made this journey all the more meaningful. I am immensely grateful to Adama Science and Technology University for providing the resources necessary to pursue my academic aspirations.

Finally, I thank my family for their help, encouragement, unwavering love, and understanding throughout this journey. Your continuous support and prayers have been a source of my strength and motivation.

TABLE OF CONTENTS

CONTENTS **PAGE**

LIST OF TABLES

TABLE PAGE

LIST OF FIGURES

LIST OF ACRONYMS AND ABBREVIATIONS

ANN	Artificial Neural Network
ASTM	American Standard for Testing and Materials
CFRPs	Carbon Fiber Reinforced Polymers
CHITM	Charpy Impact Test Machine
CMCs	Ceramic Matrix Composites
DGC	Department Graduate Council
DOE	Design of Experiment
FRP	Fiber-Reinforced Plastic
GFRPs	Glass Fiber-Reinforced Polymers
GRA	Grey Relational Analaysis
GPa	Gigapascals (= 10^9 Pascals)
MPa	Megapascals (= 106 Pascals)
MMCs	Metal Matrix Composites
NA	Not available
NFRC	Natural Fiber Reinforced Composite
OMCs	Organic Matrix Composites
OPGS	Office of Postgraduate Studies
PMCs	Polymer Matrix Composites
RSM	Response Surface Method
SCJ	Scarf lap joint
SGC	School Graduate Committee
SiC	Silicon Carbide
SEM	Scanning Electron Microscope
SLJ	Single Lap Joint
STJ	Stepped joint
UTM	Universal Testing Machine
Wt. %	Weight Percentage
WSFRPC	Woven Sisal Fiber Reinforced Polymer Composite

ABSTRACT

Polymer-based composite materials are widely used in various industries. Composite joining using the adhesive joining method is an increasing concern in various industries worldwide. The main problems of natural fiber-based polymer matrix composites are their lower mechanical properties than other materials. In other ways, composite joining was challenging while controlling the adhesive joining parameters. This thesis aims to develop a hybrid composite from polyester resin-sisal fiber-E-glass-SiC and study the adhesive joining of this composite. The composite tensile, flexural, impact, and hardness properties were analyzed as per ASTM standards. The wt.% of the sisal and E-glass fibers (0,10 and 15) were optimized using Taguchi-based GRA. Further, morphology analysis was analyzed. The parameters influencing the adhesive joint performance, such as joint configuration (SLJ, SCJ, and STJ), SiC filler (0, 1.5, and 3)wt.%., and overlap lengths of (20, 25, and 30)mm, were analyzed and optimized using Taguchi-based GRA. The results from the fabricated composite show that 42.13 MPa, 185.56 MPa, 24.75 J, and 97.93 HV of tensile, flexural, impact, and Vickers hardness were achieved respectively. The 15 wt. % of both sisal and E-glass fibers have more effects on the mechanical properties of the composite. The results of composite adhesive joining reveal that, a maximum of 32.63 and 90.15 MPa of joint tensile and flexural strengths were achieved. Based on the Taguchi-based GRA, an optimum joining parameter of SCJ, 3 wt.% SiC filler and overlap length of 30mm were obtained and had more influence on the joint strength of the composite. This research work is expected to help different industries, governments, and researchers working on developing composite and composite adhesive joining areas.

Keywords: *Composite, hand lay-up, GRA, composite joining, mechanical properties.*

CHAPTER-1

INTRODUCTION

1.1 Background of the Study

In recent years, there has been a growing interest in developing advanced materials such as composite with enhanced mechanical properties for various applications in engineering and industry. Composite materials are multiphase systems developed by mixing two or more distinct materials to give them particular qualities that vary from the materials from which they are developed. The matrix and reinforcement are the two essential phases of composite materials that result from the physical and chemical mixing of two or more materials with differing characteristics, and the matrix phase is the most important of them. The primary responsibility of the matrix is to wrap the reinforcing component around it and hold it together in the proper shape. To obtain a composite material with high mechanical, chemical, and physical properties, at least one reinforcement element in the form of particles, flakes, fabric, or others must be added to the matrix material. Composite materials made with more than one reinforcement are known as hybrid composite materials. The constituent materials of the composite exist in two or more phases and are physically as well as mechanically separable. The properties and performance of the composite depend upon the reinforcement and matrix materials(Mbeche *et al*., 2020; Kumar Sharma *et al*., 2022).

Based on the matrix constituents, composite materials are classified into organic matrix composites (OMCs), metal matrix composites (MMCs), and ceramic matrix composites (CMCs) (Figure 1.1). Organic matrix composites can be categorized into two classes of composites, such as polymer matrix composites (PMCs) and carbon matrix composites, commonly known as carbon-carbon composites. Based on reinforcement, composite materials are classified as fiber-reinforced, laminar, and particulate composites (Nagavally, 2016).

Polymer matrix composites (PMCs) have emerged as promising materials due to their exceptional strength-to-weight ratio, corrosion resistance, and design flexibility. Depending on the different bases, polymers can be classified into different types. Based on the raw material used, polymers can be classified as natural, synthetic, or semi-synthetic polymers. Naturally occurring polymers such as proteins, starch, and cellulose exist in the human body, animals, and plants. Polymers like nylon and polyethylene are prepared artificially. Semi-synthetic polymers such as cellulose acetate (rayon) are made by modifying the naturally

occurring polymers. The classification of polymers based on molecular structure is either connected by straight-long chains of identical links (linear chain polymers) or branches formed from linear chains (branch chain polymer) or monomers connected by covalent bonds in a three-dimensional structure (cross-linked polymer). Based on polymerization, polymers are classified as addition polymers (the monomers connected and added linearly in three-dimensional space, such as polyethylene) and condensation polymers (molecules of water or alcohol are removed through a chemical reaction) (Chohan *et al*., 2022; Sumithra *et al* 2023).

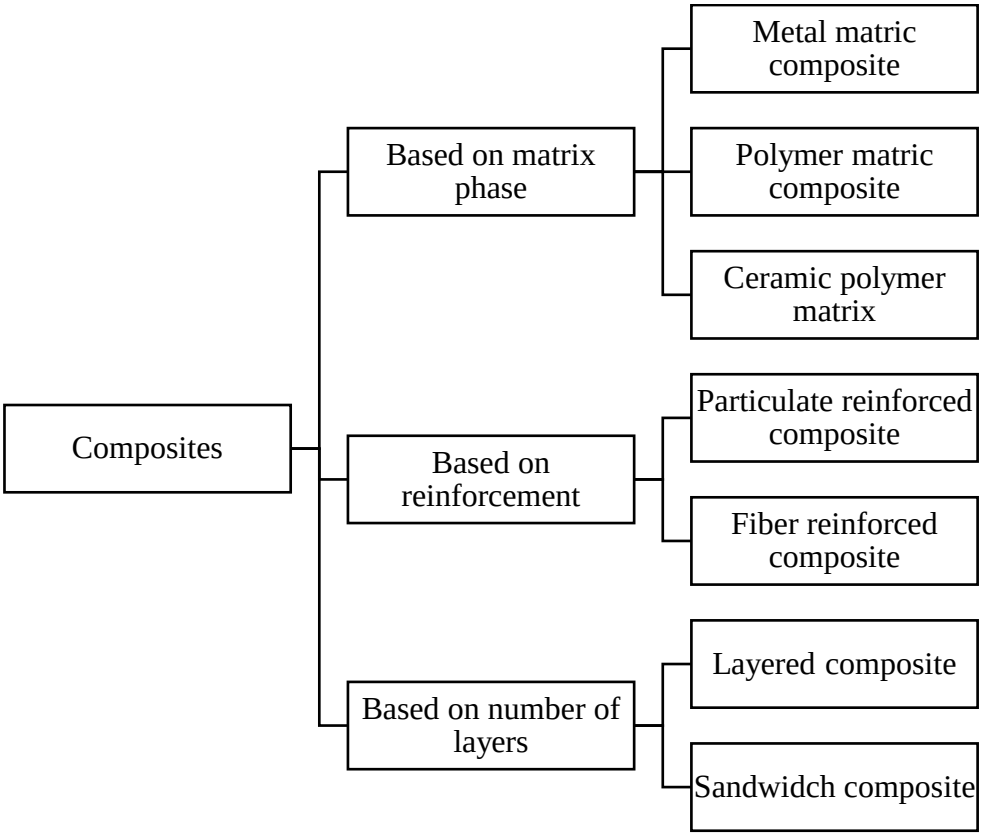

Figure 1. 1 Classification of composite materials(Sumithra et al., 2023)

Polymer matrix composites (PMCs) have a wide range of uses, including the construction of airplanes, ships, automobiles, military equipment, and sports equipment, due to their higher size-to-strength ratio, minimum cost, and ease of production processes. *(Chohan et al., 2022; Kumar Sharma et al*., 2022). The reinforcement of PMCs with natural fibers, synthetic fibers, and ceramic particles has been extensively investigated to further enhance their mechanical and physical properties.

The utilization of natural fibers as reinforcements in composites has gained significant attention due to their abundant availability, low cost, renewable nature, and biodegradability. Sisal fiber is a natural fiber derived from the leaves of the Agave sisalana plant, which is

predominantly grown in tropical and subtropical regions. It possesses good mechanical properties, including high strength, stiffness, and good dimensional stability(Bichang'A et al., 2022; Appadurai et al., 2022). Sisal fiber is a potential reinforcement for polymer composites. Beyond its traditional applications such as ropes, carpets, mats, etc, sisal fiber has potential application in automobile sectors, and aircraft and is effectively used for higher structural applications. Incorporating sisal fibers into polymer matrices can Improve the strength, impact resistance, and fracture toughness of the composite (Mbeche et al., 2020; Sharma et al., 2023).

Alongside natural reinforcement, synthetic fiber reinforcement has also been widely explored. E-glass fiber, a type of fiberglass, is a commonly used synthetic fiber in composites. It offers excellent mechanical properties, such as tensile strength, flexural strength, impact strength, modulus, and resistance to chemical attack due to the enhanced tension distribution between the fiber and matrix as a result of the improved interfacial adhesion between the polyester matrix and the glass fiber (Cavalcanti et al., 2019s). E-glass fiber has been extensively employed in various applications including aerospace, automotive, and construction industries, to enhance the mechanical performance of the composite(Begum et al., 2020; Gangil et al., 2020).

In addition to fiber reinforcement, the incorporation of ceramic particles into polymer matrix has been investigated to further enhance the mechanical properties of composites. Silicon carbide (SiC) is a widely used ceramic material due to its exceptional hardness, high thermal conductivity, good tribological properties, and excellent mechanical strength(Madhu et al., 2018). It is less expensive, and an easily available earth product in comparison to other engineering oxides with similar properties(Ganesamoorthy et al., 2022). SiC particles can improve the wear resistance, thermal stability, stiffness of composites, and mechanical properties suitable for industrial applications. It plays a crucial role in enhancing the properties of structural materials, especially in the aerospace and automotive industries (Choudhary et al., 2020; Praveenkumara et al., 2022).

To meet certain design specifications, a variety of fabrication techniques for composite components were developed. Thus, the choice of technique is the main process required in composite fabrication to shape the resin and reinforcement. To shape the resin and reinforcements, molding is the main process required in composite fabrication(Sumithra et al., 2023). Hand layup is the most basic fabrication method from different types of composite fabrication methods for thermoset composites. It consists the laying dry fabric layers, or

"plies," manually onto a tool from a laminate stack, and resin is applied to the dry plies following the completion of the layup (Nagavally, 2016).

The post-processing methods like joining are equally crucial for determining the sophisticated and complex composite products for structural integrity (Melese et al., 2021). Joining methods are crucial for creating large-scale structures and achieving structural integrity. Adhesive joining is the most versatile joining technology in many engineering applications, and it is the most practical way to combine and bond composite materials with other materials such as polymers and metals (Banea & Da Silva, 2009; Worrall *et al*., 2020). Low stress concentration, ease of maintenance, and minimum manufacturing cost influence adhesive joining to become one of the most widely used in different industrial applications. To ensure the safety, efficiency, and reliability of adhesive bond joints one must understand their properties and behavior of them (Melese *et al*., 2022).

1.2 Statement of the Problem

Polymer-based natural fiber-reinforced composites are extensively used in the automotive, marine industry, and structural applications. However, they have low mechanical properties. To overcome this problem e-glass, and SiC reinforcements were used with a polyester resin matrix. Natural fibers cannot be used solely because of certain drawbacks such as low mechanical strength but it requires the combined advantages of both fibers as natural with synthetic. Adhesive joining has a predominant advantage such as lower structural weight, modified damage tolerance, and minimum fabrication cost. The lower joint strength of adhesively joined composite components occurs due to the lower strength of the adhesive material used, the type of joint configuration, and the overlap length. This challenge can be solved by adding SiC nanoparticles to epoxy adhesive material to increase bonding strength and improve adhesion. Furthermore, in addition to introducing filler particles, different adhesive joining process parameters such as joint configuration, and overlap length are considered and optimized. This study aims to enhance mechanical properties such as tensile, flexural, impact, and hardness by fabricating a polymer-based hybrid composite reinforced with sisal fiber, E-glass, and SiC. Moreover, the study aims to enhance the joint strength and investigate the optimized joining parameters of the composite.

1.3 Objectives of the Study

1.3.1 General objectives

The main objective of this thesis study is to develop and investigate the mechanical properties of polymer matrix hybrid composite reinforced with sisal fiber, E-glass, and SiC; its adhesive bonding parameters (Joint configuration, filler material, and overlap length) investigation.

1.3.2 Specific objectives

1. To develop hybrid polymer composites reinforced with sisal fiber, E-glass, and SiC samples at different weight percentage ratios through hand lay-up technique.
2. To test the mechanical properties of the developed composite material including tensile strength, flexural strength, impact strength, and hardness as per ASTM standards and morphology analysis using SEM.
3. To optimize the combination percentage of the fibers for the composite using Taguchi-based GRA analysis.
4. To optimize the adhesive bonding technique process parameters such as joint configuration, filler material, and overlap length for the selected sample with optimal combination parameters using Taguchi-based GRA.

1.4 Significance of the Study

Focusing on the fabrication, testing, and adhesive bonding of hybrid PMC reinforced with sisal fiber, E-glass, and SiC, this research has the following basic significances.

- Sisal fiber a biodegradable material that is abundantly available in Ethiopia can be used highly in composite materials for various applications.
- The combination ratio of sisal and E-glass fiber used in polyester resin matrix was optimized and this minimizes the material waste and inappropriate usage of these fibers.
- Introducing the filler into epoxy adhesive has improved the joint strength of the composite and this results in reducing the damage of composite material components in different applications.
- An understanding of the adhesive bonding performance can benefit the manufacturing and joining process of composite structures, leading to improved product performance and reliability.
- This research also adds to the body of scientific knowledge in the field of composite materials, providing valuable data and insights for future studies.

1.5 Scope of the Study

This study covers the development and investigation of a polyester resin polymer matrix hybrid composite reinforced with sisal fiber, E-glass, and SiC, to enhance the mechanical properties of polyester-based composite. The hand lay-up technique was used to fabricate the composite. The research involved testing mechanical properties such as tensile strength and flexural strength using UTM, impact test using Charpy impact tester, hardness test using Vickers hardness tester, as well as characterization of the composite materials, including morphology analysis of the composite material using SEM. The research also optimized the adhesive joining parameters, including joint configuration, overlap length, and effect of filler into the adhesive, for obtaining the best parameters of composite joining using Taguchi-based GRA as well as experimental data analysis using analytical methods, Minitab software, and Excel.

1.6 Research Motivation

Due to light-weight material application in different sectors, demand was high while controlling the quality of fabricated composite for required purposes was challenging for researchers and industries. The raw materials such as natural plants, and agricultural by-products were highly available to enhance the use of composite fabrication. In other ways joining composites was challenging for the researchers while controlling adhesive joining parameters.

1.7 Limitations of the Study

- The lack of a sisal decortication machine to extract fiber, and hence manual extraction, causes damaged sisal fibers, which could impact the composite performance.
- The laboratories utilized for this research work are located across the country, which wastes time and could impact the outcome.
- The mechanical property testing performed did not fully capture the properties of composites and joints. Additional properties like compression and fatigue tests are necessary for specific applications.
- There is a shortage of literature related to composite adhesive joining.

1.8 Research Questions

The research questions that were raised with this research work are mentioned below.

1. What is the effect of varying fiber composition?
2. What are the effects of incorporating sisal fiber, E-glass, and SiC on the mechanical properties of polymer-based composite?
3. What are the effects of adding filler into adhesive on the joint strength of adhesively joined composite?
4. What is the contribution of this study?

1.9 Thesis Organization

The overall structure of this research work is summarized below.

Chapter One: Introduce the background of polymer-based hybrid composite, composite joining, objectives, statement of problems, significance of the study, scope of the research, research motivation, and limitations. **Chapter Two:** It reviews relevant research papers regarding natural and synthetic fiber composites, effects of reinforcements, factors affecting properties of natural fiber composites, joining of polymer-based composite, application area of natural and synthetic fiber reinforced composites, and research gaps. **Chapter Three:** Materials required for the research work, methodology, experimental setups and testing, and analysis methods were included. **Chapter Four:** The experimental findings and their deep discussion as well as optimization have been done. **Chapter Five:** Conclusion of the overall work, recommendations from findings, and future works were covered. Finally, References and various appendices are tabulated.

CHAPTER-2

LITERATURE REVIEW

2.1 Introduction

This chapter reviews previous literature on polymer-based matrix hybrid composites and adhesive joining of the composite. Effects of reinforcements on polymer-based matrix composite were reviewed. Factors affecting the properties of the polymer-based hybrid composite material were discussed. Further studies on the factors affecting the joint strength of adhesively bonded composite were discussed in detail. Finally, the research gap was identified and the literature summary was provided.

2.2 Polymer Matrix Composite Materials

A composite material is a heterogeneous material that is synthesized through the mixing of two or more components that form a compatible matrix and a reinforcing matrix to achieve particular features and characteristics. The reinforcing and matrix materials that make up the composites have qualities superior to those of the individual components. The matrix, often made of resin, distributes the weight among the fibers while shielding them from external and environmental harm. In turn, the fiber gives the matrix strength and stiffness to reinforce and help it withstand defects like fractures and cracks. Lightweight, environment-friendly, bio-degradable, low-cost, plentily available, sustainable, low density, and high strength are the unique characteristics of composites over conventional materials (Madhu Kumar & Murthy, 2020; Nagaraj et al., 2020; Rajamahendran et al., 2021).

Based on the matrix constituents, composite materials are classified into organic matrix, metal matrix, and ceramic matrix composites. Organic matrix composites can be categorized into two classes of composites, such as polymer matrix composites and carbon matrix composites, commonly known as carbon-carbon composites. Based on reinforcement, composite materials are classified as fiber-reinforced, laminar, and particulate composites (Nagavally, 2016). PMCs are one of the most sorted materials replacing traditional materials due to its excellent strength-to-weight ratio. PMCs are classified into particle and fiber-reinforced composites. Furtherly, fiber-reinforced composites are classified as glass fiber and carbon fiber-reinforced polymers (Begum et al., 2020).

The most frequently employed matrices to create hybrid natural fiber composites are polymeric (thermoset or thermoplastic) because they are lightweight and can be processed at low temperatures. Epoxy and unsaturated polyesters are the two primary thermoset resins

utilized in hybrid natural composites (Neto et al., 2022). Unsaturated polyester resins are a significant category of thermoset polymers. They are widely used due to their low cost, superior corrosion resistance, ease of processing, and availability in a variety of grades. Their inability to release volatile byproducts during the curing process adds to their attractiveness(Athawale & Pandit, 2019).

Better mechanical properties are obtained with the hybrid natural fiber-reinforced polymer composite when compared to a single fiber-reinforced polymer composite. Hybridization between synthetic and natural fiber may enhance the strength, moisture resistance, stiffness, modulus, and thermal resistance of the composite (Begum et al., 2020). The mechanical performance and water resistance of NFRCs can be greatly enhanced by hybridizing natural fibers with synthetic fibers. The most common fiber utilized in hybridization of NFRCs is glass fiber (Neto et al., 2022).

2.3 Natural Fiber-Reinforced Polymer Composite

Natural fiber composites (NFCs) are composite materials composed of a polymer matrix reinforced with natural fibers, such as sisal, jute, hemp, and coir. They have gained significant attention due to their eco-friendly nature, lightweight properties, and cost-effectiveness (Pereira et al., 2020). Gopal Krishna et al., (2019), stated that minimized dependence on non-renewable energy, lower pollution, and greenhouse emission are the environmental advantages offered by natural fiber-reinforced composite materials. Natural fiber-reinforced composites are employed in a variety of nonstructural automotive applications, including instrument panels, package trays, door panels, internal engine covers, boot liners, oil filter liners, and oil air filters (Bichang'A et al., 2022). Low mechanical properties and absorption of humidity due to the hydrophilic properties of the natural fibers are the main drawbacks of NFRCs. Furthermore, the poor adhesion between fibers and matrix, inconsistent fiber quality, thermal stability, and moisture absorption of natural fibers are the main issues that need to be resolved to improve performance and consequently the use of NFRCs in the industry (Neto et al., 2022).

2.3.1 Natural fiber

Natural fibers are materials that are obtained directly from plants, animals, and minerals and can be spun into yarn, made into fabric, or for other industrial purposes. The primary constituents of these naturally occurring fibers include cellulose, hemicellulose, pectins, lignin, and trace amounts of extractives (Karthi et al., 2019).

Venkatesan & Bhaskar, (2020) stated the automotive, construction, different energy sources, and packaging industries use natural fibers such as jute, flax, hemp, coir, and sisal because they are effective reinforcement in thermoset and thermoplastic matrices. Based on their source, natural fibers are classified into three as shown in Figure 2.1.

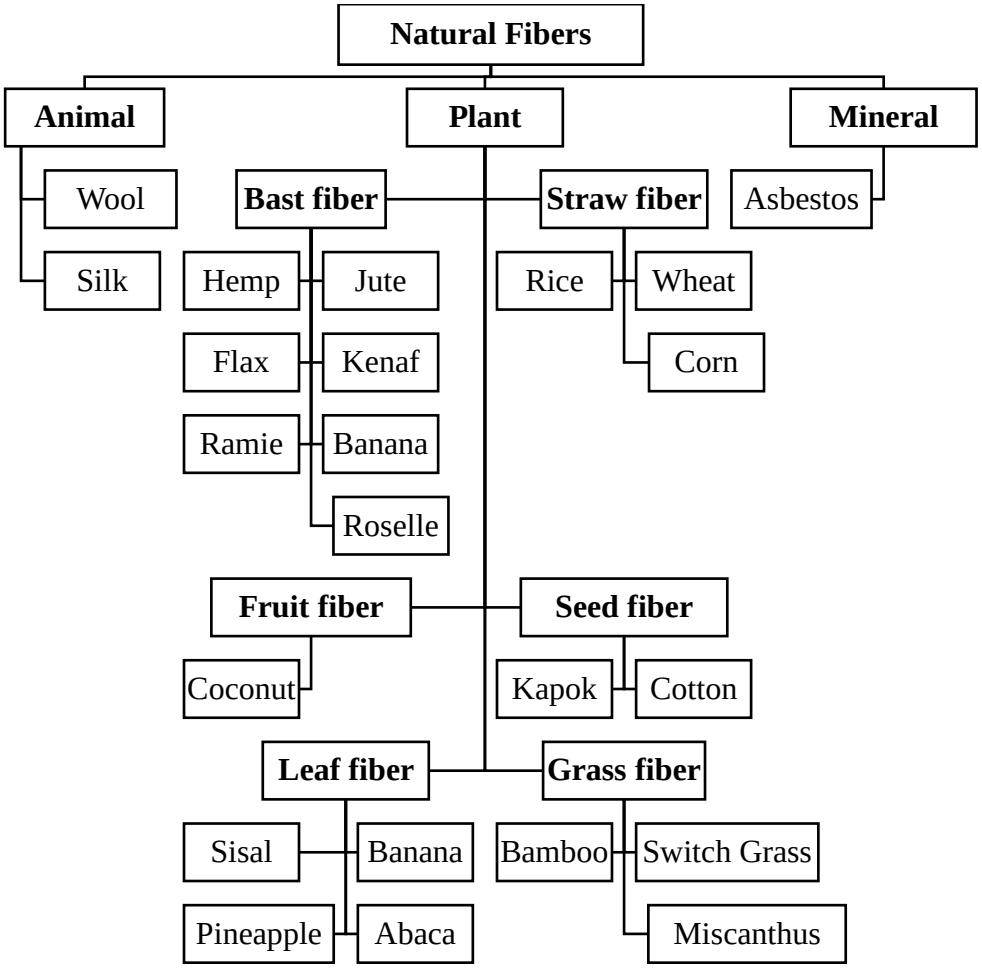

Figure 2. 1 Classification of Natural fibers redrawn from (Karthi et al., 2019)

Sisal fiber

Sisal fiber is a natural, biodegradable, derived from the leaves of the agave sisalana plant, which can be developed in many countries of the world including Ethiopia. It is one of the most extensively used natural fibers which is also very easy to cultivate. Nearly, 4.5 million tons of sisal fibers are produced every year throughout the world. Sisal fibers range in length from 1 to 1.5 mm and in diameter from 100 to 300 μm. Sisal fiber has a high tensile strength and high cellulose content. After two years of planting, the fibers can be taken out of the leaves, and the plant has a 12-year productive life (Alemayehu et al., 2020; Mosisa & Batu, 2021; Ramasubbu & Madasamy, 2022).

Naveen et al., (2018) reported that sisal fiber is one of the potential reinforcements for polymer composite. In addition to its source, age, and location, the physical and mechanical

properties of sisal fibers are further influenced by gauge length, experimental temperature, fiber diameter, and strain rate. Sisal fiber can be used in the aircraft and automotive industries in addition to its more conventional uses in ropes, carpets, and mats. Rajak et al., (2022) reported that sisal fiber has superior tribological, mechanical, thermal, and chemical durability as compared to conventional metals. The primary benefits of sisal fibers include their durability, stretchability, waterproofing, resistance to strain and wear, and resistance to moisture. However, they also have several drawbacks, including the ability to be flammable, incompatibility for hot washing, contribution to microplastic pollution, low insulation capacity, susceptibility to heat damage, and lack of environmental friendliness.

2.3.2 Factors affecting properties of natural fiber composite

The properties of natural fibers depend on several factors, including fiber extraction method, fiber treatment, fiber orientation, and, hybridization, which are discussed in this section.

- **Fiber extraction**

Naveen et al., (2018) described that retting, scaraping, or mechanical decortication are the methods used to extract sisal fiber from leaves. Decortication is the most common technique for extracting sisal fiber. This method separates the fleshy pulp from the fiber by crushing the leaves between blunt knives and moisture. The debris contained in the leaves is cleaned with water. Retting is a conventional method for the extraction of sisal fiber. The sisal leaves were initially broken down by bacteria, and then fibers were extracted from the pitch. Radoor et al., 2020; Sathish et al., (2021) described the decoration method involves removing the sisal leaf's fleshy green portion while keeping its long fibers in place. The process requires skill and precision to avoid damaging the fibers. Jaballi et al., (2017) prepared sisal fiber from the leaves of the sisal (agave sisalana) by cutting off from the mother plant and removing their higher pointed parts. The remaining leaves were cut to the needed length. The fiber bundles containing impurities can be easily extracted from recently obtained sisal leaves, fiber bundles containing impurities are easily retrieved, and they are rapidly scraped between nails' hands until all matter is removed. Finally, fibers were dried in the air.

- **Fiber treatment**

Natural fibers like sisal are chemically treated to remove lignin, waxy substances, pectin, and natural oils coating the external surface of the fiber cell wall. Sodium hydroxide is the most often used chemical for bleaching and/ or cleaning plant fiber surfaces. Different treatments are used to improve the adhesion between the matrix and fiber of fiber-reinforced

composite. The alkali treatment of sisal fiber for surface modification results in optimum impact and tensile strength (Karthi et al., 2019).

Kumaresan *et al*., (2015) prepared a 5% NaOH solution using sodium hydroxide pellets and distilled water. The study shows that increasing the percentage of NaOH affects the fiber's properties by reducing the bonding capacity during the preparation of composites. Concluded that sodium hydroxide (NaOH) is the most commonly used alkali treatment for bleaching and cleaning the surface of natural fibers to produce high-quality fibers. Tesfay & Kahsay, (2020) stated that to remove any NaOH that might be left the alkaline-soaked fibers were washed using water before they were allowed to dry at room temperature for 72 h. The result showed that treatment of sisal fibers with NaOH and $NaHCO_3$ improves the tensile and impact strength of the composite laminates. Khan *et al*., (2018) suggested treating the fibers with a 5% weight alkali for NFRPCs can have good tensile and flexural characteristics.

- **Fiber orientation**

Dress *et al*., (2021) prepared the 30°/60°, 30°/−45°, 0°/90°, and 45°/−45° woven sisal fiber using a nailed wooden frame as a warp and weft guide. The result showed that the average absorbed energy and impact strength of 0/90° and 45°/−45° woven sisal fiber reinforced polymer composite(WSFRPC) was greater compared to 30°/60° and 30°/−45° WSFRPC. Compared to all other orientation test specimens, the 30°/60° WSFRPC showed less absorbed energy and impact strength. A 45°/45° oriented woven sisal fiber-reinforced polyester composite showed better toughness and absorbed energy. It also has better impact strength than the other orientations of woven sisal fiber-reinforced polyester composites. Khan *et al*., (2018) investigated the combination of long/short fibers and particulates that results in good tensile and flexural properties because particulates reduce the voids between the fiber and matrix. To achieve good tensile and flexural properties of NFRPCs a fiber length of 20–50 mm can be used. When a high strength-to-weight ratio is required, NFRPCs are the material of choice.

- **Hybridization**

Suriani et al., (2021) mentioned that hybridization is recommended by the majority of researchers to address the shortcomings of natural fibers and reduce the usage of synthetic fibers that are harmful to the environment. Pereira et al., (2020) investigated that combining natural fibers allows for the creation of hybrid composites that fully use the qualities of each constituent. The hybrid natural fiber-reinforced composites may eventually replace glass fiber-reinforced composites in applications where very high load-bearing capacities are not required. Saba et al., (2016) stated hybridization technology facilitates easy manufacturing

of cost-effective components as well. Composite materials based on natural and synthetic fibers have proved their potential as effective materials for structural uses.

- **Fiber volume**

Neto et al., (2022) reported the volume fraction of each type of fiber has an impact on how the failure occurs. For composites with high-strain fiber volume, fibers dominate the stress distribution. If the fiber fraction is reversed, the composite's strength is limited by the low-strain fiber.

2.4 Synthetic Fiber-Reinforced Polymer Composite

Neto et al., (2022) investigated that, synthetic fibers like glass, carbon, and aramid are being used in hybrid polymer-based composites due to their biodegradability, initial processing cost, recyclability, health hazard, energy consumption, and machine abrasion. Cavalcanti et al., (2019), studied that the addition of synthetic fiber increases the flexural and impact strength of the composite due to better interfacial adhesion between glass fiber and polyester matrix which contributed to a better distribution of tension between fiber and matrix.

2.4.1 Synthetic fiber

Synthetic fibers are materials made by humans through chemical synthesis. Carbon and glass fibers are synthetic fibers widely used as reinforcements (Karthi et al., 2019). The entire process of creating synthetic fibers takes place in a lab using synthetic polymers which are typically derived from petroleum byproducts. Synthetic fibers can be processed via spinning, polymerization, and filament winding processing. The major classifications of synthetic fibers are organic (such as polyamides, polyesters, polyvinyl derivatives polyolefins), inorganic (such as glass, carbon, boron, and silicon carbide), and others (Bicomponent and multicomponent) (Rajak et al., 2022).

- **E-glass fiber**

Glass fibers are widely used preferred materials in high-performance composite applications due to their highly attractive physical and mechanical qualities, ease of manufacturing, and comparably cheap cost to carbon fibers. E-glass fiber is easily mouldable, lightweight, extremely strong, and robust materials. Fiberglass is frequently used in boats, cars, bathtubs, hot tubs, water tanks, roofing, pipes, and exterior door skins (Begum et al., 2020; Gangil et al., 2020).

E-glass fiber reinforced polymer has major advantages including a high strength-to-weight ratio and combination of lightweight and it is easy to fabricate, which is better than many conventional materials, (Rajamahendran et al., 2021). EL-Wazery *et al*., (2017) investigated

how the percentage of glass fiber affected mechanical properties like impact, bending, and tensile strength by developing an E-glass fiber reinforced polymer composite with randomly oriented, with different fiber percentages (15%, 30%, 45%, and 60%) using a hand lay-up technique. The composites' hardness was assessed using a Brinell hardness tester. The best mechanical qualities of the fabricated composites were attained at 60% glass fiber weight.

2.5 Ceramic Particle-Reinforced Polymer Composite

Ceramic particle-reinforced polymer composites exhibit enhanced mechanical and thermal properties due to the synergistic effects of the constituents. The microstructure of these composites plays a crucial role in determining their properties, with factors like filler particle ratio and orientation influencing mechanical and thermal behavior significantly (Hassan et al., 2022). By incorporating ceramic particles into polymer matrices, these composites can achieve improved fracture toughness and thermal conductivity, surpassing the individual properties of the constituent materials (Article et al., 2022). Khan *et al*., (2018) reported that the addition of coupling agents further improves the tensile and flexural properties. SiC, graphite, ZrO_2, and Al_2O_3 are commonly utilized as coupling agents.

2.5.1 Silicon carbide

Silicon carbide is a synthetic material with good mechanical, electrical, tribological, and thermal properties for industrial applications. Particles of SiC are produced when sand and carbon undergo a high-temperature electrochemical reaction (Ravi Raj & Vijaya Ramnath, 2021). Silicon carbide is a low-density materials that have good resistance to oxidation, high temperatures, and chemicals. This filler material lowers costs without compromising the properties of composites by minimizing the amounts of reinforcement added. Adding these fillers could result in a 5-10% reduction in volume cost (Choudhary et al., 2020; Praveenkumara et al., 2022).

Sharma et al. (2018) fabricated epoxy composites reinforced with glass fiber and silicon carbide (SiC) filler to investigate processing and characterization through the hand layup method. The result shows that the strength of glass epoxy composites increases as the filler material volume percentage increases. Also, the bending, hardness, and compressive strength increased as the percentage of glass fibers and SiC increased. However, the fracture Strength of GFRP was decreased.

Madhu *et al*., 2018; Ramadan et al., (2017) conducted an additional investigation into SiC particles and jute-reinforced epoxy composites revealing 8% and 15% increases in tensile and flexural strength, respectively. According to the SEM images, material breakdown

happens when fibers envelop the particles, causing the connection between the fibers to weaken. The main benefit of SiC particles in hybrid composites developed from natural and synthetic fiber is improving their hardness.

(Mullaikodi et al., 2019) developed a new composite using SiC nanoparticles as secondary reinforcement and Kevlar 49 and S-Glass fibers as main reinforcement. The amounts of the SiC nanoparticles were varied. A comparison was done between the laminates' tensile strength with and without SiC particles. There was a 35% increase in tensile strength for 5% SiC and an 18% increase for 10% SiC. Maximum tensile strength was obtained when the laminate was developed with 5% SiC.

2.6 Hybrid PMCs Reinforced with Natural, Glass, and Ceramic

Arpitha et al., (2017) incorporated the sisal and E-glass fabrics with the epoxy matrix and added silicon carbide filler to the sisal fabrics. The physical and mechanical properties of composite laminates were evaluated according to ASTM standards, and the results showed that the voids were reduced and the physical properties were enhanced by the incorporation of E-glass and silicon carbide filler. Njoku *et al*., (2011) studied hybrid composites of sisal/periwinkle shell and E-glass/periwinkle shell prepared at a fixed fiber-to-polyester ratio of 30:70 through the hand lay-up method. The results showed that the mechanical properties of the E-glass fiber-reinforced polyester composite improved while those of the sisal fiber-reinforced composite decreased due to the addition of periwinkle shell particles.

Ramesh *et al*. (2021) investigated the tribological behavior of polyester composites reinforced with natural/synthetic fiber. The study was focused on sisal fiber, glass fiber, and hybrid sisal/glass fiber reinforced polyester composites. The samples were fabricated with the fiber volume fraction varying between 20 and 40% via the compression molding method. The result revealed a significant improvement in the tensile, flexural, and impact properties of the hybrid composite.

2.7 Fabrication Techniques of Hybrid Polymer Composite

The polymer composites can be developed by using various fabrication methods (Chohan *et al.*, 2022) as shown in Figure 2.2.

a. Pultrusion

Pultrusion is a fabrication technique that creates desired cross-sectional shapes without regard to length by pulling layers of fabric bathed in resin through a heated die. High productivity, minimal material waste, high quality, and quick composite processing are the

results of this technique. However, incorrect fiber wet-out, die jamming, and fiber breaking are the draw drawbacks of this method (Chohan *et al*., 2022).

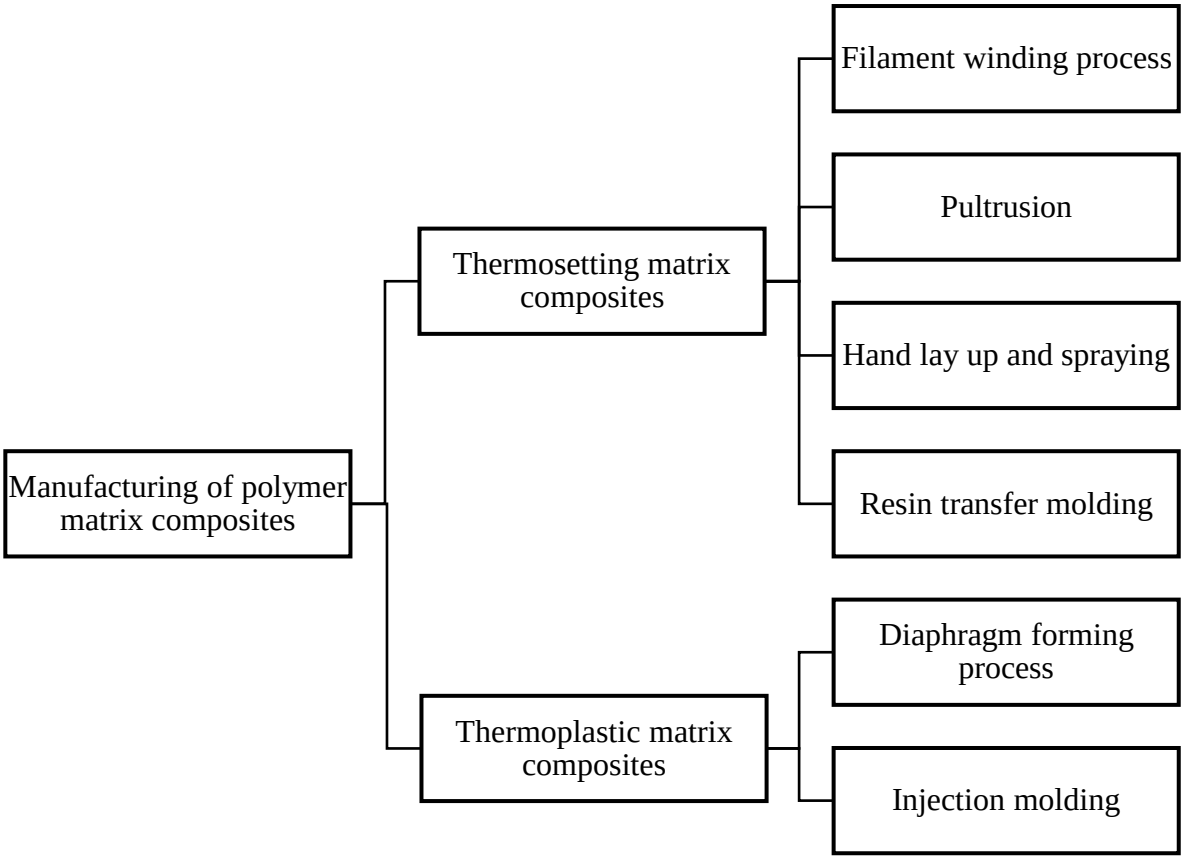

Figure 2. 2 Classification of manufacturing techniques (Chohan et al., 2022)

b. Resin transfer molding

It is a process used for the fabrication of thermosetting polymer composites. The pre-shaped, dry reinforcements are pressed into a heated die mold. The heated mold is then closed, pushing liquid resin into it to cure the component; at last, the mold is opened to remove the portion. The advantage of this approach is that it allows for the automation of massive, complex patterns and curves at low cost and with skilled labor (Chohan *et al*., 2022).

c. Filament winding process

In this method, fiber trails are spooled in various directions on a spindle after being forced through a liquid resin solution. This quick and affordable method allows for precise control of the resin composition, making it ideal for usage in gas cylinders, pressure vessels, pipes, and chemical storage tanks (Chohan *et al*., 2022; Begum et al., 2020).

d. Hand lay-up method

Hand layup is the simplest method of developing the thermosets-based fibers composite. It is the most common and least expensive open-molding method because it requires the least

amount of equipment (Chohan *et al*., 2022;Yogeshwaran et al., 2020). Fiber reinforcements are placed by hand in a mold and resin is applied with a roller. This process is used to make both large and small items. Relatively lower mold costs, easy availability of the tools required for production, and mold maintainability are advantages of the hand lay-up method. To avoid the sticking of polymer to the surface of a mold and to get a good surface finish of the product, fibers as a reinforcement are placed at the upper surface of the mold thin plastic sheets are used on the bottom of the mold and then a releasing agent is sprayed on it(Abas *et al*., 2018; Venkateshwaran *et al*., 2011). The hybrid composite was made using a hand lay-up method. Hand lay-up is the most common and least expensive open-molding method because it requires the least amount of equipment(Sayam et al., 2022).

2.8 Testing and Characterization of Hybrid Composite

The hybrid composite's stacking order is very important for its flexural properties. a specimen's tensile and compressive stresses reach their maximums on its top and bottom faces, respectively, and then linearly decline towards the neutral line, or the middle of the specimen under a 3-point bending flexural load. The impact resistance of hybrid composites is closely related to the mechanical characteristics of the fibers, layer stacking order as well as the fiber's and matrix's interfacial adhesion (Cavalcanti et al., 2019; Neto et al., 2022).

2.9 Adhesive Bonding of Polymer-Based Composite

Polymer-based composite joining refers to the process of connecting or bonding different components or sections of a composite material made primarily of polymers. It involves the fusion or adhesion of multiple components to create a unified structure. Joining methods for these composites can vary depending on the specific materials involved, the desired properties of the final structure, and the application requirements (Melese & Tesfie, 2023). Casas Pulido et al., (2019), report that adhesion is the state in which two surfaces are held together by an interfacial junction (the region where two materials come into contact and form a bond) while cohesion is the term used to indicate the state that tends to associate the particles of substance by secondary valence forces (attractive forces that act between molecules to hold atoms together). Depending on its chemical and physical properties, an adhesive's cohesive strength changes as it cures or sets.

Malekinejad et al., (2023) reported that adhesive joining is a joining mechanism in which adhesive material is added between the adherend surfaces to hold them together by the formation of adhesive bonds after solidifications. It is the highest versatile joining technology in many engineering applications, and it is the most practical way to combine

and bond composite materials with other materials such as polymers and metals. Adhesively bonded joints are becoming good alternatives to mechanical joints in engineering as they provide predominant advantages such as lower structural weight, modified damage tolerance, and minimum fabrication cost over conventional fasteners (Banea & Da Silva, 2009; Worrall et al., 2020). Melese et al., (2022) stated that low-stress concentration, ease of maintenance, minimum manufacturing cost, and other factors influence adhesive joining to become one of the most widely used in different industrial applications. To ensure the safety, efficiency, and reliability of adhesive bond joining one must understand the properties and behavior of adhesively bonded joints

2.9.1 Advantage of adhesive joining over other joining methods

Composite materials joining methods can be categorized into three methods. These are adhesive joining, mechanical joining, and welding joining. Mechanical joining is the process of forming joins using mechanical forces. Fiber-reinforced plastic materials are not well-suited for mechanical joining, especially in intricate designs such as wind turbine systems or aircraft. This is because things like adding structural discontinuities, adding extra weight, and having protruding bolt heads and nuts enhance aerodynamic drag (AİKHUELE, 2019). Compared to mechanical fastening, adhesive bonding has several advantages in composite joining applications. Compared to riveted connections, adhesively bonded joints have a higher degree of stiffness due to their more uniform stress distribution along the bonded surface. They also offer superior fatigue strength, shock absorption, dampening, and sealing as well as electrical insulation. Adhesive bonding is also a manufacturing-friendly technology that has a lower overall fabrication cost than other joining techniques, frequently only requires single-side access, and permits a high degree of automation with quick cycle durations for quick production (Omairey et al., 2021).

Welding is a joining technique in which materials of the same type, such as metals, polymers, or ceramics, are joined by chemical bonds due to the attraction of ions, atoms, or molecules to one another under the combined action of heat and pressure. The kinds of bonds that develop across the joint are the same kinds of bonds present in the materials that are being joined. Adhesive bonding is different from welding since welding does not require chemical reactions (Messler, 2004; Siddique et al., 2023). In composite materials with a polymeric matrix, when traditional joining techniques like welding and mechanical joining may result in a stress concentration or are impractical, they prove to be particularly beneficial (Barbosa et al., 2018; Casas Pulido et al., 2019).

2.9.2 Parameters that affect the strength of adhesively bonded composites

The strength of adhesive bonded composites is influenced by several key parameters, including, surface preparation, adhesive type, adhesive thickness, overlap length, joint configuration, and manufacturing bonding process.

- **Surface Preparation**

Surface preparation has a direct impact on how well the bonded joint performs. Surface treatment of adherend should ensure the removal of contaminants (lubricants, dust, microorganisms) from surfaces. The key factors to get a strong and durable join are good surface wettability, good activation of the material surfaces being bonded, and surface energy (Banea *et al*., 2014; Budhe *et al*., 2017). Etching is the method of surface treatment applied to composites to eliminate impurities, change the chemistry and surface roughness, or create a lot of pores. Typically, the treated composite is submerged completely in a bath of acidic or basic solution for a predetermined amount of time, temperature, and concentration. Sodium hydroxide, or NaOH, is a base solution that is frequently applied to composite materials treatments(Yudhanto et al., 2021). Melese & Tesfie, (2023) effective joint preparation greatly depends on surface preparation. Acetone washing and 200-grit sandpaper grinding improve adhesion in the join region.

- **Adhesive types**

The adhesives used in structural applications are epoxies (a high strength and temperature resistance), cyanoacrylates (which bond to plastic and rubber quickly but have poor resistance to moisture and temperature), an-aerobics (suitable for bonding cylindrical shapes), acrylics (cure quickly and tolerate dirty and poorly prepared surfaces), polyurethanes (good flexibility at low temperatures and fatigue resistance), polyurethane (which have flexibility at low temperatures and fatigue resistance), silicones(excellent low-stress applications, high degree of flexibility and very high-temperature resistance), and high-temperature adhesive (phenolics, and polyimides) (Banea & Da Silva, 2009; Omairey et al., 2021).

- **Adhesive thickness**

Different adhesive systems require different adhesive thicknesses depending on the; **Function/properties:** An adhesive thickness can be small (less than 100 μm) for maximum peak strength. However, if impact resistance is needed or the joint dimensions vary, the bond line can be much larger, more than 1 mm, and

Type of cure: The thickness of adhesives that are cured chemically (such as epoxies, and acrylics) can be extremely small, but those cured by external factors (such as moisture-curing

polyurethanes, and silicones) need a much larger adhesive thickness to provide a large enough external surface area for efficient moisture diffusion from the atmosphere (Worrall *et al*., 2020).

- **Overlap length**

Overlap length is the length of the contact area between the adherents and the adhesive. It influences the stress distribution and the load transfer capacity of the joint. *(Rangaswamy et al*., 2020) revealed the effects of overlap length performance for single lap adhesively bonded joint within fiber-reinforced polymer tubular adherents subject to static and cyclic torsional loading conditions of overlap length (12 mm, 20 mm,30 mm, and 40 mm) and constant thickness (0.8mm). It was concluded that the static capacity of the composite joints increased, but not so significantly at overlap lengths above the effective length, and under cyclic loading, the increase in overlap length increased the life cycle of the bond.

Kadioglu *et al*. (2018) used materials of woven carbon fiber-reinforced polymer matrix composite and film adhesive, and employed parameters such as an SLJ configuration of overlap lengths (15 mm, 25 mm, and 40 mm), and two distinct composite adherend thicknesses of 2 mm and 3 mm, respectively.

- **Joint configuration**

Typically, single-lap, double-lap, scarf, and stepped-lap joints are joint configurations that have been examined in the literature(Siddique et al., 2023). Bonded joints are usually anticipated to withstand static or cyclic loads for extended periods without negatively affecting the structure's ability to support loads(Nascimento *et al*., 2021). Commonly, scarf joints, stepped-lap joints, double-lap joints, and single-lap joints are the types of joint configurations. Melese *et al*., (2021) experimentally investigated the joining behavior of jute/sisal fibers epoxy laminates using different joint configurations. Joint configuration (single lap, scarf, and double strap butt joints), types of adhesive material, and adherents were the parameters for joint strength. Among the various joint configurations investigated, the double-strap butt joint was found to be most suitable for all types of material systems (sisal/epoxy, jute/epoxy, and hybrid/epoxy).

- **Manufacturing bonding process**

The bonding process is one of the factors to consider because it has an impact on all aspects of joint strength. Three bonding processes namely co-curing, co-bonding, and secondary bonding are primarily used to manufacture the bonded connection between composite adherend. The co-curing of both substrate parts are simultaneously cured while the co-bonding process is performed when the substrate or adherend is cured with the adhesive.

Secondary bonding is when the adhesive layer is cured between two pre-cured substrates. The multi-material bonding process is similar to secondary bonding except with a combination of metal and composite substrates instead of only cured composite substrates (Budhe *et al*., 2017).

2.9.3 Effect of additive/ filler on joint strength of composite materials

Fillers are solid materials that are insoluble in adhesive and are added to adhesives to improve adhesion, lower adhesive costs, modify mechanical properties, raise viscosity, improve electrical and/or thermal conductivity, and increase bonding strength. Biobased fillers (cellulose nanoparticles, tree bark powders), carbon-based fillers (carbon black, carbon nanotubes,), ceramic fillers (aluminum oxide, silicon carbide), metallic fillers (aluminum, copper), silicon-based fillers (silica), and hybrid fillers (consisting more than one type of filler) are some of the filler substances used. The type and quantity of filler used will have an impact on the characteristics of the adhesive (Anaç, 2023; Sanghvi et al., 2022). Anaç, (2023) investigated that, an epoxy adhesive was mixed with powdered mussels, olive pomace, and walnuts in varying weight ratios (5 percent, 15%, and 30%), and diameters (38 and 45 micrometers). The obtained adhesives with additives were used to link the steel materials in the form of single-lap joints. The results revealed that, in comparison to pure adhesive, binding strengths increased when the particle size was 45 µm; however, for 38 µm powders, the strength value improved only at the 5% additive ratio. When 45 µm powder additives were added to joints, the strength increased up to 38% as compared to pure adhesive; for 38 µm, this rate was found to be 31%.

Chavooshian et al., (2017) presented research on how silicon carbide nanoparticles affect the strength of adhesion in steel-glass/epoxy composite joints joined by two-part structural acrylic adhesives. The shear and tensile strength of the composite joints were significantly increased by the addition of nano silicon carbide to the two-part acrylic adhesive. When filler was added up to 1.5 weight percent, the shear and tensile strengths of the adhesive joints increased; however, as filler was added further, they dropped. Additionally, the peel strength of the joints decreased as a result of the nanoparticle addition. SEM micrographs indicated that the fracture was altered by the incorporation of nanoparticles.

The summary of adhesive joining process parameters from the previous work of different researchers was given in Table 2.1.

Table 2. 1 Summarized literature review for selection of process parameters

Authors, Years	**Materials**	**Process Parameters**			
		Filler wt.%	**Joint configuration**	**Overlap length(mm)**	**Layer thickness(mm)**
(Afendi *et al*., 2011)	Epoxy-(Al-alloy)	-	Scarf joint (SCJ)	-	Ranged between 0.1 to 1.2
(Campilho *et al*., 2013)	Carbon-epoxy composite	-	Stepped lap joint (STJ)	10,20,30,40, 50,60,70 and 80	0.2
(Chavoos hian et al., 2017)	Steel–epoxy composite	SiC nano-particle	Single lap joint (SLJ)	-	0.2
(Kadioglu *et al*., 2018)	C-fiber-reinforced PMCs	-	Stepped lap joint (STJ)	15, 25 and 40	Constant at 0.2
(Alves et al., 2018)	A7075 and stainless steel 30 4	-	30º scarf angle	59	0.2
(Brito *et al*., 2020)	Carbon-fiber reinforced polymer	-	Stepped lap joint (STJ)	12.5, 25, 37.5, and 50	-
(Hyeon-Seok et al., 2020)		-	Scarf joint (SCJ)	99	0.2
(Khashaba et al., 2022)	Carbon fiber composite	SiC nano-particle	Scarf joint (SCJ)	5º scarf angle	0.17-0.25
(Anaç, 2023)	DX51D+Z galvanized steel	Bio-fillers	Single lap joint (SLJ)	12.5	-
(Melese & Tesfie, 2023)	Natural fiber-PMCs.	-	Single lap joint (SLJ)	$>$ 20 (25.4 is optimal)	0.1 to 2
(Venugop al & Sudhagar P, 2024)	Glass fiber-reinforced polymer	Graphene nanoparticles	Single lap joint (SLJ)	-	-

2.10 Optimization Process

Mosisa & Sirhabizu, (2019) described that Taguchi experimental design is a suitable design since it minimizes the number of runs and applies to process optimization, product creation, and quality control of diverse products. This set of fractional factorial designs is focused on main effect estimation. According to the Taguchi design approach, the product quality (signal) to uncontrollable conditions (noise) should be high. Lilly Mercy *et al*., (2017) used Taguchi's design of experiment to conduct the experiments by varying the levels of input parameters and resulting responses were identified and converted to a grey scale to get the optimal combination. The quality of data was validated through Analysis of Variance (ANOVA). Grey relational analysis (GRA) was used for optimizing multi-response (tensile and flexural strength). The natural composites from durian skin fiber and PP matrix were analyzed using the response surface methodology (RSM) and design of experiment (DOE) method (Sumesh & Kanthavel, 2022).

(Pandya & Rathod, 2020) employed grey relational analysis to address the interdependencies among multi-responses. Events with no information are categorized as black, and those with all the information are categorized as white. Grey or hazy refers to the conditions that lie between these extremes. The ANOVA method is applied when multiple cases are involved. This method analyses the degree of homogeneity between several data sets. An F-test is used to compare the two necessary estimates of population variance (the variation between and within samples).

2.11 Application of Hybrid Polymer Composite

Hybrid fiber composites are now used in the fabrication of automotive parts, including door panels, instrument panels, armrests, headrests, seat shells, and parcel shells (Satyanarayana et al., 2009). Natural fiber polymer composites can also be used to manufacture thermally sound materials that need fire-resistant qualities. This is because natural fibers have microstructures that are porous and give them fire resistance(Gangil et al., 2020; Shahinur & Hasan, 2020). Polymer-based natural fiber-reinforced Hybrids composites are also utilized in a variety of structural and outdoor applications, such as marine constructions, aircraft parts, leisure equipment, and automobile exterior underfloor panels (Nurazzi et al., 2021).

Figure 2.3. shows the application of natural fibers in Mercedes-Benz components (Li et al., 2020), where (a) A-glass, (b) C-glass, (c) E-glass, and (d) S-glass.

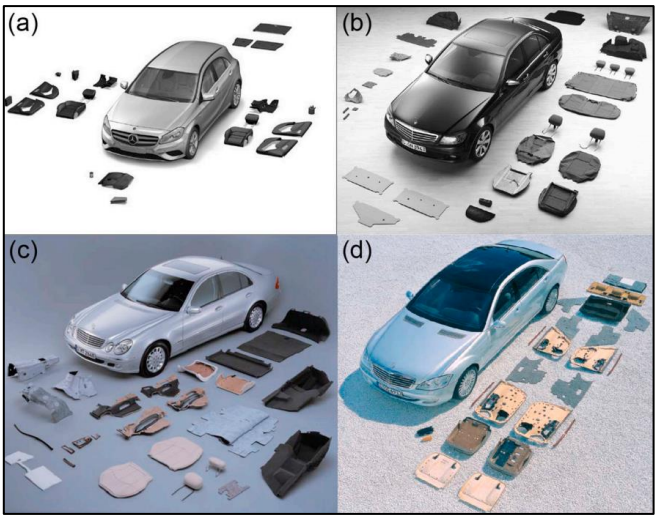

Figure 2. 3 Mercedes-Benz components containing natural fibers (Li et al., 2020)

2.12 Literature summary

Various research have been done on the development and investigation of polymer-based composites reinforced with natural and synthetic fibers, and fillers using the hand layup method. NFRCs have gained significant attention due to their eco-friendly nature, lightweight properties, and cost-effectiveness. Low mechanical properties and absorption of humidity due to the hydrophilic properties of the natural fibers are the main drawbacks of NFRCs. Furthermore, poor adhesion between fibers and matrix, inconsistent fiber quality, and moisture absorption of natural fibers are the main issues that need to be resolved to improve performance and consequently the use of NFRC composites in the industry. Synthetic fiber increases the flexural and impact strength of the composite due to better interfacial adhesion between glass fiber and polyester matrix, which contributes to a better distribution of tension between fiber and matrix. Silicon carbide is a synthetic material with good mechanical, electrical, tribological, and thermal properties for industrial applications. Based on the previous work results, the mechanical performance and water resistance of PMCs can be greatly enhanced by hybridizing natural fibers with synthetic fibers and adding filler.

The joining of polymer-based composites refers to the process of connecting or bonding different components or sections of a composite material made primarily of polymers. Adhesive joining is a joining mechanism in which adhesive material is added between the adherend surfaces to hold them together through the formation of adhesive bonds after solidification. As discussed in various literature, the joint strength of the adhesively joined composite materials is highly affected by surface preparation, joint configuration, adhesive type, overlap length, and manufacturing bonding processes. Additives are solid materials

that are insoluble in adhesive and are added to adhesives to improve adhesion, lower adhesive costs, modify mechanical properties, raise viscosity, improve electrical and/or thermal conductivity, and increase bonding strength.

2.13 Research Gaps

Although polymer-based composite materials are reinforced with both natural fiber and synthetic fiber, their mechanical performance is not sufficient. However, the mechanical performance of composite materials depends on several factors, including the fibers (type, orientation, and length), matrix material, the interface between fiber and matrix, and fabrication methods as studied (Lokesh et al., 2020; Sadasivuni et al., 2020). Epoxy polymer-based composites reinforced with sisal fiber, SiC, and E-glass are most commonly studied by many researchers and used for different applications. However, few studies are available on a polyester-based composite reinforced with sisal fiber and E-glass and the effect of hybridization with SiC has not yet been well studied. In addition to this, a lot of research has been conducted around composite joining through the adhesive joining technique by considering a single process parameter of the joint without integrating multi-process parameters (Joint configuration, filler wt.%, and overlap length together) that can affect the bond strength of adhesive joining. Furthermore, few studies are available on utilizing the filler or additives in adhesive materials to enhance the joint strength of composite adherends. In this research, the effects of fiber weight percentage were studied for mechanical performance. It has been revealed that void creation during the fabrication process lowers the composite's strength. To overcome this, SiC filler was used to close the space between the fiber and the matrix, creating dense composite structures and lowering the number of gaps and pores in the material(Sen et al., 2021). Finally, the SiC powder was added to the adhesive material (epoxy) to enhance the joint strength of the adhesively joined composite of "Polyester-sisal fiber-E-glass-SiC".

CHAPTER-3

MATERIALS AND METHODS

3.1 Introduction

In this chapter, the required materials, and sample preparation process for developing the hybrid polymer composite material reinforced with sisal fiber-E Glass-SiC composite as well as for joining using the adhesive joining technique were discussed. The methodology of the experimental process was provided. Testing and characterization methods of the composite were discussed. Adhesive joint samples were prepared based on the selected process parameters as per ASTM and their testing methods were also provided. Figure 3.1 shows the research methodology of this research.

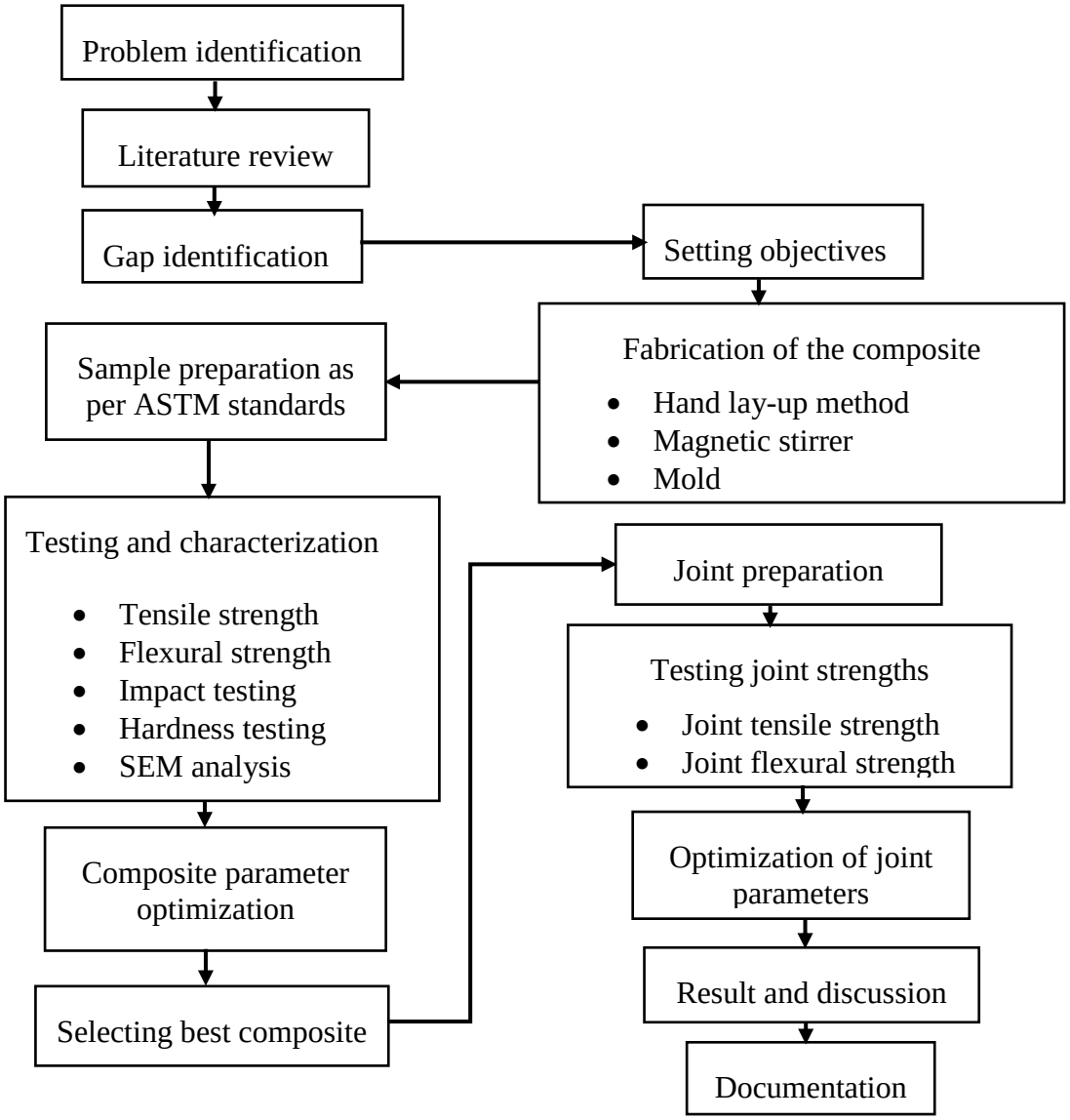

Figure 3. 1 Research methodology

3.2 Materials

The basic materials selected for this research to produce the new and modified composite material are matrix material (polyester resins), and reinforcements (sisal fiber, SiC, and E-glass). Other materials, such as release agents, hardeners, sodium hydroxide, and distilled water, were used to facilitate the fabrication, increase the bonding between matrix and reinforcements, and clean up the fibers before the fabrication of the composite were discussed in the following sub-sections.

Figure 3. 2 Basic required materials

3.2.1 Polyester resins

Polyester resins are thermosetting polymer materials and are cured when mixed with hardener. The general-purpose polyester resin was a matrix material that was mixed with reinforcements to fabricate the required composite material. Unsaturated polyester known as “TOPAZ-1110 Phthalic Anhydride,” used for general purposes, was purchased from World Fiber Glass and Water Proofing Engineering, Addis Ababa, Ethiopia, and utilized for this research. The properties of matrix and reinforcement materials are given in Table 3.1.

Figure 3. 3 Polyester resin

Table 3. 1 Properties of the materials (Naveen et al., 2018; EL-Wazery et al., 2017; Begum et al., 2020)

Properties	Properties of Polyester resins	Properties of the reinforcement materials	
		SiC	E-glass
Density (g/cm^3)	1.2-1.5	3.22	2.55
Melting point (C^0)	60	2730	1725
Tensile strength (MPa)	20-40	240-1625	3400
Young Modulus (GPa)	2-4.5	90-170	71
Modulus of elasticity (GPa)	3.23	410	72

3.2.2 Sisal fiber

Sisal fiber is a natural fiber derived from the leaves of the Agave sisalana plant. Two to four-year-old sisal fiber was collected from Ejere, Oromia, Ethiopia, located 42 km from Addis Ababa the capital city. Based on the different literature, the mechanical properties, chemical composition, and moisture content of sisal fiber are described in Tables 3.2 and 3.3.

Table 3. 2 Properties of sisal fiber Source: (Naveen et al., 2018)

Properties	Density (g/cm^3)	Tensile strength (MPa)	Young Modulus (GPa)
Sisal fiber	1.33-1.5	400-700	9.0-38.0

Figure 3. 4 a) Agave sisalana plant b) Sisal fibers

Table 3. 3 Chemical composition and moisture content of sisal fiber (Bekele et al., 2022)

Cellulose (%)	Hemicellulose (%)	Lignin (%)	Moisture content (% w.b)
65	12	9.9	10

3.2.3 Silicon carbide (SiC)

SiC particles are used to strengthen fibers, enabling them to bear greater compressive, tensile, flexural, and shear stresses, as discussed in section 2.5. It has been revealed that void creation during the fabrication process lowers the composite's strength. SiC was added as the filler particle and a black powder of silicon carbide with a 50-150-micron particle size was used for this research work. The properties of SiC are described in Table 3.1 and the SiC powder is shown in Figure 3.5.

Figure 3. 5 Silicon carbide (SiC) powder

3.2.4 E-glass

E-glass, or electrical-grade glass, is a type of glass that is commonly used as a reinforcement fiber in composite development. It is a popular choice due to its excellent mechanical properties, high strength, and cost-effectiveness as explained in section 2.4. The chemical composition of E-glass is given in Table 3.4 and random-type fiberglass is shown in Figure 3.6.

Table 3. 4 Chemical composition of E-glass (Naveen et al., 2018), (Arpitha et al., 2017)

SiO_2	Al_2O_3	CaO+MgO	B_2O_3	Na_2O+K_2O
54wt%	14wt%	22wt%	10wt%	less than 2wt%

Figure 3. 6 Chopped straight mat E-glass fiber (Fiber mat 450)

3.2.5 Release agents

One of the release agents known as honey waxes was utilized for easy removal of developed composite samples from mold. This release agent is given in Figure 3.7.

Figure 3. 7 White petroleum jelly - A mold release agent

3.2.6 Hardener

A hardener material or catalyst was used to solidify the fabricated composite laminate following the mixture with polyester resins in a ratio of 10:1. For this purpose, "methyl ethyl ketone peroxide hardener," was purchased from World Fiber Glass and Water Proofing Engineering, Addis Ababa, Ethiopia. This material is given in Figure 3.8.

Figure 3. 8 Hardener (Catalyst)

3.2.7 Sodium hydroxide

Sodium Hydroxide was used for sisal fiber treatment to remove the lignin, pectin, hemicellulose, and waxy elements that may result in the deprived fiber. This chemical was purchased from the local market of "Labcoom Trading PLC. Addis Ababa". This material is shown in Figure 3.9.

(a) Sodium hydroxide and (b) Pellet form NaOH

Figure 3. 9 Fiber treating material

3.2.8 Distilled water

Distilled water removed contaminants such as bacteria, algae, lead, and rust and dissolved minerals such as sodium, calcium, potassium, and other impurities. This material is given in Figure 3.10.

Figure 3. 10 Distilled water

3.2.9 Adhesive material

Epoxy adhesive is the fitting and available adhesive material for joining the developed composite. Araldite is a two-component, rapid-curing transparent epoxy used to bond a variety of substrates. These materials are depicted in Figure 3.11 and the materials properties are shown in Table 3.5.

Table 3. 5 Properties of the adhesive araldite(Özer & Erbayrak, 2018)

Adhesive	Tensile strength (MPa)	Tensile yield strength (MPa)	Elasticity modulus (MPa)	Tensile failure strain (%)	Poisson's ratio
Araldite	21.6	12.6	1850	4.77	0.33

Figure 3. 11 Epoxy resin with hardener (Araldite)

3.3 Methodology

Design of the experiment, sample fabrication methods, testing and characterization of composite, composite adhesive joining, and grey relational analysis methods were provided in this section.

3.3.1 Design of Experiment

Factors such as fiber orientation, fiber treatment, and hybridizations are affecting mechanical properties of the polymer-based composite. The sisal fiber treatment effect was kept constant because it was suggested that a 5% NaOH solution is best, as discussed in Section 2.3, while random fiber orientation was used and different wt.% ratios of the reinforcements were considered, as described in Table 3.6. Chopped sisal fiber was used as it was recommended to be used with hybridization of the composite, and the detail was given in section 2.3.

a. Design of experiment for composite fabrication

Based on the previous literature on different related works, the compositions of reinforcements with three factors and three levels were selected as described in Table 3.6. The wt.%. of sisal and E-glass fibers was selected based on their optimum combination wt.%. ratio in hybridization as investigated by the authors (Njoku et al., 2011; Chokshi et al., 2017; Chaudhary et al., 2017; Ahmed & Khanna, 2020), and SiC as discussed in section 2.5.

Table 3. 6 Process parameters for composite fabrication

S/No	Parameters	Levels		
1	Wt.% of sisal fiber	0	10	15
2	Wt.% of E-glass	0	10	15
3	Wt.% of SiC	5	5	5

The combinations of matrix and reinforcements were designed as described in Table 3.7.

Table 3. 7 DOE for composite fabrication based Taguchi L9 orthogonal array

S/No	Reinforcements			Matrix
	Sisal fiber (Wt.%)	E-glass (Wt.%)	SiC (Wt.%)	(Polyester resin) (Wt.%)
1	0	0	5	95
2	0	10	5	85
3	0	15	5	80
4	10	0	5	85
5	10	10	5	75
6	10	15	5	70
7	15	0	5	70
8	15	10	5	70
9	15	15	5	65

b. Design of experiment for adhesively joined composite

Adhesive joining process parameters were selected based on the previous work of different researchers from the literature review as discussed in section 2.9. Joint configuration, overlap length, and addition of filler to adhesive were selected based on their optimum combination weight percentage ratio in hybridization as investigated by the authors (Kadioglu et al., 2018; Fenta & Tsegaw, 2023; Brito et al., 2020; Banea et al., 2018; Anaç, 2023; Chavooshian et al., 2017; Sanghvi et al., 2022) as given in Table 3.8, to assess their effects on the joint performance.

Table 3. 8 Process parameters for composite adhesive joining

Process parameters	**Levels**
Joint configuration	SLJ, SCJ, and STJ
Overlap length(mm)	20, 25 and 30
SiC filler to epoxy adhesive (wt. %)	0, 1.5, 3

Based on Taguchi orthogonal array L_9 of the design of the experiment for adhesive joints, nine specimens were prepared, and experimental investigations were conducted. Nine trial specimens obtained by Minitab 20 software are given in Table 3.9.

Table 3. 9 DOE for composite adhesive joining based on Taguchi L_9 orthogonal array

Sample	**Joint configuration**	**Filler (wt.%)**	**Overlap length**
1	SLJ	0	20
2	SLJ	1.5	25
3	SLJ	3	30
4	SCJ	0	25
5	SCJ	1.5	30
6	SCJ	3	20
7	STJ	0	30
8	STJ	1.5	20
9	STJ	3	25

From the design of the experiment based on L_9 that was described in Table 3.9, 9 different samples were required due to the effect of the considered process parameters. Mechanical properties such as joint tensile and joint flexural testing were performed for each specimen.

3.3.2 Sample fabrication methods

This section discusses fabrication methods such as fiber extraction method, fiber treatment method, chopping fiber, mold preparation, sample preparation process, and hand layup methods.

(a) Harvesting sisal leaf (b) Manual extraction (c) Extracted sisal fibers

Figure 3. 12 Sisal fiber extraction process

a) Fiber extraction method

Sisal fiber was extracted from the leaf part of **Agave sisalana**, which was collected from Ejere, Oromia Region, Ethiopia. The fibers were extracted by the manual method using non-serrated knives. The extracted fibers dried in the sun for 8 hours. Once dried, the fibers were ready for chemical treatment.

b) Sisal fiber treatment method

Alkali treatment involves immersing the sisal fiber in the NaOH solution. The extracted fibers were immersed in a NaOH solution for about 12 hours at room temperature. Then, after being treated with NaOH these fibers were thoroughly washed with fresh water and distilled water to remove any sticking of NaOH on the fiber surface, and finally dried at room temperature for 24 hours. The good tensile and flexural properties of NFRPCs can be achieved by using a 5% wt alkali treatment of the fibers (Khan et al., 2018). Therefore, Chemical treatment for sisal fiber was done by using sodium hydroxide (NaOH 5%). The required temperature and soaking time to treat in the solution were in the range of 20-180 °C and 15min-48hrs, respectively (Naveen & Maheswaran., 2015). In the present research, the following steps were followed for NaOH treatment as shown in Figure 3.13.

1. **Prepare the NaOH solution:** Dissolve a 5% concentration of NaOH in 95% distilled water to create a solution.
2. **Soak the sisal fibers:** Immersing the sisal fiber in the NaOH solution for 12 hours at room temperature.

3. **Rinse and Neutralize:** After soaking, the fibers were rinsed thoroughly with water to remove excess NaOH, and any remaining alkalinity was neutralized by rinsing with distilled water. The fiber was washed repeatedly with water.
4. **Drying:** Finally, the neutralized sisal fiber was dried in sunlight for two days.

(a) Solution preparation (b) Soaking in solution (c) Drying

Figure 3. 13 Sisal fiber treatment process

c) Chopped sisal fiber preparation

The good tensile and flexural properties of NFRPCs can be achieved by using the optimum fiber length of 20 to 50mm as discussed in section 2.3. Therefore, the sisal fiber was re-sized to a length of 25mm by using a ruler and scissors.

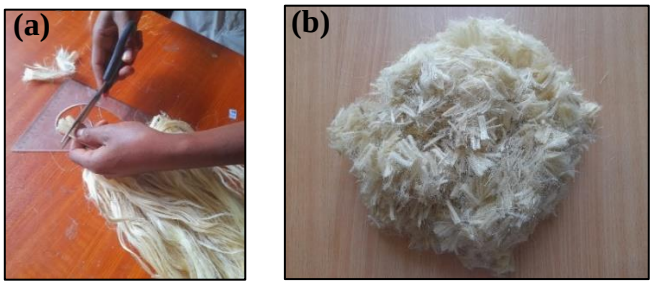

(a) Chopping sisal fiber (b) Chopped sisal fiber

Figure 3. 14 Chopping process

d) Mold preparation

The mold of rectangular shape was prepared from sheet metal material with the dimension of $(270 \times 180 \times 5)$mm.

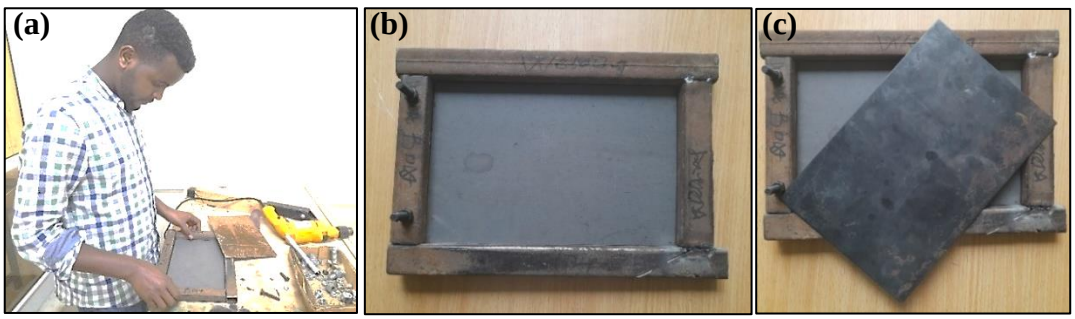

(a) Mold preparation in a shop (b) Prepared mold (c) Mold with top cover plate

Figure 3. 15 Mold for fabrication of the composite

e) Mass and volume fraction of the matrix and reinforcements of the composite

The volume fraction of each material can be calculated by using their weight fraction and density. This calculation was based on the formulation available in published papers (Sen et al., 2021). The basic formulas used to calculate the weight fraction were given in Eqs. 3.1 to 3.3.

$$Fiber\ weight\ fraction\ = \frac{\text{Fiber weight}}{Total\ Weight}, Wf_s = \frac{W_s}{W_t}, Wf_g = \frac{W_g}{W_t} \tag{3.1}$$

$$Filler\ weight\ fraction\ = \frac{\text{Filler weight}}{Total\ Weight},\ Wf_{sc} = \frac{W_{sc}}{W_t} \tag{3.2}$$

$$Matrix\ weight\ fraction\ = \frac{\text{Matrix weight}}{Total\ Weight}, Wf_m = \frac{W_m}{W_t} \tag{3.3}$$

$$W_t = W_c = W_s + W_g + W_{sc} + W_m \tag{3.4}$$

$$Wf_t = Wf_s + Wf_g + Wf_{sc} + Wf_m = 100\%\ or\ 1 \tag{3.5}$$

The volume and volume fraction of fibers, matrix, and their composite were given in Eqs. 3.6 to 3.10.

$$V_s = \frac{W_s}{\rho_s}, V_g = \frac{W_g}{\rho_g}, V_{sc} = \frac{W_{sc}}{\rho_{sc}}, V_m = \frac{W_m}{\rho_m} \tag{3.6}$$

$$V_t = V_c = V_s + V_g + V_{sc} + V_m \tag{3.7}$$

$$Fiber\ volume\ fraction\ = \frac{\text{Fiber volume}}{Total\ \text{volume}};\ Vf_s = \frac{V_s}{V_t}, Vf_g = \frac{V_g}{V_t} \tag{3.8}$$

$$Filler\ volume\ fraction\ = \frac{\text{Filler volume}}{Total\ \text{volume}}, Vf_{sc} = \frac{V_{sc}}{V_t} \tag{3.9}$$

$$Matrix\ volume\ fraction\ = \frac{\text{Matrix volume}}{Total\ \text{volume}}, Vf_m = \frac{V_m}{V_t} \tag{3.10}$$

$$Vf_s + Vf_m + Vf_g + Vf_{sc} = 1 \tag{3.11}$$

The density of the composite can be calculated as Eqs. (3.12) and (3.13), and the weight of the composite can be calculated as Eq. 3.14.

$$\rho_c = \frac{1}{V_s+V_g+V_{sc}+V_m}, \text{but } V = \frac{W}{\rho} \tag{3.12}$$

$$\rho_c = \frac{1}{\frac{W_s}{\rho_s} + \frac{W_g}{\rho_g} + \frac{W_{sc}}{\rho_{sc}} + \frac{W_m}{\rho_m}} \tag{3.13}$$

$$W_c = V_c \times \rho_c \tag{3.14}$$

The mass of the matrix, reinforcements, and composite laminate was calculated based on the formula provided in equations 3.15 and 3.16.

$$\text{Mass of compsite } (C_m) = C_\rho * C_v \quad (3.15)$$

Where $C_m, C_\rho, and\ C_v$- mass, density and volume of composite respectively

By considering the dimension of the mold $= 270, w = 180, and\ t = 5$) the volume of the composite can be calculated based on the volume of the mold as follows.

$$\text{The volume of mold } (M_v) = l \times w \times t \quad (3.16)$$

$$M_v = 270 \times 180 \times 5 \ = 243 cm^3$$

Where M_v - volume of mold, *w*- width, and *t*- thickness

The density value for each parameter was taken from published research work on the same area, especially for sisal fibers, from related work based in Ethiopia(Bekele et al., 2022) as well as based on the material specifications. These density values were given in Table 3.10.

Table 3. 10 Density of matrix and reinforcements

Materials list	**Density (g/cm^3)**
Unsaturated polyester resins	1.15
Sisal fiber (5% NaOH treated)	2.31
E-glass	2.55
SiC	3.22

For sample 1, by considering their weight percentage as described in Table 3.7.

Sisal fiber = 0 wt.% = 0.00, E-glass = 0 wt.% = 0, SiC = 5 wt.% = 0.05, and Polyester resin = 95 wt.% = 0.95.

From Eq. 3.13.

$\rho_c = \frac{1}{\frac{W_s}{\rho_s}+\frac{W_g}{\rho_g}+\frac{W_{sc}}{\rho_{sc}}+\frac{W_m}{\rho_m}} = \frac{1}{\frac{0}{2.31}+\frac{0}{2.55}+\frac{0.05}{3.22}+\frac{0.95}{1.15}} = \mathbf{1.19\ g/cm^3}$, and

From Eq. 3.16,

$V_c = 243$, $W_c = V_c \times \rho_c \ = 243 \times 1.19 \ = \mathbf{288.73\ g}$

Therefore, the calculated masses were;

Mass of sisal fiber $= 0$g,

Mass of E-glass = 0g,

Mass of SiC=$0.05 \times 288.73 \ = 14.44$g, and

Mass of polyester resin $= 0.95 \times 288.73 = \mathbf{274.29g.}$

Accordingly, the mass of reinforcements and matrix material in each of the rest eight samples (S_2, S_3, S_4, S_5, S_6, S_7, S_8, and S_9) were calculated and tabulated in Table 3.11.

Table 3. 11 Mass of reinforcements and matrix material

Samples	Composition (Wt.%)				Calculated mass (g)				
	Sisal fiber	E-glass	SiC	Polyester resin	Sisal fiber	E-glass	SiC	Polyester resin	Total
S_1	0	0	5	95	0	0	14.44	274.29	288.73
S_2	0	10	5	85	0	30.61	15.30	260.18	306.09
S_3	0	15	5	80	0	47.34	15.78	252.46	315.58
S_4	10	0	5	85	30.45	0	15.23	258.85	304.53
S_5	10	10	5	75	32.29	32.29	16.2	242.93	323.71
S_6	10	15	5	70	33.46	50.18	16.73	234.19	334.56
S_7	15	0	5	70	52.89	0	17.63	246.82	317.34
S_8	15	10	5	70	50.04	33.36	16.68	233.53	333.61
S_9	15	15	5	65	51.74	51.74	17.25	224.2	344.93

f) Hand layup

The hand lay-up method was used to fabricate nine laminates for composite testing and characterization.

Figure 3. 16 Hand layup process

g) Sample preparation process for composite material

The materials used to fabricate these laminates are listed in section 3.2. Initially, the releasing agent (petroleum jelly) was applied over the mold surface to facilitate the removal of laminates from the mold. Then SiC was mixed with polyester resin by using a mechanical stirrer and a uniform mixture was obtained. Next, the chopped fibers were mixed manually for the hybrid composite. The fibers were laid manually after a thin layer of resin mixed with SiC was applied to the mold. The roller was used to achieve a homogeneous structure and a c-clamp was applied to the entire setup to remove the air bubbles and for applying equal load. It was left for 24 hours to cure. The mixing ratio for each nine samples was tabulated

in Table 3.7, and the basic procedures used for sample preparation were shown in Figure 3.17.

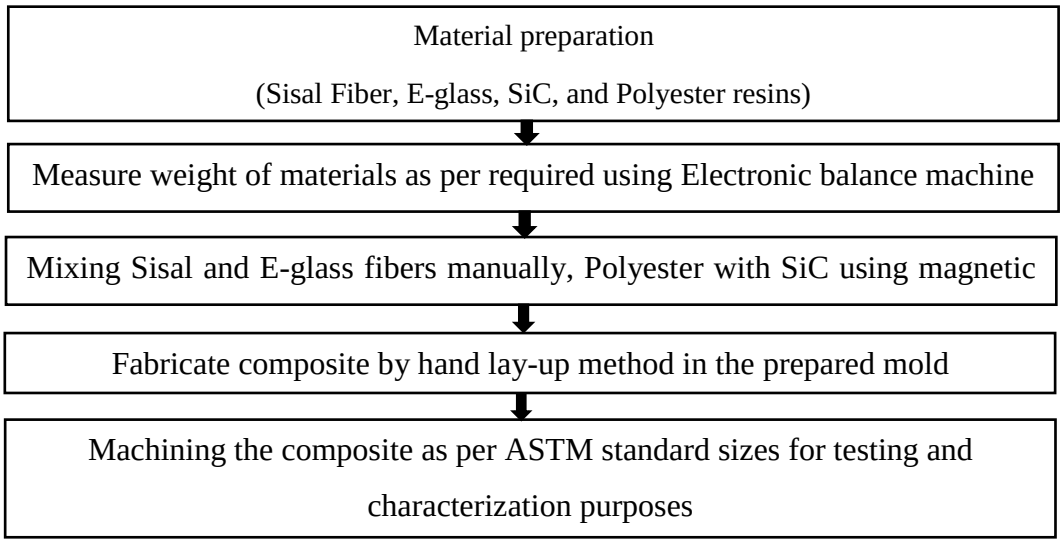

Figure 3. 17 General flow diagram of composite development

The general procedures utilized in the composite fabrication are shown in Figure 3.18.

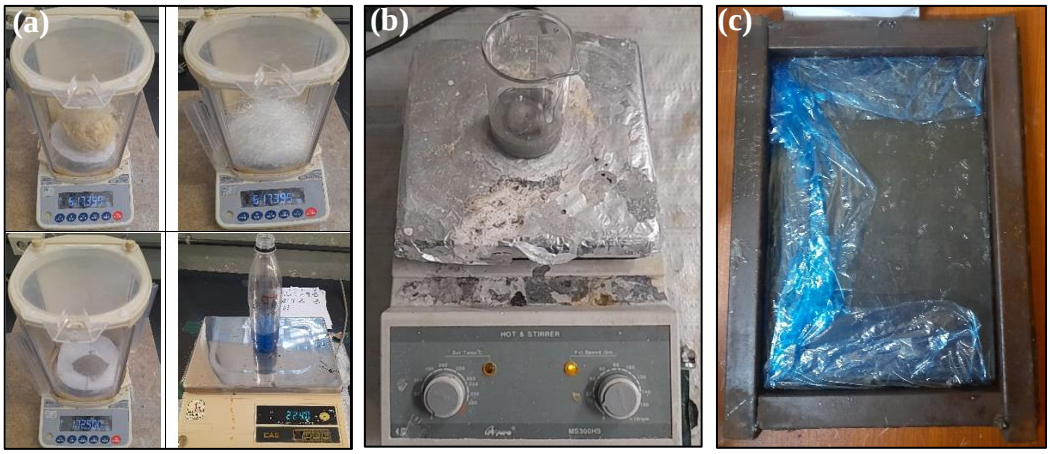

(a) Weight measuring (b) Mixing using stirrer (c) Preparing laminate in mold

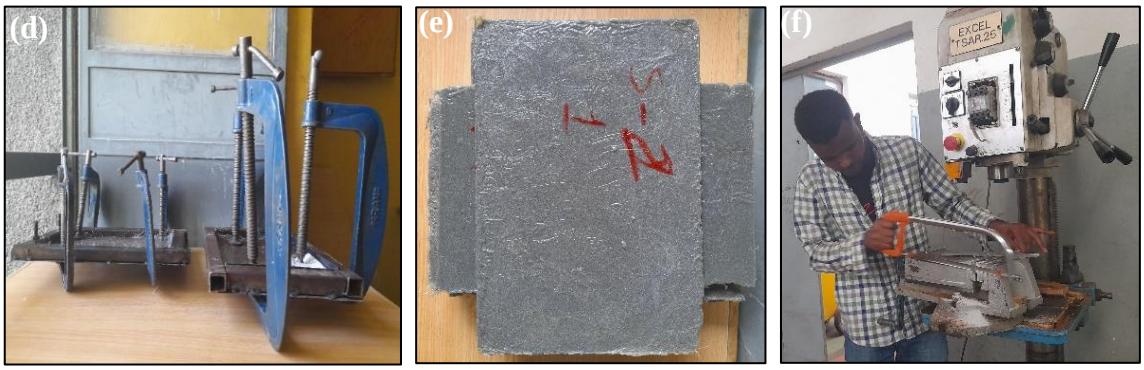

(d) Tightening using C-clamp (e) Laminates (f) Machining for tests

Figure 3. 18 Composite fabrication process

3.3.3 Testing and Characterization of the Composite

The testing and characterization of this composite material are crucial to assess its mechanical and physical properties as well as its overall performance and suitability for specific applications. These assessments involve a range of experimental techniques, including tensile testing, flexural testing, impact testing, Vickers hardness testing, and SEM analysis.

Figure 3. 19 Prepared specimens as per ASTM standards

3.3.3.1 Tensile strength testing

A tensile strength test is used to determine how much load a composite sample can withstand before it fractures. The test was performed by using a universal testing machine called INSTRO 5985 UTM with a capacity of 50KN that exists in Federal Engineering University College, bishoftu, Ethiopia. The tensile test specimen was prepared as per ASTM D3039 standard. In each case, three specimens were tested to determine the average result. a constant rectangular cross-section $(250 \times 25 \times 5)$ mm were used.

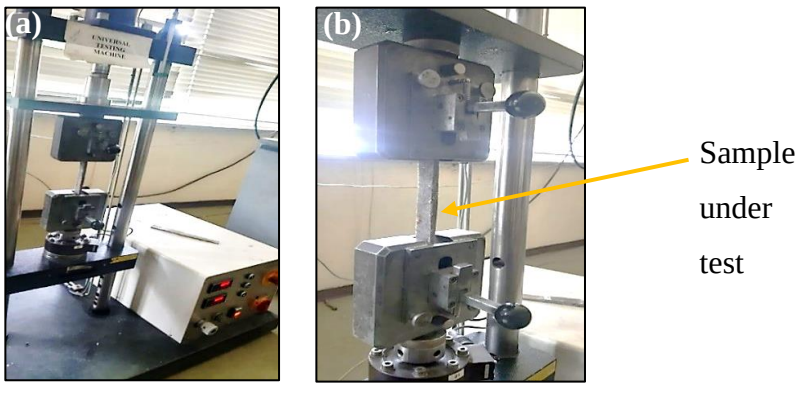

(a) Machine setup and (b) Sample adjusted

Figure 3. 20 Tensile strength testing

Test procedure- Specimens were inserted into a UTM's grips at a specified grip separation and pulled until they broke. The 2 mm/min standard test speed was taken in to account.

Finally, the tensile stress and elongation were measured using an extensometer. The samples before and after the test are shown in Figure 3.21.

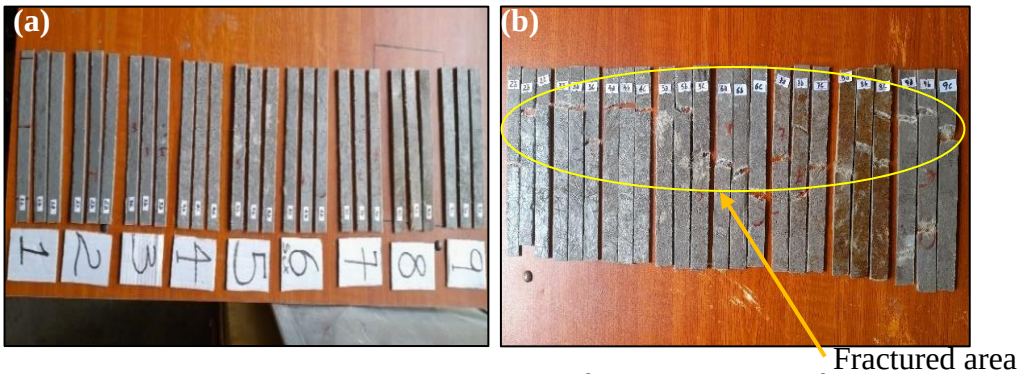

Figure 3. 21 Tensile strength test (a) Before test and (b) After test

3.3.3.2 Flexural strength testing

A flexural strength test was performed to identify how composite samples behave under transverse compressive load. The test was conducted by using a universal testing machine with a capacity of 50KN as per the ASTM-D790 standard. The specimen dimension is $(127 \times 13 \times 5)$ mm and the test speed was maintained between 0.5 and 1mm/min.

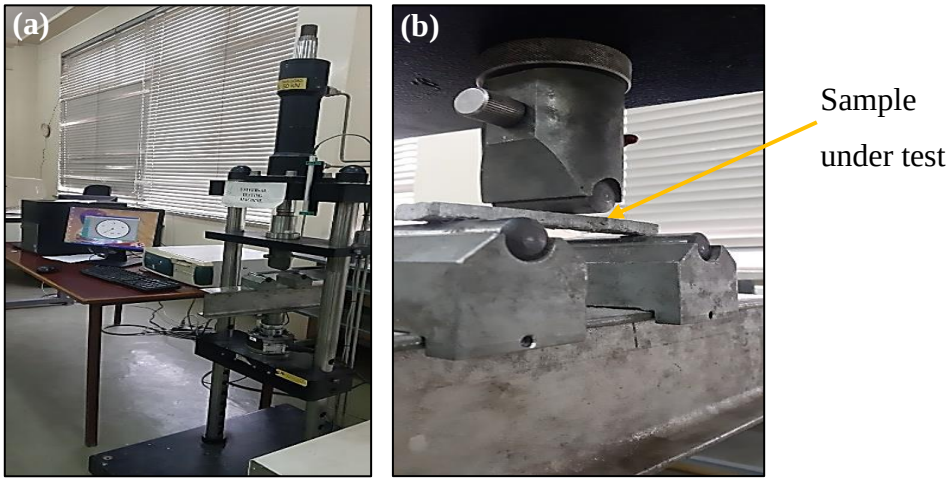

Figure 3. 22 Flexural strength testing: (a) Machine setup and (b) Sample adjustment

Test method: A bar of rectangular cross-section supported as a beam is deflected at a constant rate as shown in Figure 3.23. The bar rests on two supports and is loaded using a loading nose midway between the supports known as a three-point loading system. Where P is load.

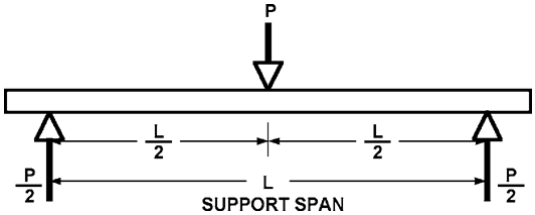

Figure 3. 23 A three-point loading system loading diagram

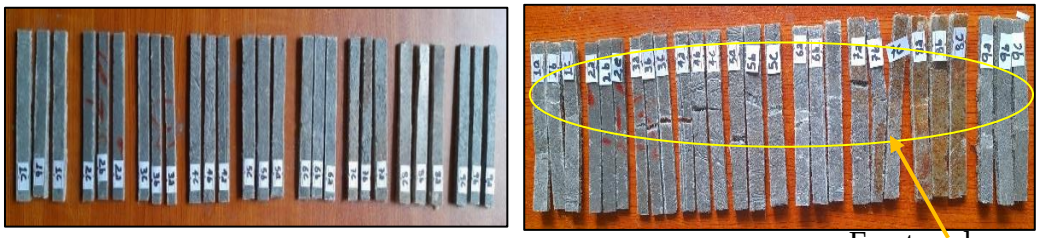

Figure 3. 24 Flexural strength test (a) Before test (b) After test

3.3.3.3 Impact Test

An impact test is a technique used to determine a material's ability to resist deformation when subjected to a sudden shock or impulse load. The Charpy impact test is a standardized impact test that determines the amount of energy absorbed by a material during fracture. It involves striking a notched test specimen with a pendulum hammer from the side. The test was conducted as per the ASTM D6110 standard, using a Charpy impact testing machine at Engineering Defense University College, Bishoftu, Ethiopia. The specimen dimension was given $(55 \times 12.7 \times 3.5)\ mm$ with a depth under the notch of $2.5\ mm$.

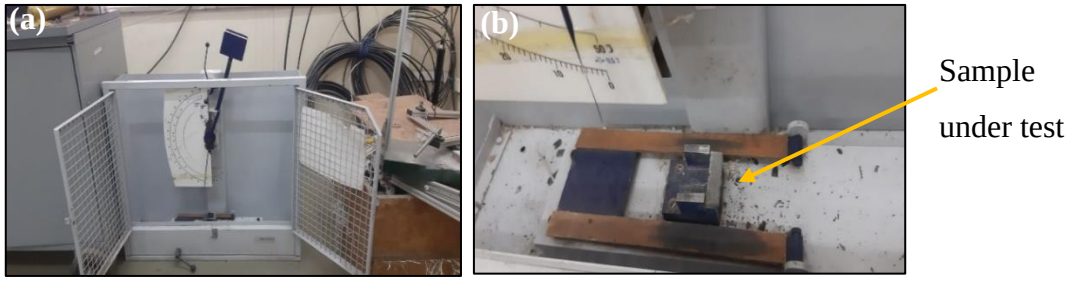

Figure 3. 25 Impact testing: (a) Machine setup and (b) Sample adjustment

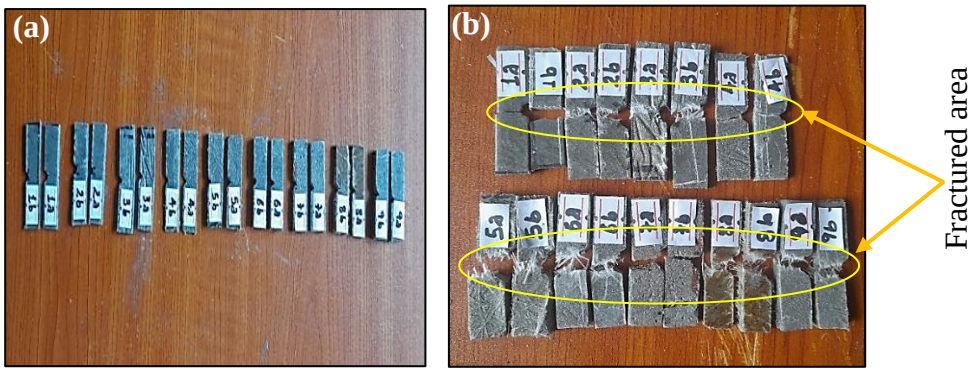

Figure 3. 26 Impact strength test (a) Before test and (b) After test

3.3.3.4 Vickers hardness testing

The Vickers hardness test is based on optical measurement. The ASTM E-384 standard was used with a specimen dimension of 20 x 20 x 5 mm, microhardness test procedures define various loads utilizing a diamond indenter to make an indentation that is measured and translated to a hardness value. The hardness of specimens was measured using a Vickers

hardness tester (HVS-50) with a load of 10 Kg and dwelling time of 10 seconds. Three measurements were taken for each sample and the average values were reported.

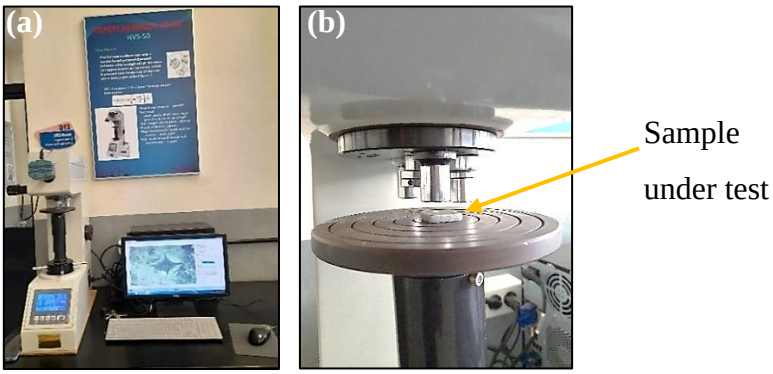

Figure 3. 27 Vickers hardness testing: (a) Machine setup and (b) Sample adjustment

The basic formula used to calculate the HV was given as follows.

HV = Test for surface indentation * hardness constant

$= 0.102* 2F (\sin 13602)d^2$

Where HV is the Vickers hardness value, F is load in kg, and d- Arithmetic mean of two diagonals, $(d_1+ d_2)^2$, d_1 and d_2 are in mm.

Figure 3. 28 Vickers hardness test samples

3.3.3.5 Morphological analysis

In the present study, the composite's morphology and topography were analysed using an SEM device. Five samples were selected for morphology analysis based on their mechanical property performances. An SEM known as JEOL7500 Field Emission Scanning Electron microscopy that was found in the biology department of ASTU was utilized for this purpose.

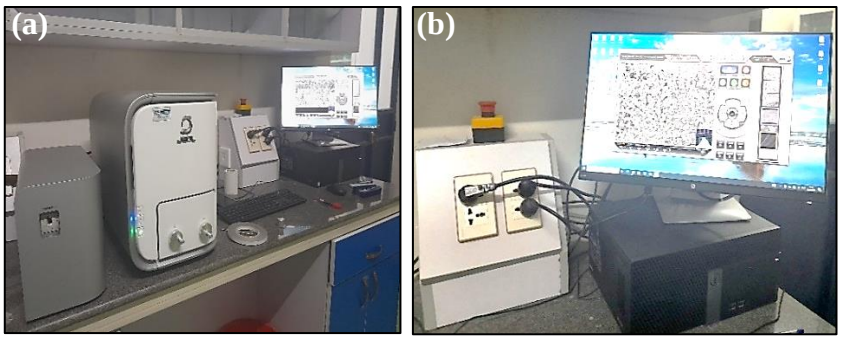

(a) Machine setup (b) Sample image

Figure 3. 29 SEM analysis

Figure 3. 30 Specimens for SEM analysis

3.3.4 Composite-Adhesive Joint Preparation

The specimens for testing and characterizing the adhesively joined composite were prepared according to the ASTM standards. Grinding with 200-grit sandpaper was used for surface preparation as discussed in section 2.9.2. Surface treatment was done for the specimens. The procedure of specimen preparation for adhesive joining tests was discussed in the section below and clearly shown in Figure 3.31.

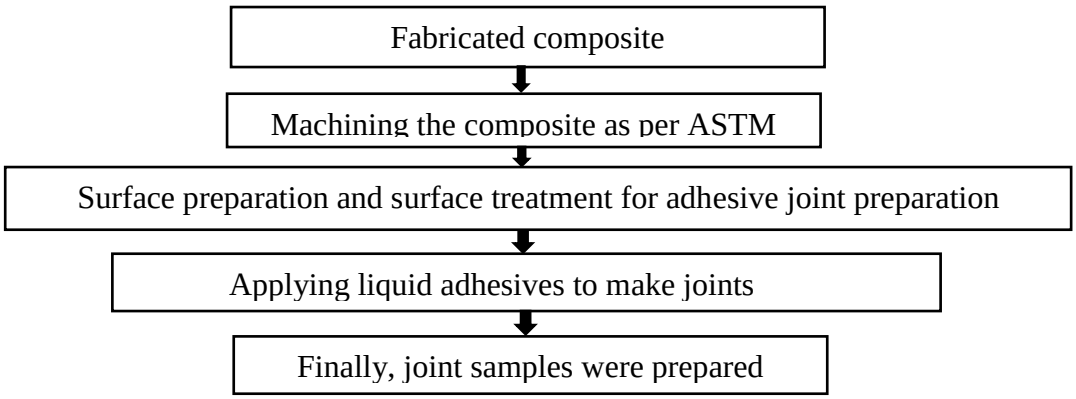

Figure 3. 31 Composite adhesive joint preparation

a) Machining composite samples for preparation of the specimens

The specimens were machined based on ASTM standards by jig saw into required samples with distinctive design configurations. Samples with a single lap joint, stepped lap joint, and scarf lap joint type of joint configurations were prepared.

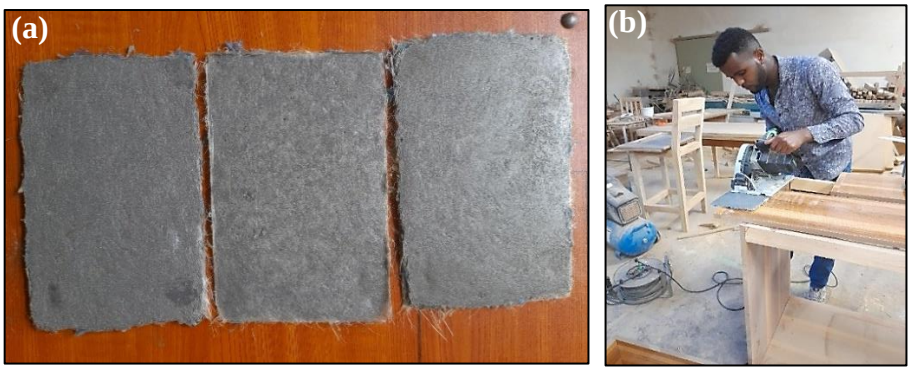

(a) Laminates (b) Machining

Figure 3. 32 Machining process

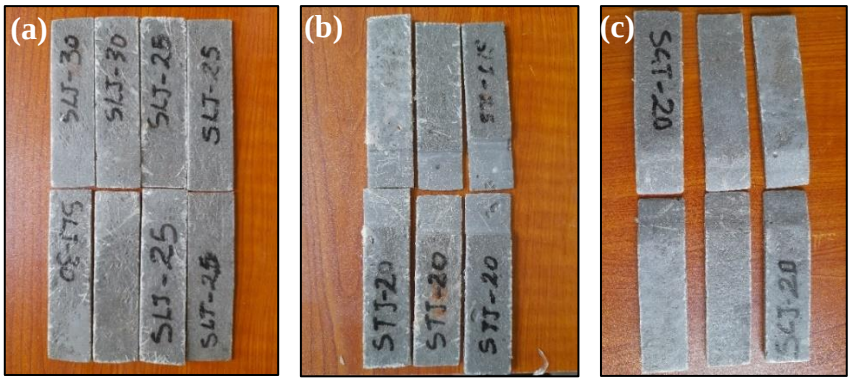

(a) Single lap (b) Stepped lap and (c) Scarf lap

Figure 3. 33 Sample preparation for joining

b) Surface treatment of adhesively bonded composite

Surface treatment is the process of removing contaminants, dust, and the release agent used during composite fabrication and it's the very critical process of preparing adhesive joints. In the present study, NaOH is used for surface treatment of the adhesively joined area of the composite. After machining the composite, surface treatment of the samples was done and then the samples were ready to be bonded by using adhesive materials. In this study, the following basic procedures were followed for surface treatment of the adhesive joints.

a. Cleaning: Contaminants such as dust, dirt, grease, or any others were removed by cleaning the surface using 5 % NaOH solvent.
b. Mechanical Abrasion: Abrading the surface helps to improve adhesion by creating a roughened texture for the adhesive to bond with. Sanding methods created a roughened surface profile that enhances mechanical interlocking between the adhesive and the composite material. The joined surfaces were abraded using 200-grit sandpaper.

Figure 3. 34 Abrading the joining surface area using sandpaper

c. Degreasing: After mechanical abrasion, it is essential to degrease the surface to remove any remaining contaminants. 5% NaOH solvent was used to ensure the surfaces were cleaned and free from contaminants that could interface with the bonding process.

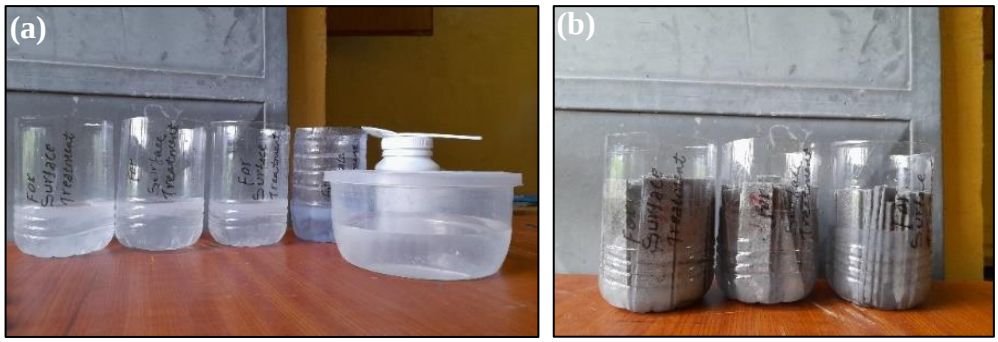

(a) Solution preparation and (b) Rinsing in the solution

Figure 3. 35 Surface treatment of the adhesive joining areas

c) Mixing liquids and preparing the samples

Once surface treatment was completed, the epoxy adhesive was mixed with nanoparticles SiC (20-30 nm diameter) using a magnetic stirrer, and later with the hardener thoroughly until uniform color could be achieved. The thickness of the adhesive in the joint was controlled to 0.95 mm. Sheet metal spacers were utilized to control the adhesive thickness added between adherends. Finally, the mixed resin and hardener were applied to the surface of the prepared samples. The specimens were allowed to be cured at room temperature for seven days.

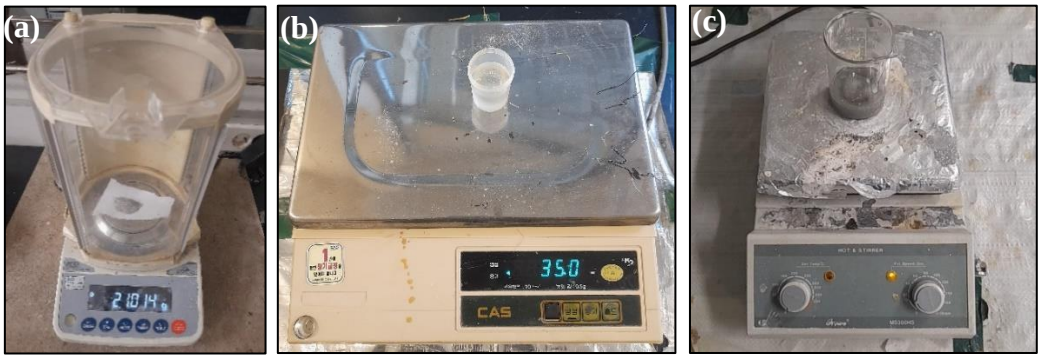

(a) Measuring SiC filler (b) Measuring adhesive material (c) Mixing filler with adhesive

(d) After mixing (e) Preparing the joints

Figure 3. 36 Specimens preparation process

3.3.5 Testing of the adhesively bonded composite

The joint strength testing of the adhesively joined composite was conducted after the identification/selection of composite materials with high mechanical properties. Mechanical properties such as joint tensile strength and joint flexural strength were conducted for the adhesively joined composite to analyze the joint strength of the composite. The adhesive layer thickness was adjusted by using sheet metal spacers. Therefore, this section presents joint strength testing of the adhesively joined composite.

3.3.5.1 Joint tensile strength testing adhesively bonded composite

To minimize the impacts of varying environmental conditions, all specimens were examined at room temperature (23C^{o}) and relative humidity of 50%. The ASTM-D5868 standard specifications were followed in the preparation of specimens and the geometrical details of the SLJ, SCJ, and STJ of the specimens as given in Table 3.12 and Figure 3.36. For each type of joint, three separate specimens were tested to ensure the repeatability of the findings. The specimens after being prepared by machining and machine setup for tensile strength testing are shown in Figures 3.37 and 3.38.

Table 3. 12 Summary of dimensional parameters (Brito et al., 2020)

S/N$_{o}$	Dimensional Parameters	Joint configurations		
		SLJ	SCJ	STJ
1	Thickness of Adherend (mm)	3	3.5	3
2	Adhesive thickness (mm)	0.95	0.95	0.95
3	Overlap length (mm)	20,25,30	20,25,30	20,25,30
4	Total length of specimen (mm)	170-180	170-180	170-180
5	Specimen width (mm)	25.4	25.4	25.4
6	Number of steps	-	-	1

(a) Single lap joint (SLJ)

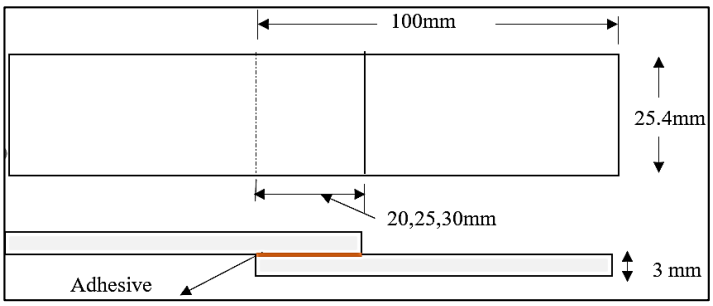

(b) Scarf lap joint (SLJ)

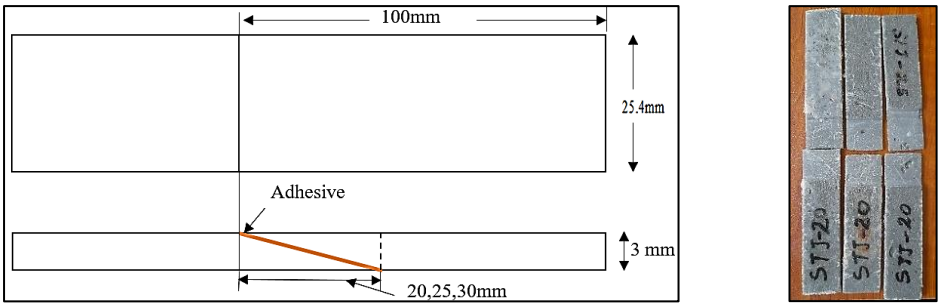

(c) Stepped lap joint (STJ)

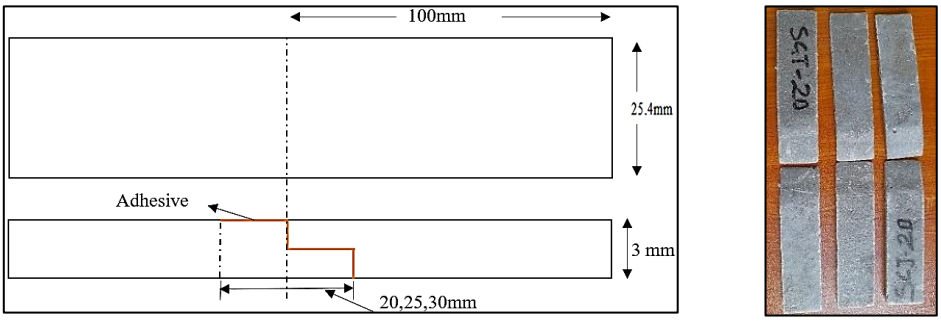

Figure 3. 37 Joint configurations; (a) SLJ, (b) SCJ, and (c) STJs respectively

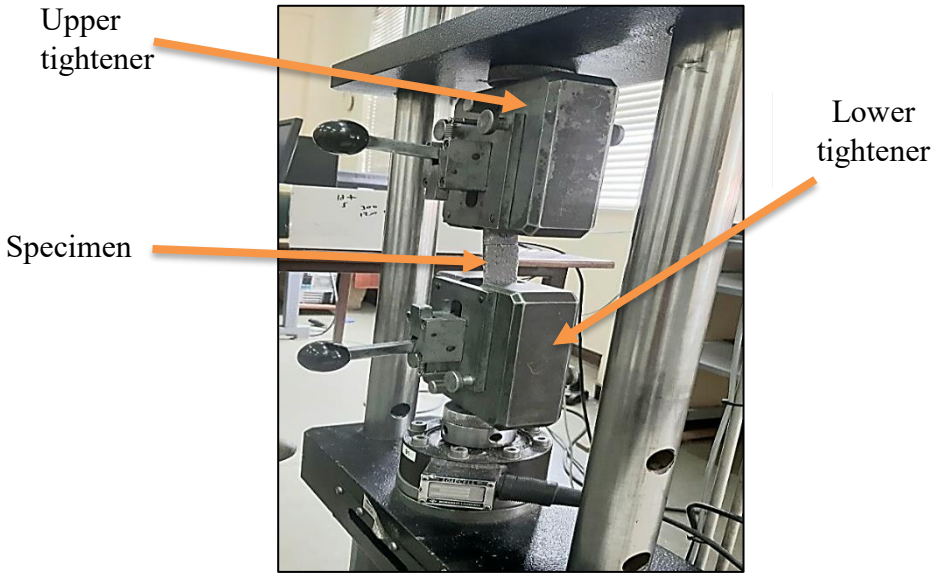

Figure 3. 38 Machine setup and specimen loading

(a) Samples before joining (b) Samples after joining

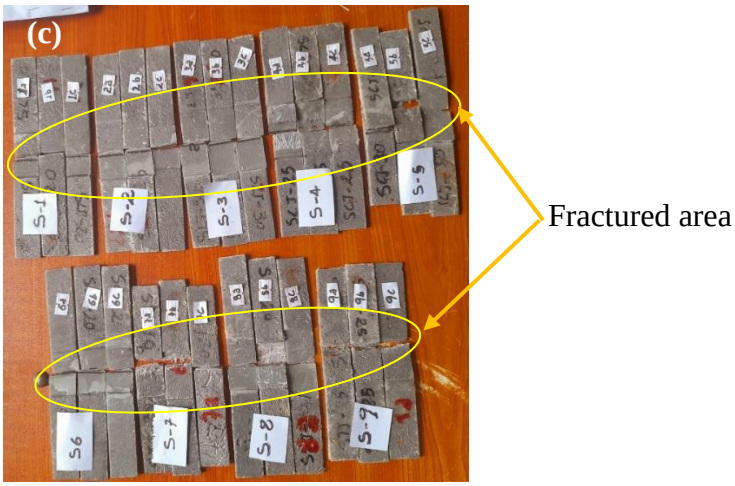

(c) After experimental testing

Figure 3. 39 Specimens for a tensile test

3.3.5.2 Joint flexural strength for adhesively bonded composite

The joining dimension parameters for joint flexural strength tests are similar to the dimensional parameters shown in Table 3.12 as per ASTM standards. The samples before and after tests are shown in Figure 3.40.

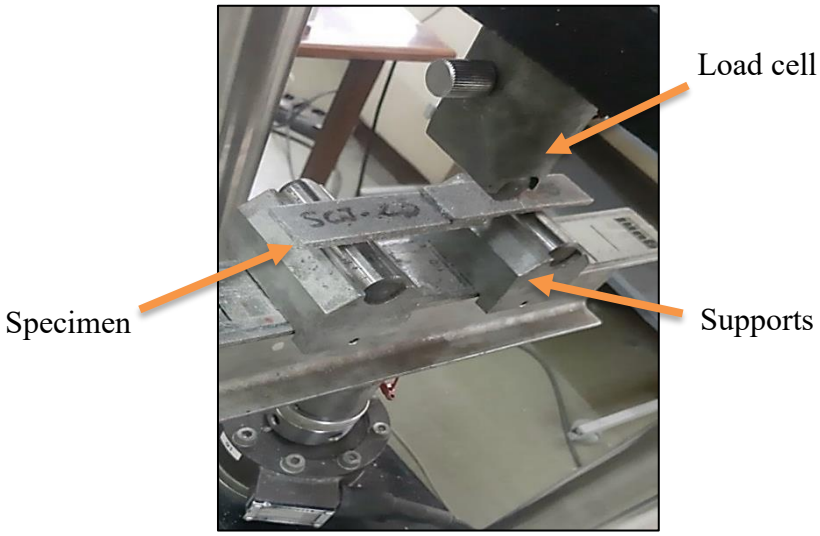

Figure 3. 40 Machine setup and specimen loading

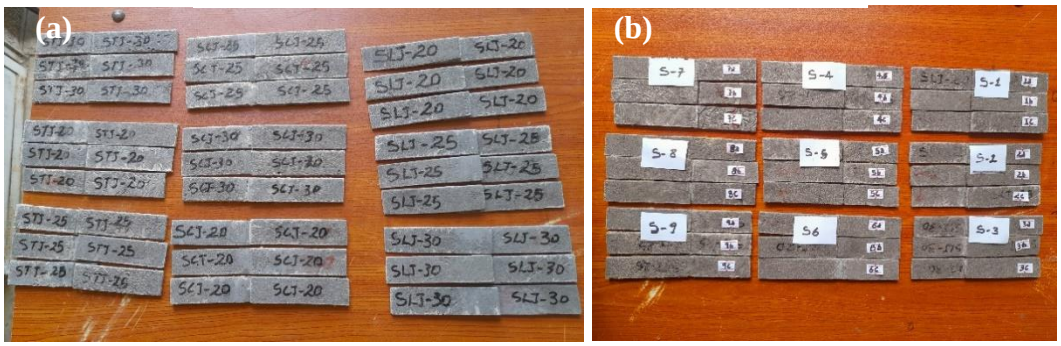

(a) Samples before joining (b) Samples after joining

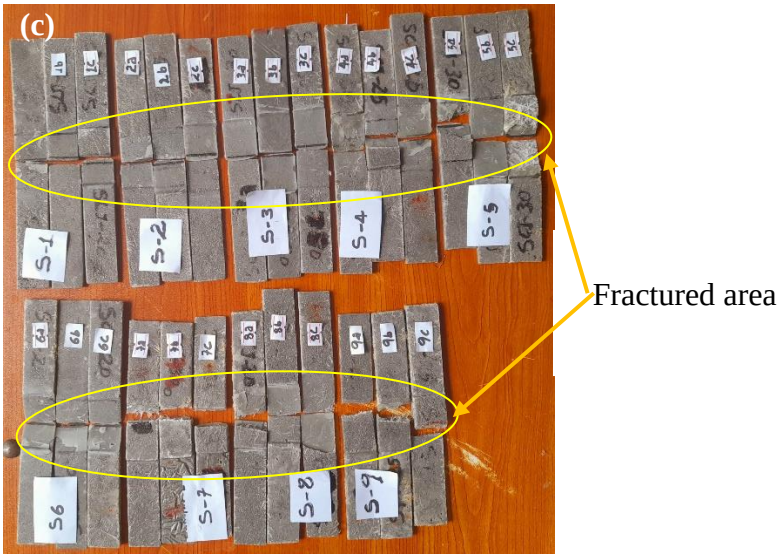

(c) After experimental testing

Figure 3. 41 Specimens for joint flexural test

3.3.6 Taguchi based-grey relational analysis

In this section, the weight percentage of fibers in composite fabrication, and the adhesive joining parameters, such as overlap length, filler wt.%, and joint configuration, were optimized for the proper and efficient adhesive joining of the composite material under the study. Taguchi-based GRA was implemented for this purpose. In grey relational optimization, data pre-processing is necessary because different data sets may have different ranges and units. For this reason, the results of various mechanical properties are normalized in the range between 0 and 1 during GRA as given by Eq.3.19, and 3.20. To conduct the grey relational analysis, the following simple steps were followed.

1. S/N was calculated by using Minitab 20 software based on Eqs. (3.17) and (3.18)

For larger the better

$$\frac{S}{N}\text{ ratio} = -10\ (\log \frac{1}{n}) + (\frac{1}{Y_{ij}^2}) \tag{3.17}$$

For smaller the better

$$\frac{S}{N}\text{ ratio} = -10\ (\log \frac{1}{n}) + (\ Y_{ij}^2\ ) \tag{3.18}$$

Where, n number of replication for each experiment and, Y_{ij}^2 response values

2. Normalization of the S/N ratio

For larger the better

$$\text{Xij} = \frac{(Yij - \min(Yij))}{(\max(Yij) - \min(Yij))} \tag{3.19}$$

For smaller the better

$$Xij = \frac{(\max(Yij) - Yij))}{(\max(Yij) - \min(Yij))} \quad (3.20)$$

Where Xij Normalized S/N ratio and Yij S/N ratio obtained from Taguchi

3. Calculation of the deviation sequence and quality loss

$$\Delta = 1 - Xij \quad (3.21)$$

Where 1 is the highest value of quality loss and Δ is quality loss

4. Determination of the grey relation coefficient (GRC) calculated from the normalized data obtained from Eq belows.

The distinguishing coefficient lies between 0 and 1, most of the researchers consider the distinguishing coefficient value for GRA as 0.5, to weaken the influence if the deviation sequence Delta max gets too big. Therefore, in this research, the coefficient is taken as 0.5.

$$GCij = \frac{\delta \min + \varphi\ \delta max}{\delta ij + \varphi\ \delta max} \quad (3.22)$$

Where φ is distinguishing coefficient

5. Determination of grey relational grade (GRG) is by utilizing Eq 3.23.

$$Gi = (\frac{1}{m}) \sum GCij \quad (3.23)$$

Where m is the number of process responses. In this work, tensile, flexural, impact, and hardness strengths are the four responses. Therefore m is $1/4$ which is 0.25.

The GRG is used to average the GRC associated with every performance characteristic. It is used as the basis for evaluating the multiple performance characteristics. The level of the input parameter with the highest GRG is the optimum level. Furthermore, a statistical ANOVA is conducted to determine the statistical significance of the process parameters.

CHAPTER-4

RESULTS AND DISCUSSION

4.1 Introduction

This chapter discusses the results obtained for all experimental tests and the findings of each specific objective of this research work. These were shown for both the developed composite material and the composite adhesive joining. Tensile testing, flexural testing, impact testing, hardness testing, and SEM analysis were utilized to assess the composite material's properties and performance. GRA was performed to convert all mechanical properties into single results, optimizing the fiber wt.% sisal fiber, and E-glass. The joining parameters such as joint configuration, filler wt.%, and overlap lengths were analyzed to assess the strength of adhesive joined composite, focusing on the joint tensile and flexural strengths for joint quality. Finally, the maximum experimental results obtained in this research were compared to the related literature to determine the significance of the findings.

4.2 Testing and Characterization for Composite

The composite materials' tensile, flexural, impact, and hardness strengths were analyzed in the following sub-sections.

4.2.1 Analysis of Tensile Strength

The experimental results obtained for each sample are given in Table 4.1, and the average tensile strength values for each sample were calculated from the trial values.

Table 4. 1 Experimental results for tensile testing of composite

Samples	S-1	S-2	S-3	S-4	S-5	S-6	S-7	S-8	S-9
Sisal fiber (wt.%.)	0	0	0	10	10	10	15	15	15
E-glass (wt.%.)	0	10	15	0	10	15	0	10	15
SiC (wt.%.)	5	5	5	5	5	5	5	5	5
Tensile strength(MPa)	10.06	27.61	33.11	22.67	36.43	41.74	25.46	37.11	42.13

Figure 4.1 shows the tensile strength results of nine samples. The highest strength of 42.13 MPa was achieved for sample number nine. This was developed from 15 wt.% of sisal fiber and glass fiber with 5 wt.% of SiC. Samples 6, 5, 8, 3, 2, 7, and 4 were the listed samples in

descending order of their impact strength results, resulting from the variations of wt.% of sisal fiber, and E-glass, SiC, and their hybridization effects. This maximum strength was achieved due to the maximum weight percentage of fibers (E-glass fiber with sisal fiber) and the filler SiC. The strength of composite samples was different due to different wt.% of the materials used. The lowest strength was achieved for sample one (10.06 MPa) due to the non-availability of fibers in the polyester resin. This sample was developed from 5 wt.% of SiC and 95 wt.% of polyester resin matrix.

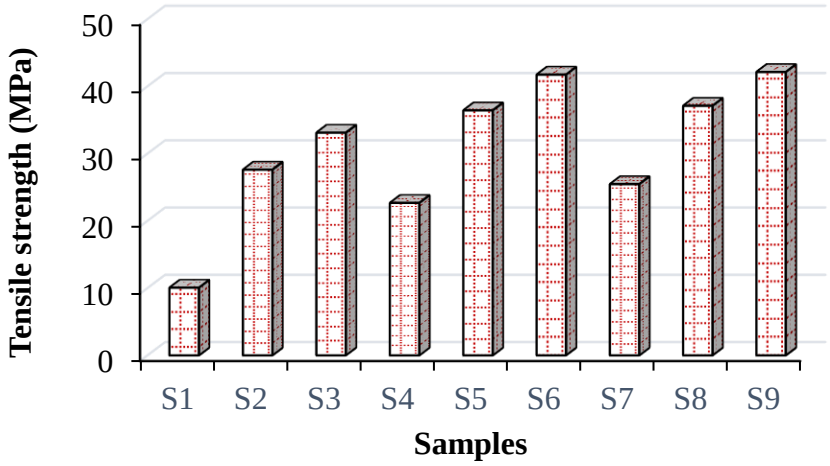

Figure 4. 1 Tensile strength experimental test results

Based on the results of Figure 4.1, the composite strength is affected by fiber materials wt.% and filler material used. Research by (Hapuhinna & Gunaratne, 2022) demonstrated that an escalation in E-glass fiber weight percentage enhanced the tensile strength of the polyester-based composite. In this investigation as the weight percentage of E-glass fiber increases in the matrix and SiC filler, the strength of the composite also increases. Research on sisal fiber-reinforced composites (Sahu et al., 2021) demonstrates that parameters including tensile strength improve up to a maximum point with increased fiber content, and in the present study, tensile strength was high with 15 wt.% of sisal fiber. The addition of SiC filler has a positive effect on the strength of the hybrid composite. The hybridization process has improved the tensile strength of the composite and therefore, the tensile strength of samples 5,6, 8, and 9 are high. A balancing effect was achieved by hybridizing natural and synthetic fibers within the polyester resin matrix. This kind of investigation was also reported by (Gangil et al., 2020).

Figure 4.2 shows the stress vs elongation (%) diagram, the elongation of sample 1 was low as compared to other samples due to its material composition.

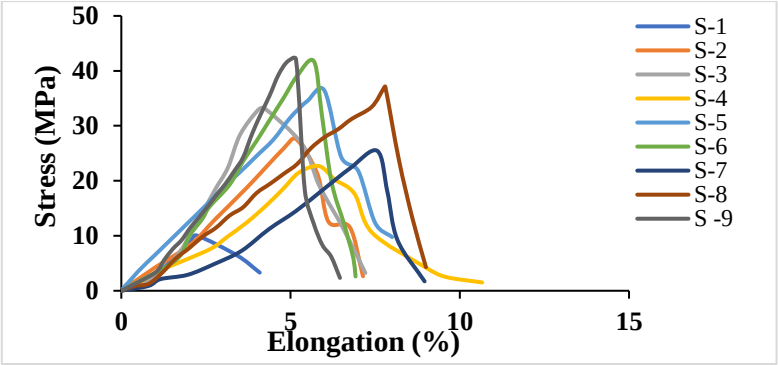

Figure 4. 2 Stress– elongation diagram

A sample with maximum tensile strength has shown minimum elongation compared to others. The elongation % Samples nine and six were 5.69 and 5.11% respectively. The maximum elongation of 7.8 % was recorded for sample 8.

4.2.2 Analysis of flexural strength

The experimental results of flexural strength obtained for each sample are given in Table 4.2, and the average flexural strength values for each sample were calculated from the trial values.

Table 4. 2 Experimental results for flexural testing of composite

Samples	**S-1**	**S-2**	**S-3**	**S-4**	**S-5**	**S-6**	**S-7**	**S-8**	**S-9**
Sisal fiber (wt.%.)	0	0	0	10	10	10	15	15	15
E-glass (wt.%.)	0	10	15	0	10	15	0	10	15
SiC (wt.%.)	5	5	5	5	5	5	5	5	5
Flexural strength (MPa)	25.40	76.20	97.30	68.87	163.81	185.56	91.83	119.19	158.26

Table 4.2 shows the flexural strength results of nine samples. The obtained flexural testing results for sample 1 of combosition (0 wt.% of sisal and E-glass, 5 wt.% of SiC, and 95 wt.% of polyester resin) was 25.40 MPa, sample 2 of combosition (0 wt.% of sisal, 10 wt.% E-glass, 5 wt.% of SiC, and 85 wt.% of polyester resin) was 76.20 MPa, sample 3 of combosition (0 wt.% of sisal, 15 wt.% E-glass, 5 wt.% of SiC, and 80 wt.% of polyester resin) was 97.30MPa, sample 4 of combosition (10 wt.% of sisal, 0 wt.% E-glass, 5 wt.% of SiC, and 85 wt.% of polyester resin) was 68.87MPa, sample 5 of combosition (10 wt.% of sisal, 10 wt.% E-glass, 5 wt.% of SiC, and 75 wt.% of polyester resin) was 163.81 MPa,

sample 6 of combosition (10 wt.% of sisal, 15 wt.% E-glass, 5 wt.% of SiC, and 70 wt.% of polyester resin) was 185.56 MPa, sample 7 of combosition (15 wt.% of sisal, 0 wt.% E-glass, 5 wt.% of SiC, and 80 wt.% of polyester resin) was 91.83 MPa, sample 8 of combosition (15 wt.% of sisal, 10 wt.% E-glass, 5 wt.% of SiC, and 70 wt.% of polyester resin) was 119.19MPa, and sample 9 of combosition (15 wt.% of sisal, 15 wt.% E-glass, 5 wt.% of SiC, and 65 wt.% of polyester resin) was 158.26 MPa.

The highest strength of 185.56 MPa was achieved for sample number six. This maximum strength was achieved due to the maximum concentration of E-glass fiber, medium wt.% of the sisal fiber, and the filler SiC. The lowest strength was achieved for sample one (25.40 MPa) due to the non-availability of fibers in the polyester resin.

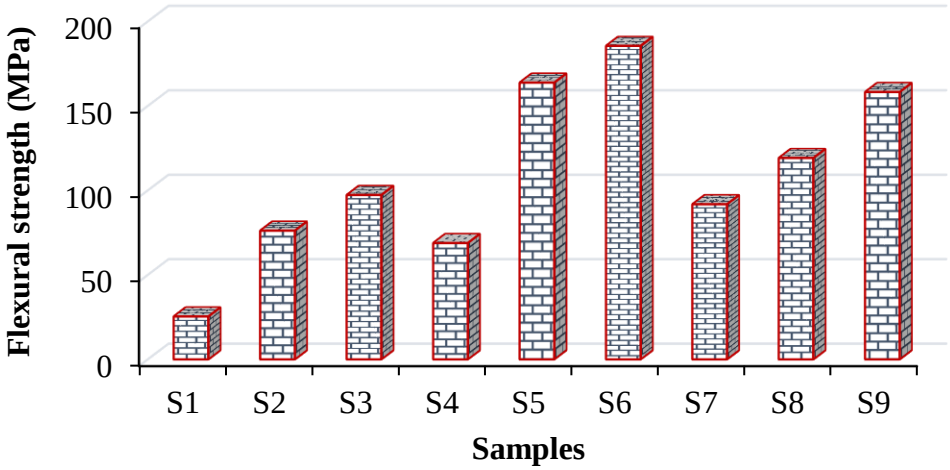

Figure 4. 3 Flexural strength experimental test results

The results of Figure 4.3 indicate that the composite strength was affected by the fiber materials weight percentage and filler material used. The material strength of samples 1, 2, and 3 increases uniformly due to the increases in E-glass fiber wt.%, while it was highly increased for samples 5, 6, 8, and 9 due to the use of sisal fiber and E-glass fiber materials with each other. (Athith et al., 2021) investigated that, the incorporation of SiC filler modifies the flexural strength of composite. The addition of sisal fiber in the polyester resin matrix and with SiC filler increases the flexural strength of the composite as it was observed from the results of samples 4, and 7 as well as the addition of E-glass fiber in samples 2, and 3. Based on the obtained results, the strengths of samples 5, 6, 8, and 9 have been improved by the hybridization of natural and synthetic fibers within the polyester resin matrix. This kind of investigation was reported by (Mohamad et al., 2023). According to (Hatti et al., 2022) the value of flexural strength rises with the addition of E-glass fiber, and the flexural strength results shown in Figure 4.3 depict the same observation.

4.2.3 Impact test analysis

The experimental results obtained for each sample are given in Table 4.3, and the average impact strength values for each sample were calculated from the trial values.

Table 4. 3 Experimental results for impact test analysis of composite

Samples	**S-1**	**S-2**	**S-3**	**S-4**	**S-5**	**S-6**	**S-7**	**S-8**	**S-9**
Sisal fiber (wt.%.)	0	0	0	10	10	10	15	15	15
E-glass (wt.%.)	0	10	15	0	10	15	0	10	15
SiC (wt.%.)	5	5	5	5	5	5	5	5	5
Impact energy(J)	4.5	6.5	10.25	9.5	11.5	13.5	17	21	24.75

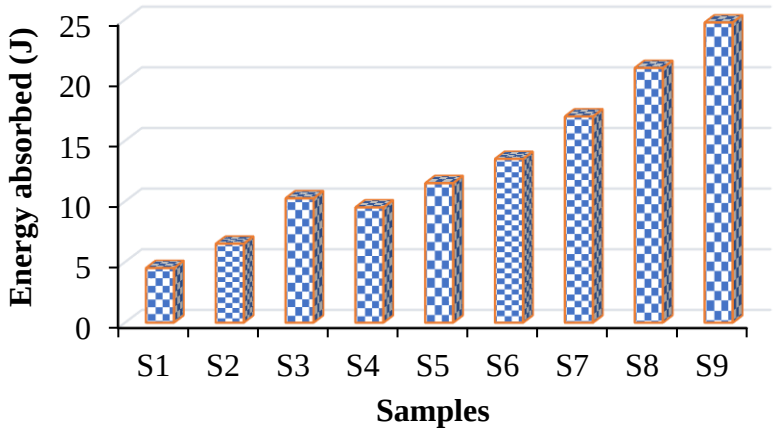

Figure 4. 4 Impact strength experimental test results

Figure 4.4 shows the impact strength plots of nine samples. The obtained impact testing results for sample 1 of combosition (0 wt.% of sisal and E-glass, 5 wt.% of SiC, and 95 wt.% of polyester resin) was 4.5 J, sample 2 of combosition (0 wt.% of sisal, 10 wt.% E-glass, 5 wt.% of SiC, and 85 wt.% of polyester resin) was 6.5 J, sample 3 of combosition (0 wt.% of sisal, 15 wt.% E-glass, 5 wt.% of SiC, and 80 wt.% of polyester resin) was 10.25 J, sample 4 of combosition (10 wt.% of sisal, 0 wt.% E-glass, 5 wt.% of SiC, and 85 wt.% of polyester resin) was 9.5J, sample 5 of combosition (10 wt.% of sisal, 10 wt.% E-glass, 5 wt.% of SiC, and 75 wt.% of polyester resin) was 11.5J, sample 6 of combosition (10 wt.% of sisal, 15 wt.% E-glass, 5 wt.% of SiC, and 70 wt.% of polyester resin) was 13.5J, sample 7 of combosition (15 wt.% of sisal, 0 wt.% E-glass, 5 wt.% of SiC, and 80 wt.% of polyester

resin) was 17J, sample 8 of combosition (15 wt.% of sisal, 10 wt.% E-glass, 5 wt.% of SiC, and 70 wt.% of polyester resin) was 21J, and sample 9 of combosition (15 wt.% of sisal, 15 wt.% E-glass, 5 wt.% of SiC, and 65 wt.% of polyester resin) was 24.74.

The highest impact of 24.75 J was achieved for sample number nine. This sample was developed from 15 wt.% of sisal fiber, 15 wt.% glass fiber, and 5 wt.% of SiC. This maximum strength was achieved due to the maximum concentration of E-glass fiber, maximum wt.% of the sisal fiber, and the filler used. Samples 8, 7, 6, 5, 3, 4, 3, and 2 were the listed samples in descending order of their impact strength results that resulted from the variations of wt.% of sisal fiber, and E-glass, SiC and their hybridization effects. The lowest energy was achieved for sample one (4.5 J) due to the non-availability of fibers in the polyester resin. The impact energy of the composite is increased by adding Sisal fiber to the polyester resin matrix together with SiC filler, as seen by the results of samples 4 and 7. In a similar vein, adding of E-glass resulted in samples 2 and 3. However, the effect of E-glass fiber was maximum. Similar results were investigated by (Palanikumar et al., 2016). The impact strength of the hybrid composite was increased as it can be observed in samples 5, 6, 8, and 9. This is due to the incorporation of both sisal and E-glass fiber and SiC filler into the polyester matrix, (Begum et al., 2020; Gangil et al., 2020) reported the same outcomes.

4.2.4 Analysis of Vickery hardness test

The experimental results obtained for each sample are given in Table 4.4, and the average Vickers hardness values for each sample were calculated from the trial values.

Table 4. 4 Experimental results for Vickers hardness testing of composite

Samples	**S-1**	**S-2**	**S-3**	**S-4**	**S-5**	**S-6**	**S-7**	**S-8**	**S-9**
Sisal fiber (wt.%.)	0	0	0	10	10	10	15	15	15
E-glass (wt.%.)	0	10	15	0	10	15	0	10	15
SiC (wt.%.)	5	5	5	5	5	5	5	5	5
Vickers hardness (HV)	58.3	69.83	73.47	78.93	81.17	91.03	87.7	89.9	97.93

Figure 4.5 shows the Vickers hardness results of nine samples. The Vickers hardness of 97.93 HV was achieved for sample number nine. This sample was developed from 15 wt.% of sisal fiber and glass fiber with 5 wt.% of SiC. Samples 6, 8, 7, 5, 4, 3, and 2 were the leading composites based on their strength due to the variations of wt.% of sisal fiber and E-glass. This maximum Vickers hardness value was achieved due to the maximum wt.% of

sisal fiber as it increases the surface roughness and interfacial bonding with the polyester matrix. The lowest strength was achieved for sample one (58.3 HV) due to the non-availability of fibers in the polyester resin. This sample was developed from 5 wt.% of SiC and 95 wt.% of polyester resin matrix.

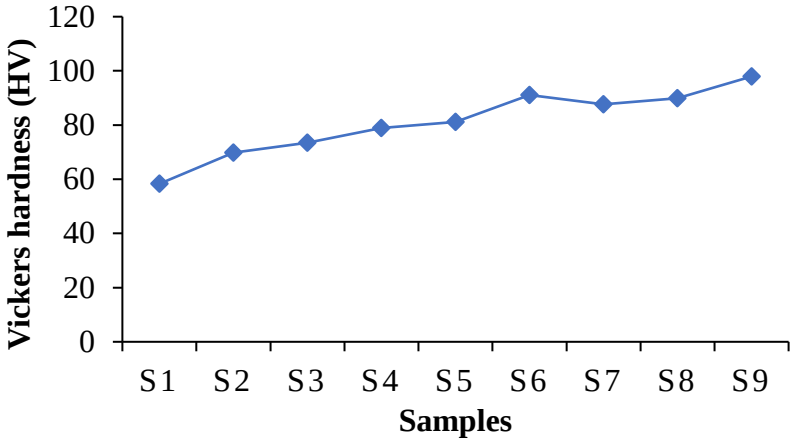

Figure 4. 5 Vickers hardness experimental test results

The results of Figure 4.5 further indicate that the hardness of the composite is influenced by the weight percentage of the fiber materials and the filler material used. The strength of samples 1, 2, and 3 shows a uniform increase as the weight percentage of E-glass fiber increases, while it significantly increases from sample 4 to sample 9 due to the incorporation of sisal fiber. Samples 5, 6, 8, and 9 exhibit the highest Vickers hardness values compared to the other samples, attributed to the combined effects of sisal fiber and E-glass fiber. However, the hardness is slightly lower for samples 1, 2, 3, 4, and 7 due to the utilized fiber types. Similar results were reported by (Rasu & Veerabathiran, 2023). Incorporation of the SiC filler into a polymer-based composite increases the hardness, contributing to improved Vickers hardness values(Praveenkumara et al., 2022), similarly, the obtained hardness values were enhanced.

4.3 Optimization of process parameters for mechanical properties

In this sub-section, the weight percentages of fibers were considered and optimized for obtaining the optimal parameters that highly influenced the mechanical properties such as tensile, flexural, impact, and hardness strengths of the composite.

4.3.1 Optimization of process parameters for tensile strength

The weight percentages of fibers were optimized for tensile strength by employing the experimental results to identify the optimal parameter combinations that maximize tensile strength.

4.3.1.1 Taguchi analysis using signal-to-noise ratio for tensile strength

The weight percentage of Sisal fiber and E-glass fibers are the parameters required to be optimized by considering the weight percentage of SiC filler as a constant variable. The tensile strength was measured by conducting the experiments according to the designed experimental matrix for each combination of factors. The SNR values were calculated based on the measured tensile strength data considering the nature of optimization larger-the-better. These experimental results and SNR values are given in Table 4.5. The S/N ratio was calculated using Eq. 3.17 in Minitab 20 software.

Table 4. 5 The result of tensile strength and S/N of the experimental result

Specimens	**Sisal fiber wt.%**	**Glass fiber wt.%**	**Tensile strength (MPa)**	**S/N ratio (dB)**
S1	0	0	10.06	20.0520
S2	0	10	27.61	28.8213
S3	0	15	33.11	30.3992
S4	10	0	22.67	27.1090
S5	10	10	36.43	31.2292
S6	10	15	41.74	32.4110
S7	15	0	25.46	28.1172
S8	15	10	37.11	31.3898
S9	15	15	42.13	32.4918

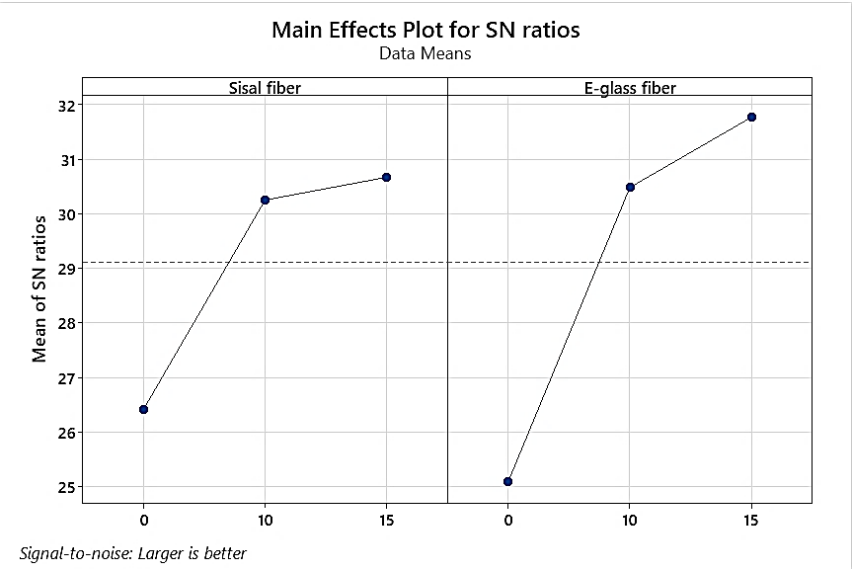

Figure 4. 6 The main effect plot for the SN ratio of tensile strength

The optimal combination of process parameters was obtained by analyzing the SNR results. Figure 4.6 shows the main effect plot for the SNR of tensile strength and the optimal parameter combinations for the increased tensile strength were observed. The optimum parameter combination for SNR was achieved at 15 wt.%. of E-glass fiber and 15 wt.%. of sisal fiber at level 3. Therefore, the optimum parameter combination for tensile strength was A3B3.

Table 4. 6 Tensile strength response table for S/N ratios (Larger is better)

Level	**Sisal fiber**	**Glass fiber**
1	26.42	25.09
2	30.25	30.48
3	30.67	31.77
Delta	4.24	6.67
Rank	2	1

Table 4.6 shows the response table for SNR of the tensile strength. From this table, E-glass fiber was the first contributor to the maximum tensile strength of the composite with a 6.67 delta number while Sisal fiber was second-ranked with a delta number of 4.24.

4.3.1.2 Analysis of variance for tensile strength of the composite

The optimum parameter combination for SNR of tensile strength was A3B3. The optimum values for maximum tensile strength were the sisal fiber of 15 wt.% and E-glass fiber of 15 wt.%. in level 3.

Table 4. 7 Analysis of variance results of the tensile strength

Source	**DOF**	**Seq SS**	**Adj SS**	**Adj MS**	**F-value**	**P-value**	**Contribution %**
Sisal fiber	2	32.80	32.80	16.402	5.14	0.039	27.15
E-glass fiber	2	75.23	75.23	37.616	11.78	0.021	62.27
Residual Error	4	12.77	12.77	3.192	-	-	10.57
Total	8	120.81			-	-	100
S = 1.7867, R-Sq = 89.43%, R-Sq(adj) = 78.86%							

From Table 4.7, E-glass fiber contributed 62.2713 % which was the maximum contribution, and the contribution percentage of sisal fiber was 27.1501%. The higher contribution percentage means more effect of that parameter on the output result. Therefore, E-glass fiber has more effects on the tensile strength of the composite. The predicted tensile strength tested under the optimum value is 43.19. The actual value was obtained from the experimental result of the tensile strength, which was 42.13 MPa.

Table 4. 8 Calculation of the percentage error value for tensile strength

Optimum parameter		**Tensile strength actual**	**Tensile strength predicted**	**Error %**
Sisal fiber	15 wt.%	42.13	43.19	2.52
E-glass fiber	15 wt.%			

The obtained percentage error was less than 5% which is acceptable.

4.3.2 Optimization of process parameters for flexural strength

The weight percentage of Sisal fiber and E-glass fibers are the parameters required to be optimized by considering the weight percentage of SiC filler as a constant variable.

4.3.2.1 Taguchi analysis using signal-to-noise ratio for flexural strength

The flexural strength was measured by conducting the experiments according to the designed experimental matrix for each combination of factors. The SNR values were calculated based on the measured flexural strength data considering the nature of optimization larger-the-better. These experimental results and SNR values are given in Table 4.9. The S/N ratio was calculated using Eq. 3.17 in Minitab 20 software.

Table 4. 9 The result of flexural strength and S/N of the experimental result

Specimens	**Sisal fiber wt.%**	**Glass fiber wt.%**	**Flexural strength (MPa)**	**S/N ratio (dB)**
S1	0	0	25.40	28.0967
S2	0	10	76.20	37.6391
S3	0	15	97.30	39.7623
S4	10	0	68.87	36.7606
S5	10	10	163.81	44.2868
S6	10	15	185.56	45.3697
S7	15	0	91.83	39.2597
S8	15	10	119.19	41.5248
S9	15	15	158.26	43.9874

The response table of SNR for the flexural strength is displayed in Table 4.6. According to this table, E-glass fiber contributed the most to the composite's maximum flexural strength with an 8.33 delta number, followed by Sisal fiber with a 6.97 delta number which ranked second.

Table 4. 10 S/N ratios response Table for flexural strength (Larger is better)

Level	**Sisal fiber**	**E-glass fiber**
1	35.17	34.71
2	42.14	41.15
3	41.59	43.04
Delta	6.97	8.33
Rank	2	1

The main effect plot for the SNR of tensile strength is displayed in Figure 4.11, and the best parameter combinations for an increase in tensile strength were found. Optimal SNR was achieved at 15% of E-glass fiber (level 3) and 10% of sisal fiber (level 2). Consequently, A2B3 was the best parameter combination for SNR of flexural strength.

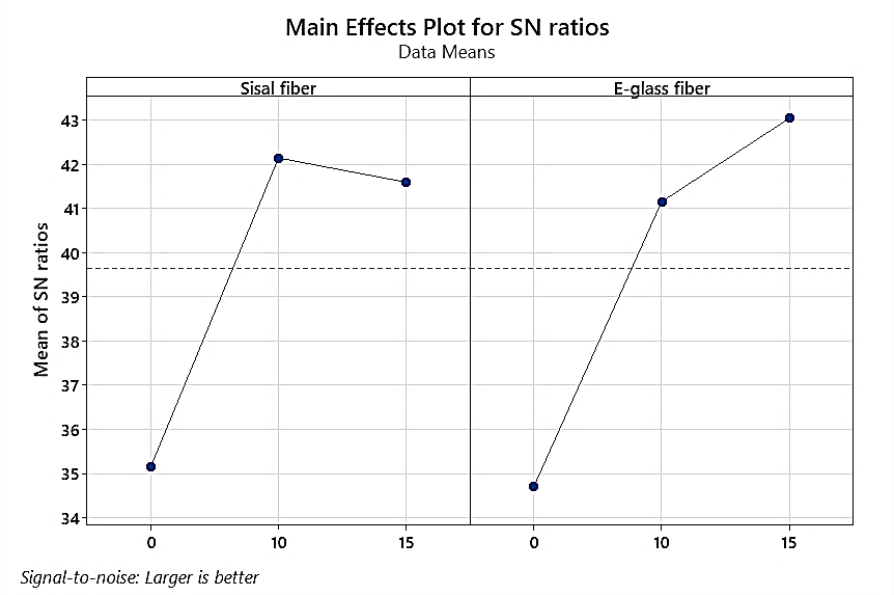

Figure 4. 7 The main effect plot for the SN ratio of flexural strength

4.3.2.2 Analysis of variance for flexural strength of the composite

A2B3 was the optimal parameter combination for SNR of flexural strength. The optimum values for flexural strength were sisal fiber at 10 wt.% in level 2 and E-glass fiber at 10 wt.% in level 3. Based on these values the predicted flexural strength values are calculated and given in Table 4.11.

Table 4. 11 Analysis of variance results of flexural strength

Source	DOF	Seq SS	Adj SS	Adj MS	F-value	P-value	Contribution (%)
Sisal fiber	2	90.20	90.20	45.100	10.13	0.027	40.52
E-glass fiber	2	114.56	114.56	57.280	12.86	0.018	51.47
Residual Error	4	17.82	17.82	4.454	-	-	8.01
Total	8	222.58	-	-	-	-	100
S = 2.1105, R-Sq = 92.00%, R-Sq(adj) = 83.99%							

Based on the optimized values of the parameters, the percentage error was calculated from the predicted flexural strength values and actual flexural strength values. These values are given in Table 4.12. The predicted tensile strength tested under the optimum value was 176.851.

Table 4. 12 Calculation of the percentage error value for tensile strength

Optimum parameter		Flexural strength actual	Flexural strength predicted	Error %
Sisal fiber	10 wt.%	186.56	176.851	4.69
E-glass fiber	15 wt.%			

The obtained percentage error was less than 5% which is acceptable. Therefore, the model was validated.

4.3.3 Optimization of process parameters for impact strength

The weight percentage of Sisal fiber and E-glass fibers are the parameters required to be optimized by considering the weight percentage of SiC filler as a constant variable.

4.3.3.1 Taguchi analysis using signal-to-noise ratio for impact strength

The impact strength results were measured and obtained by conducting the experiments according to the designed experimental matrix for each combination of factors. The SNR values were calculated based on the measured values considering the nature of optimization larger-the-better. These experimental results and SNR values are given in Table 4.13. The analysis of optimum results was identified from the response table and the plot of the main effect for the SN ratio of impact strength. The S/N ratio was calculated using Eq. 3.17.

Table 4.14 shows the response Table for S/N ratios of impact strength. In this case, the weight percentage of sisal fiber was the highest contribution factor ranked number one with a 9.8 delta value while, E-glass fiber was the second contributor with a 4.49 delta number.

Table 4. 13 The result of impact test analysis and S/N of the experimental result

Specimens	Sisal fiber wt.%	Glass fiber wt.%	Impact strength (J)	S/N ratio (dB)
1	0	0	4.50	13.0643
2	0	10	6.50	16.2583
3	0	15	10.25	20.2145
4	10	0	9.50	19.5545
5	10	10	11.50	21.2140
6	10	15	13.50	22.6067
7	15	0	17.00	24.6090
8	15	10	21.00	26.4444
9	15	15	24.75	27.8715

Table 4. 14 S/N ratios response Table for impact strength (Larger is better)

Level	Sisal fiber	Glass fiber
1	16.51	19.08
2	21.13	21.31
3	26.31	23.56
Delta	9.80	4.49
Rank	1	2

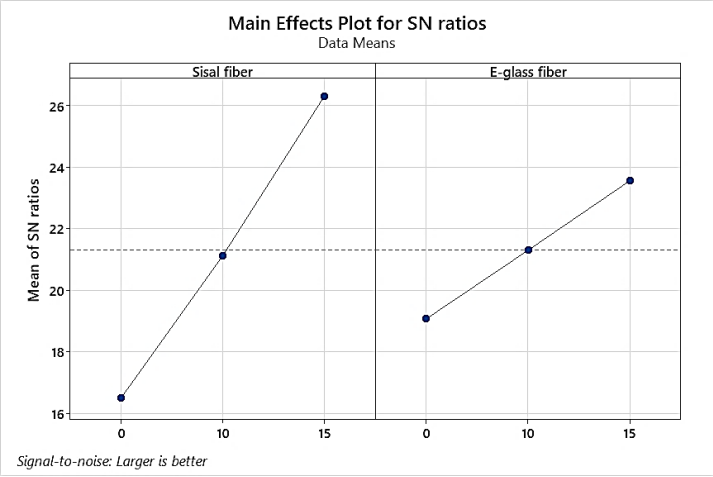

Figure 4. 8 The main effect plot for the SN ratio of impact strength

The main effect plot for the SN ratio of impact strength is displayed in Figure 4.8. shows that 15 wt.% of sisal fiber at level 3 and 15 wt.% E-glass fiber at level 3 were the optimum parameters for maximum impact strength of the composite material developed in this research work. Therefore, the optimum parameter combination for SNR of impact strength was A3B3.

4.3.3.2 Analysis of variance for impact strength of the composite

The optimum parameter combination for SNR of impact strength was A3B3 with sisal fiber at 15 wt.% and E-glass fiber at 15 wt.% in level 3.

Table 4. 15 Analysis of variance results of impact strength

Source	DOF	Seq SS	Adj SS	Adj MS	F-value	P-value	Contribution (%)
Sisal fiber	2	144.104	144.104	72.052	52.77	0.001	80.15
E-glass fiber	2	30.218	30.218	15.109	11.07	0.023	16.81
Residual Error	4	5.461	5.461	1.365	-	-	3.04
Total	8	179.783	-	-	-	-	100.00
S = 1.1685, R-Sq = 96.96%, R-Sq(adj) = 93.92%							

From Table 4.15, sisal fiber contributed the maximum amount of 80.1544 %. This shows the effect of sisal fiber was greater for the obtained maximum impact strength. E-glass shows minimum contribution. The predicted tensile strength tested under the optimum value is 23.9167.

Table 4. 16 Calculation of the percentage error value for impact strength

Optimum parameter		Impact strength actual	Impact strength predicted	Error %
Sisal fiber	15 wt.%	24.75	23.9167	3.35
E-glass fiber	15 wt.%			

The calculated percentage error was 3.35 which was ales than 5% and the percentage error was acceptable.

4.3.4 Optimization of process parameters for Vickers hardness

The weight percentage of Sisal fiber and E-glass fibers are the parameters required to be optimized by considering the weight percentage of SiC filler as a constant variable.

4.3.4.1 Taguchi analysis using signal-to-noise ratio for hardness

The hardness test was measured by conducting the experiments according to the designed experimental matrix for each combination of factors. The SNR values were calculated based on the measured Vickers hardness data considering the nature of optimization larger-the-better. These experimental results and SNR values are given in Table 4.17. The S/N ratio was calculated using Eq. 3.17.

Table 4. 17 The result of hardness test analysis and S/N of the experimental result

Specimens	Sisal fiber wt.%	Glass fiber wt.%	Vickery hardness (MPa)	S/N ratio (dB)
1	0	0	73.47	37.3222
2	0	10	78.93	37.9448
3	0	15	81.17	38.1879
4	10	0	91.03	39.1837
5	10	10	87.70	38.8600
6	10	15	89.90	39.0752
7	15	0	97.93	39.8183
8	15	10	73.47	37.3222
9	15	15	78.93	37.9448

The response for S/N ratios of the Vickers hardness displayed in Table 4.18 shows sisal fiber reinforcement was the higher contributor in this composite material for the obtained maximum hardness while, E-glass fiber is the second one. This shows that the effect of sisal fiber was maximum as compared to E-glass fiber in obtained maximum Vickers hardness.

Table 4. 18 S/N ratios response Table for Vickers hardness (Larger is better)

Level	Sisal fiber	E-glass fiber
1	36.51	37.37
2	38.44	38.05
3	39.25	38.77
Delta	2.75	1.40
Rank	1	2

The main effect plot for the SN ratio of the Vickers hardness displayed in Figure 4.9 shows that the optimum wt.% of sisal fiber and E-glass fiber were obtained at level 3. Therefore, the optimum parameter combination for SNR of the Vickery hardness test was A3B3.

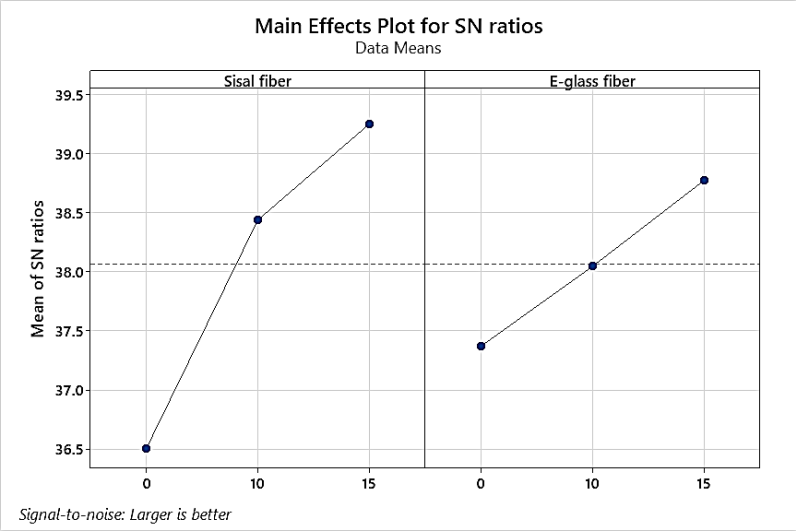

Figure 4. 9 The main effect plot for the SN ratio of the Vickers hardness

4.3.4.2 Analysis of variance for Vickers hardness of the composite

The optimum parameter combination for SNR of the Vickery hardness test was A3B3. These optimum values for maximum Vickers hardness are sisal fiber at 15 wt.% and E-glass fiber at 15 wt.%. Based on these values, the contribution percentage and percentage error were calculated and given in Tables 4.19 and 4.20 respectively.

Table 4. 19 Analysis of variance results of Vickers hardness

Source	DOF	Seq SS	Adj SS	Adj MS	F-value	P-value	Contribution %
Sisal fiber	2	11.9366	11.9366	5.9683	36.91	0.003	76.85
E-glass fiber	2	2.9497	2.9497	1.4749	9.12	0.032	18.99
Residual Error	4	0.6468	0.6468	0.1617	-	-	4.16
Total	8	15.5331	-	-	-	-	100
S = 0.4021, R-Sq = 95.84%, R-Sq(adj) = 91.67%							

From Table 4.18, sisal fiber contributes 76.8462 %, which means the effect of sisal fiber was more on the Vickers hardness of the composite. E-glass fiber contributes 18.9898 % of the total percentage.

Table 4. 20 Calculation of the percentage error value for Vickers hardness

Optimum parameter		Vickers hardness actual	Vickers hardness predicted	Error %
Sisal fiber	15 wt.%	97.93	98.4022	0.48
E-glass fiber	15 wt.%			

The predicted hardness was 98.40 and the actual was 97.93. The obtained percentage error was 0.48 which is less than 5% and hence it is acceptable.

4.3.5 Grey relational analysis for multi-response analysis of the composite

The mechanical properties (Tensile strength, flexural strength, impact test, and hardness strength) were converted into single results using GRA analysis to obtain the optimal fiber weight percentage for the composite. Tensile strength, flexural strength, impact test, and hardness strength need to be maximized, and hence larger the better case was selected throughout the responses. The basic steps for conducting the GRA are given in Section 3.3.6, and the results are given in Tables 4.21 to 4.23.

Table 4. 21 Experimental results and S/N ratio for each responses

Samples	Response for all experimental results				S/N ratio for each experimental result of the samples			
	TS	FS	IS	HV	TS	FS	IS	HV
1	10.06	25.40	4.5	58.3	20.0520	28.0967	13.0643	37.3222
2	27.61	76.20	6.5	69.83	28.8213	37.6391	16.2583	37.9448
3	33.11	97.30	10.25	73.47	30.3992	39.7623	20.2145	38.1879
4	22.67	68.87	9.5	78.93	27.1090	36.7606	19.5545	39.1837
5	36.43	163.81	11.5	81.17	31.2292	44.2868	21.2140	38.8600
6	41.74	185.56	13.5	91.03	32.4110	45.3697	22.6067	39.0752
7	25.46	91.83	17	87.7	28.1172	39.2597	24.6090	39.8183
8	37.11	119.19	21	89.9	31.3898	41.5248	26.4444	37.3222
9	42.13	158.26	24.75	97.93	32.4918	43.9874	27.8715	37.9448

The normalized values and deviation sequences were calculated based on Eq.3.19 and 3.21 respectively using Excel software. The values are given in Table 4.22.

Table 4. 22 Normalized values and deviation sequence of normalized S/N ratio

Sample	Normalized values				Deviation sequence			
	TS	FS	IS	HV	TS	FS	IS	HV
1	0	0	0	0	1	1	1	1
2	0.7049	0.5524	0.2157	0.2494	0.2951	0.4476	0.7843	0.7506
3	0.8318	0.6754	0.4829	0.3468	0.1682	0.3246	0.5171	0.6532
4	0.5673	0.5016	0.4383	0.7458	0.4327	0.4984	0.5617	0.2542
5	0.8985	0.9373	0.5504	0.6161	0.1015	0.06273	0.4496	0.3839
6	0.9935	1	0.6444	0.7023	0.0065	0	0.3556	0.2977
7	0.6483	0.6463	0.7797	1	0.3517	0.3537	0.2203	0
8	0.9114	0.7774	0.9036	0	0.0886	0.2226	0.0964	1
9	1	0.9200	1	0.2494	0	0.0800	0	0.7506

Table 4. 23 Grey relational coefficient, GRG and rank

Samples	TS	FS	IS	H	GRG	R
1	0.3333	0.33333	0.3333	0.3333	0.3333	9
2	0.6289	0.5277	0.3893	0.3998	0.4864	8
3	0.7483	0.6063	0.4916	0.4336	0.5699	6
4	0.5361	0.5008	0.4709	0.6629	0.5427	7
5	0.8313	0.8886	0.5265	0.5657	0.7030	4
6	0.9872	1	0.5844	0.6268	0.7996	2
7	0.5871	0.5857	0.6941	1	0.7167	3
8	0.8495	0.6919	0.8384	0.3333	0.6783	5
9	1	0.8620	1	0.3998	0.8155	1

Designation: GRG-grey relational grade, R-rank

The Grey relational coefficient, GRG, and ranked samples of optimum values of parameters displayed in Table 4.23 show that, sample number nine was the composite material that ranked first for its high mechanical properties. The composition of this sample was a sisal fiber of 15 wt.%, E-glass fiber of 15 wt.%, SiC of 5 wt.%, and polyester resin of 65 wt.%.

4.3.6 Analysis of mean for GRG composite

The response table for the GRG displayed in Table 4.24 shows that sisal fiber wt.% in level 3 was the more optimal composition, while the sisal fiber wt.% in levels 2 and 1 were the second and third optimal composition, respectively.

Table 4. 24 Response Table for the GRG (Larger is better)

Level	Sisal fiber	E-glass fiber
1	0.4632	0.5309
2	0.6818	0.6226
3	0.7368	0.7283
Delta	0.2736	0.1974
Rank	1	2

The parameters with the highest effect on the mean from Table 4.24 were sisal fiber with a 0.2736 of delta value ranked 1 and E-glass ranked second with a 0.1974 delta value. The actual or optimum value was calculated based on values obtained from experimental results using the linear regression equation (Pandya & Rathod, 2020).

Opm = A3 + B3 – (m) = 0.7368+ 0.7283 – (0.6273)

Opm = 0.8378 and this is the actual value.

Where m is the average performance mean value for GRG (i.e.: m = 0.6273)

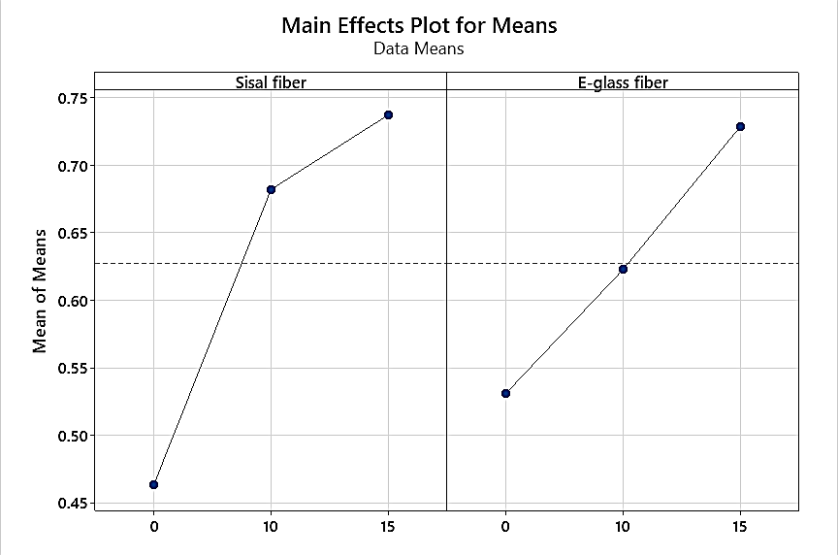

Figure 4. 10 The main effect plot for the mean of GRG

From the S/N ratio plot shown in Figure 4.10, the optimum values for the composite are sisal fiber at 15 wt.% and E-glass fiber at 15 wt.%.

4.3.7 Determining optimum condition for GRG of the composite

The optimum prediction condition for SNR in which, the GRG response result of the material was obtained with the terms set was shown in Table 4.25. The selected optimum parameters in the study were at the highest wt.% of sisal and highest wt.% of E-glass which was A3B3. Therefore optimal mechanical properties of the developed composite were achieved at 30 wt

% fibers (i.e. 15 wt % sisal fiber and 15 wt % sisal fiber E-glass fibers). The observed results are in line with the research work reported earlier by the authors (Sinitsky, et al. 2022).

Table 4. 25 The predicted optimal value of GRG

Factors	Levels	Values	Rank	Prediction SNR	Values mean
Sisal fiber	3	15 wt.%	1	-1.20777	0.8380
E-glass fiber	3	15 wt.%	2		

4.3.8 Analysis of variance for GRG of composite

Table 4. 26 Analysis of Variance for GRG (mean)

Source	DOF	Seq SS	Adj SS	Adj MS	F-value	P-value	Cont.%
Sisal fiber	2	0.12564	0.12564	0.062820	18.04	0.010	63.41
E-glass fiber	2	0.05856	0.05856	0.029281	8.41	0.037	29.56
Residual Error	4	0.01393	0.01393	0.003482	-	-	7.03
Total	8	0.19813					100
S = 0.0590, R-Sq = 92.97%, R-Sq(adj) = 85.94%							

The ANOVA table for GRG displayed in Table 4.25 shows that the sisal fiber contributed 63.41 % while E-glass fiber contributed 29.56%. The weight percentage of sisal fiber had more effects on the mechanical properties of the developed composite, while E-glass fiber was the next. Due to its cellulose-rich composition and chemically treated, sisal fiber plays a crucial role in enhancing the mechanical properties of the composite. The obtained results are in line with the work carried out earlier by (Sinitsky, et al. 2022).

Table 4. 27 Calculation of the percentage error value for GRG

Optimum parameters		Actual value of GRG	Predicted value of GRG	Error %
Sisal fiber	15 wt.%	**0.8378**	0.8380	0.024
E-glass fiber	15 wt.%			

The percentage error between the predicted value and the actual value was 0.024, which is very small. Therefore, the obtained percentage error was acceptable.

The normal probability plot obtained for GRA is given in Figure 4.11. Data points were distributed along the reference line, and it suggests the data follows a normal distribution.

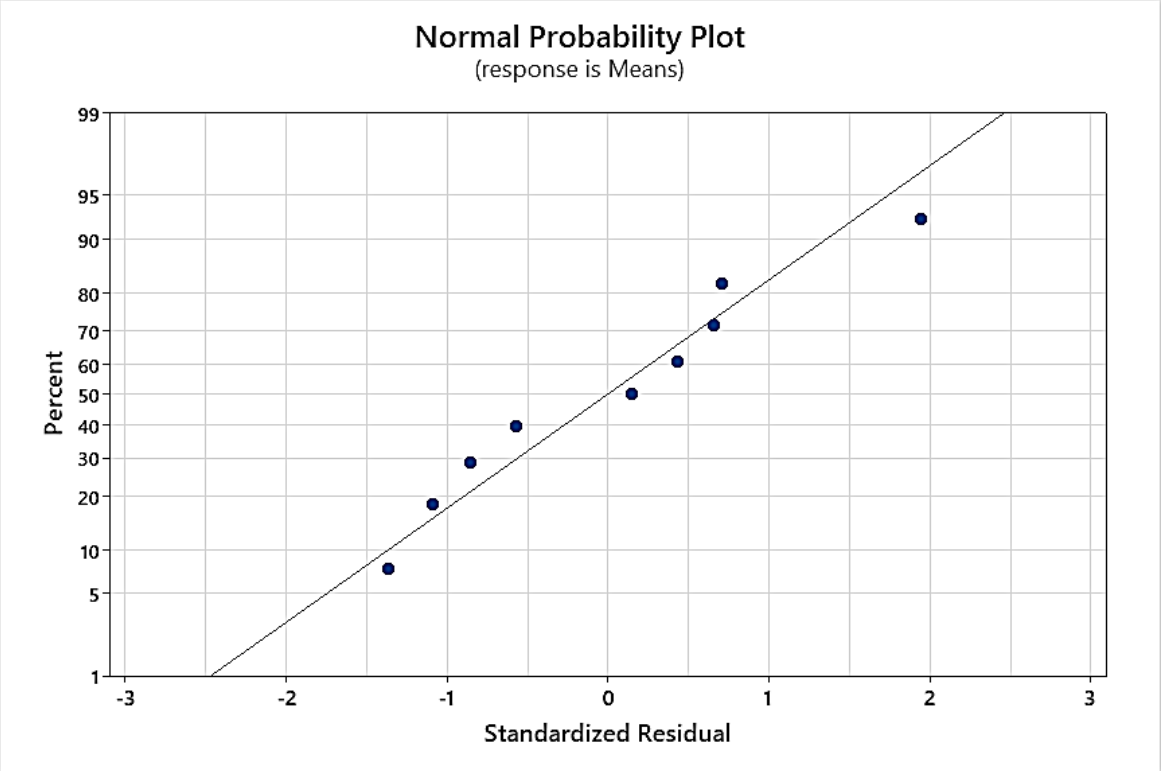

Figure 4. 11 Normal probability plot

4.4 Confirmation test for composite

After determining the optimal process parameters and their respective levels, the next step was to confirm if the predicted results disagreed with the experimental data. If the combination of optimal process parameters level matches any experimental trial in the orthogonal array, it will not be necessary to conduct a confirmation test. Unless it is appropriate to do experimentation at that new level. In this study, the optimal process parameter combination was **A3B3**, and this predicted result coincides with the experimental results of sample nine. The composition of this sample was a sisal fiber of 15 wt.%, E-glass fiber of 15 wt.%, SiC of 5 wt.%, and polyester resin of 65 wt.%. Therefore, there is no need to conduct a confirmation test.

4.5 The comparison with previous work on mechanical properties of the composite

In this section, the maximum values obtained from each test's experimental results were compared with those of the same tests obtained in other related literature papers by other researchers. The achieved value of tensile, flexural, impact, and Vickers hardness strengths in the current research were compared with the work of other researchers and tabulated in Tables 4.28 and 4.29.

Table 4. 28 Comparison of tensile (TS) and flexural strengths (FS)

Matrix material	Fibers	Filler	Fabrication method	TS (MPa)	FS (MPa)	References
Polyester resin	Sisal/E-glass	SiC	Hand layup	42.3	185.56	Current work
Polyester	Glass fiber	SiC	Hand layup	33.1	-	(Palle et al., 2022)
Epoxy	Sisal /Glass	NA	Hand layup	-	82.6± 4.77	(Pereira et al., 2020)
Polyester	Sisal /Glass	NA	Hand layup	< 18	<65	(Njoku et al., 2011)

Table 4. 29 Comparison of impact and Vickery hardness strengths

Matrix material	Fibers	Filler	Fabrication method	Impact (J)	Hardness (VH)	References
polyester resin	Sisal/E-glass	SiC	Hand layup	24.75	97.93	Current work
Epoxy	Glass	NA	Hand layup	18.4	-	(Palanikumar et al., 2016)
Epoxy	Sisal-Caryota	NA	Hand layup	-	< 90	(Atmakuri et al., 2021)

Designation: NA- Not available

As shown in Tables 4.28 and 4.29, the tensile, flexural, impact, and hardness of the developed composite in the current work were improved due to the hybridization effects of fibers and SiC particles.

4.6 Analysis of Composite Bonding

In this sub-section parameters (Joint configuration, filler wt.%, and overlap length) that affect the strength of the adhesive joined composite were analyzed for selected samples for tensile joint strength, and flexural joint strength to get the quality of the joint. This composite joining analysis was done for a composite with high mechanical properties, which were obtained after optimization of the experimental results. Therefore, this composite material was a material developed with a material composition of 15 wt.% Sisal fiber, 15 wt.% E-glass fiber, 5 % SiC filler, and 65% polyester resin as explained in section 4.3.5.

4.6.1 Effects of joining parameters on tensile strength of the adhesively joined composite

The experimental results for tensile strength of adhesively joined composite materials developed from a polyester resin matrix reinforced with sisal fiber, E-glass fiber, and SiC filler are given in Table 4.30. These results were obtained for nine different runs by considering the joining parameters.

Table 4. 30 Experimental results for tensile strength of adhesively joined composite

Runs	**Joining parameters**			**Av. Tensile strength (MPa)**
	Joint configuration	Filler (wt.%)	Overlap length	
R-1	SLJ	0	20	21.02
R-2	SLJ	1.5	25	26.51
R-3	SLJ	3	30	29.29
R-4	SCJ	0	25	23.38
R-5	SCJ	1.5	30	28.57
R-6	SCJ	3	20	27.35
R-7	STJ	0	30	25.90
R-8	STJ	1.5	20	29.18
R-9	STJ	3	25	31.44

The joint tensile increased gradually from 21.02 to 29.29 MPa (by 28.23 %), due to the increased SiC contents from 0 to 3 wt.% and an overlap length from 20 to 30mm for SLJ. With the SCJ configuration, the strength rises from 23.38 to 28.57 (increased by 18.12 %), due to the increase of SiC composition from 0 to 1.5 and length of 25 to 30mm. But strength decreased from 28.57 to 27.35 (by 4.27) due reduction in overlap length from 30 to 20mm. The joint strength was enhanced from 25.90 to 29.18 (by 11.24%) due to an increase of filler from 0 to 1.5 wt.%. The material effect and substantial geometry were found on the maximum load of SLJ, with the benefit of a large overlap length (Brito et al., 2020). Similarly, the strength increased from 29.18 to 31.44 MPa (by 2.28), due to an increase of SiC filler from 1.5 to 3 wt.%. These could be attributed to the effective stress transfer that occurs between the araldite epoxy and the nanoparticles, which is crucial in enhancing the adhesion properties of adhesive bonds.

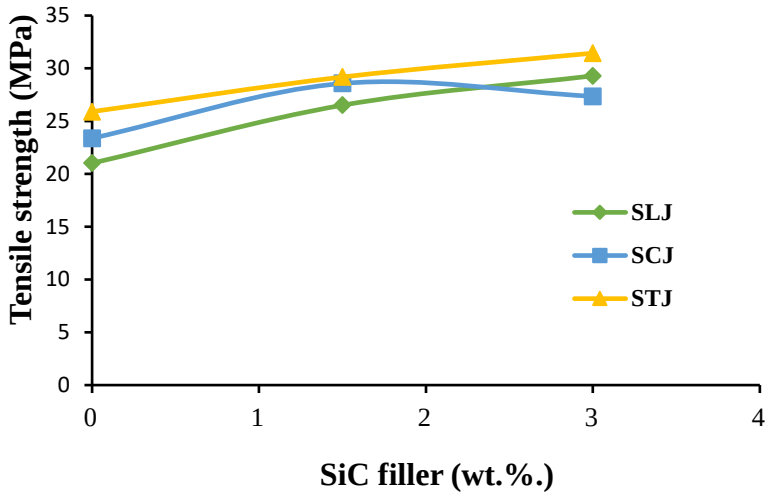

Figure 4. 12 Effects of filler wt.%. on joint strength for different joint configurations

Figure 4.12 shows that the STJ of the joint configuration achieved the highest tensile strength of 31.44 MPa at 3 wt.% SiC filler. In addition to this, the strength of 29.18 MPa and 25.90 MPa were obtained at 1.5 wt.% and 0 wt.% of SiC filler respectively. Whereas the SLJ and SCJ show a maximum strength of 28.57 MPa at 1.5 wt.% of SiC and 29.29 MPa at 3 wt.% of SiC filler respectively. The STJ shows the maximum strength over the three ranges of SiC wt.% and the SCJ shows the same results up to 1.5 wt.% of SiC. However, the strength of SCJ decreases above 1.5 wt.% of SiC filler due to the surface treatment and surface preparation. Similar phenomena were reported by (Rangaswamy et al., 2020; Shang, Marques, Machado, Carbas, Jiang, & Silva, 2019). Finally, the SLJ, STJ, and SCJ show the minimum joint strength at 0 wt.% of SiC and increased after the addition of SiC wt.%. This shows that the joint strength of composite materials can be increased using SiC filler materials in the adhesive materials. This occurred as the result of efficient stress transfer between the SiC particle and the polymer composite, which improves the adhesion properties of the adhesive material. The obtained results are in line with the work carried out earlier by (Chavooshian et al., 2017).

Figure 4.13 shows the effects of SiC filler wt.%. on joint strength for different overlap lengths. With varying overlap lengths, the effect of SiC filler weight percentage on joint strength in adhesive materials varies. The maximum joint strength of 29.29 MPa (with SLJ) and 28.57 (with SCJ) MPa were achieved for 30mm overlap length at 3 wt.% and 1.5 wt.% respectively. The minimum joint strength values were identified with a 20mm overlap length at 0 wt.% of SiC filler and the medium joint strength was obtained with a 25 mm overlap length at 0 wt.% of SiC filler.

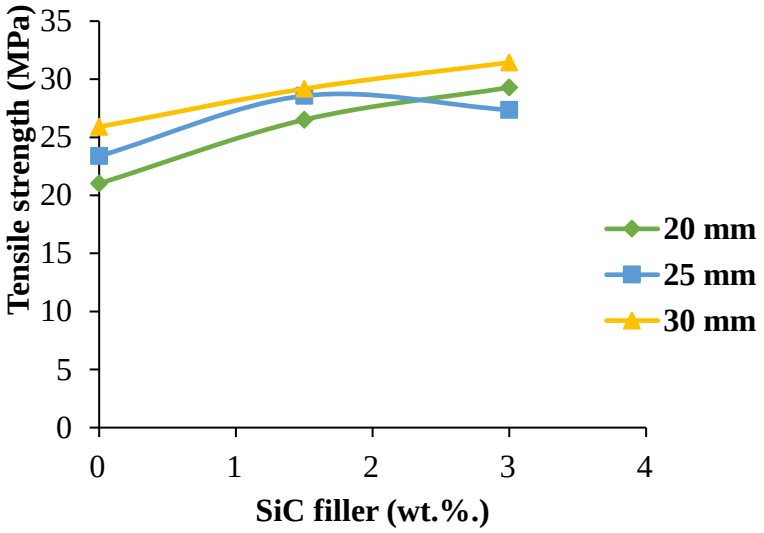

Figure 4. 13 The effects of SiC filler wt.%. on joint strength for overlap lengths

Figure 4.13 further explains that as the overlap lengths of joining surfaces increase the joint strength between the adherends increases. Based on the results tabulated in Figure 4.13, the joint strength increases as filler wt % increases with the overlap lengths, and similar results were reported by (Kadioglu et al., 2019; Mejbel et al., 2019).

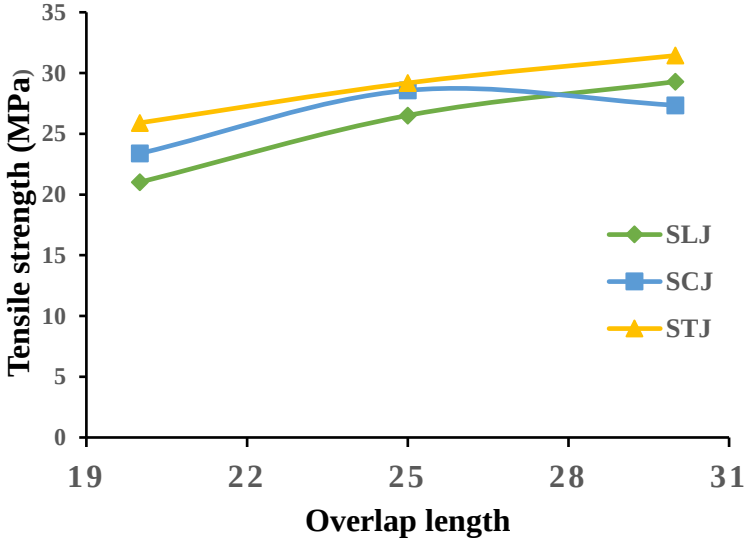

Figure 4. 14 The effects of overlap length on joint strength for joint configurations

Figure 4.14 shows the effects of overlap length on joint strength for different joint configurations. The maximum joint strength of 25.90 MPa was obtained with an overlap length of 30mm at 0 wt.% of SiC filler. The effect of overlap length increases for SLJ and STJ over the ranges of overlap lengths and highly increases up to 25mm of overlap length for the SCJ. Increasing the overlap length generally increases the joint strength for all three

types of joint configurations, because a longer overlap length provides more surface area for the adhesive to bond to, which increases the strength of the joint. The observed results align with the research work reported earlier by authors (Jeevi et al., 2019; Abbasi et al., 2023).

4.6.2 Effects of bonding parameters on joint flexural strength of the adhesively joined composite

The experimental results for joint flexural strength of adhesively joined composite were given in Table 4.31. Nine different joint flexural strength results were obtained by considering different adhesive joining process parameters.

Table 4. 31 Experimental results for joint flexural strength testing of adhesively joined

Runs	Joining parameters			Av. Flexural strength (MPa)
	Joint configuration	Filler (wt.%)	Overlap length	
R-1	SLJ	0	20	55.74
R-2	SLJ	1.5	25	61.71
R-3	SLJ	3	30	67.96
R-4	SCJ	0	25	64.96
R-5	SCJ	1.5	30	70.59
R-6	SCJ	3	20	76.69
R-7	STJ	0	30	66.76
R-8	STJ	1.5	20	72.40
R-9	STJ	3	25	79.23

Based on Table 4.3, the joint flexural strength increased gradually from 55.74 to 67.96 MPa (by 17.98 %), due to the increased SiC contents from 0 to 3 wt.% and an overlap length from 20 to 30mm with SLJ configuration. With the SCJ configuration, the strength rises from 64.96 to 70.59 (by 7.98 %), due to the increase of SiC composition from 0 to 1.5 and length of 25 to 30mm, similarly increases from 70.59 to 76.69 (by 7.95 %) as SiC increased from 1.5 to 3 wt.% and overlap length reduce from 30 to 20mm. With STJ configuration the joint strength was enhanced from 66.76 to 72.40 (by 7.79%) due to an increase of filler from 0 to 1.5 wt.%. Similarly, the strength increased from 72.40 to 79.23 MPa (by 8.62 %), due to the increase of SiC filler from 1.5 to 3 wt.%. A slight rise in joint strength was recorded over 20mm of overlap length (Melese et al., 2022), and the effect of overlap length was minimal with the SCJ and STL.

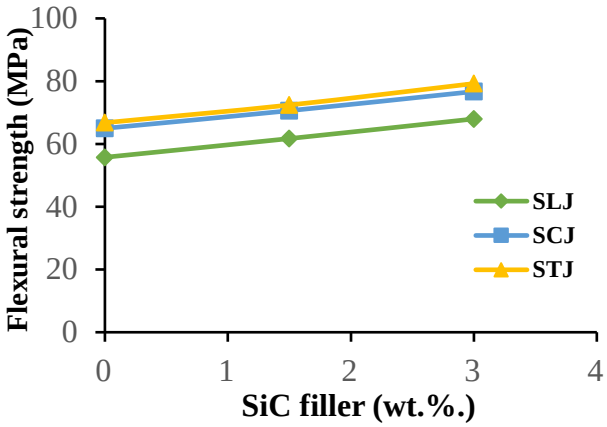

Figure 4. 15 The effects of filler wt.%. on joint flexural strength for joint configurations

Figure 4.15 shows the effects of SiC filler wt.%. on joint flexural strength for different configurations. The joint flexural strength for the three joint configurations increases as the SiC filler wt.% increases. The maximum joint flexural strength of 79.23 MPa was achieved by STJ at 3 wt.% of SiC, 76.69 MPa with SCJ at 3 wt.% of SiC, and 72.40 MPa with STJ at 1.5 wt.% of SiC. These results occurred due to the SiC filler with varying weight percentages. The minimum joint flexural strength of 55.74 MPa, 64.96 MPa, and 66.76 MPa for the three joint configurations of SLJ, SCJ, and STJ respectively was obtained at 0 wt.% of the SiC filler. The observed results align with the research work reported earlier by (Sanghvi et al., 2022).

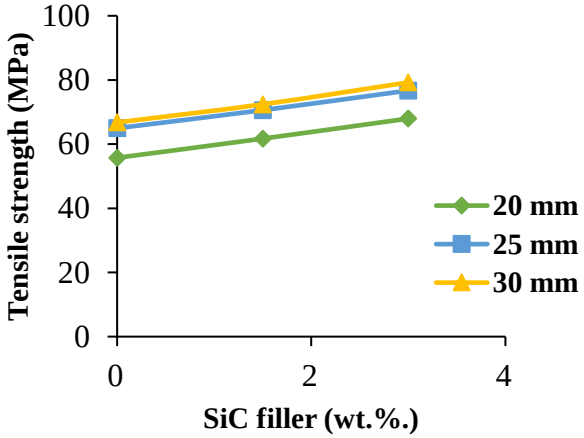

Figure 4. 16 The effects of filler wt.%. on flexural strength for overlap lengths

Figure 4.16 displays the effects of SiC filler wt.%. on the joint flexural strength for different overlap lengths. The joint strength for the adhesive joints was increased with the addition of filler and an increase in overlap lengths. The maximum joint strength of 79.23 MPa was achieved in run number nine of STJ at 3 wt.% of SiC. A 67.96 MPa was obtained for SLJ at 3 wt.% of SiC and 76.69 MPa resulted for SCJ at 3 wt.% of SiC. Based on the graph of

Figure 4.16, the wt.% of SiC filler and the increment of overlap lengths have a positive impact on the joint strength of composite materials developed from polyester resin matrix and sisal fiber, glass fiber, and SiC reinforcement. Similar findings were reported by authors (Kadioglu et al., 2018).

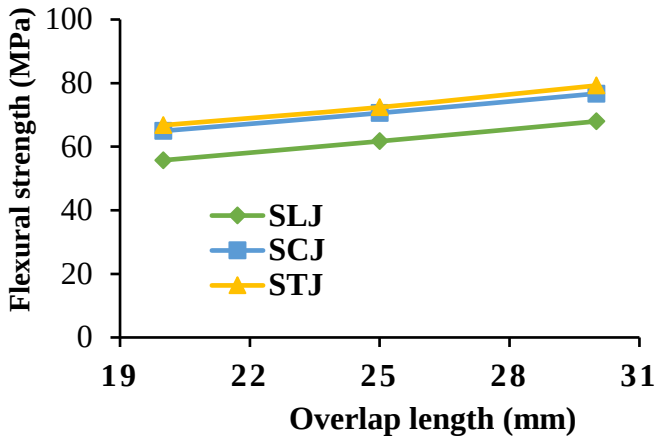

Figure 4. 17 The effects of overlap length on flexural strength for joint configurations

Figure 4. 17 displays the effects of overlap length on joint flexural strength for different joint configurations. As the the overlap length increases the joint strength increases for each joint configuration. The maximum flexural strength was obtained for STJ at 3 wt.% of SiC and 25 mm overlap length. A 55.74 MPa of the joint strength was the minimum joint strength value achieved by SLJ, 20 mm of overlap length, and 0 wt.% of SiC. This implies that the smaller overlap length results in the minimum joint strength of the adhesive joint especially for an adhesive without filler materials. The observed results were in line with the research work reported earlier by the authors (Rangaswamy et al., 2020).

4.7 Optimization of process parameters for adhesive joint strength

4.7.1 Optimization of process parameters for joint tensile strength

The joint configuration, wt.% of SiC filler, and overlap lengths were optimized for joint tensile strength by employing the experimental result to identify the optimal parameter combinations that maximize the tensile strength of the joint.

The joint configuration, wt.% of SiC filler, and overlap lengths are the parameters required to be optimized by considering the adhesive type, and adhesive layer as a constant variable. The joint tensile strength was measured by conducting the experiments according to the designed experimental matrix for each combination of factors. The SNR values were calculated based on the measured tensile strength data considering the nature of optimization larger-the-better. These experimental results and SNR values are given in Table 4.32.

Table 4. 32 Tensile strength and S/N ratio of the adhesive joint

Specimens	Joint configuration	Wt.% of SiC filler	Overlap joint	Tensile strength (MPa)	S/N ratio (dB)
S1	SLJ	0.0	20	21.02	26.4540
S2	SLJ	1.5	25	26.51	28.4682
S3	SLJ	3.0	30	29.29	29.3344
S4	SCJ	0.0	25	23.39	27.3794
S5	SCJ	1.5	30	28.57	29.1172
S6	SCJ	3.0	20	27.35	28.7381
S7	STJ	0.0	30	25.90	28.2660
S8	STJ	1.5	20	29.17	29.3007
S9	STJ	3.0	25	31.44	29.9506

Table 4.33 shows the response table for SNR of the joint tensile strength. From this table, filler (with a 1.97 delta number) was the first contributor in the obtained maximum joint tensile strength, and joint configuration (with a delta number of 4.24) was the second ranker while overlap length (0.74 with a 1.97 delta number) was the third-ranked contributor.

Table 4. 33 Response Table for S/N ratios of Tensile strength

Level	Joint configuration	Filler wt.%	Overlap length
1	28.09	27.37	28.16
2	28.41	28.96	28.60
3	29.17	29.34	28.91
Delta	1.09	1.97	0.74
Rank	2	1	3

The main effect plot for the SNR of joint tensile strength displayed in Figure 4.18 shows the optimal parameter combinations for the increased joint tensile strength observed at the optimum SNR of STJ joint configuration in level 3, 3 wt.% SiC filler in level 3, and an overlap length of 30mm in level 3. Therefore, the optimum parameter combination for SNR of tensile strength was A3B3C3.

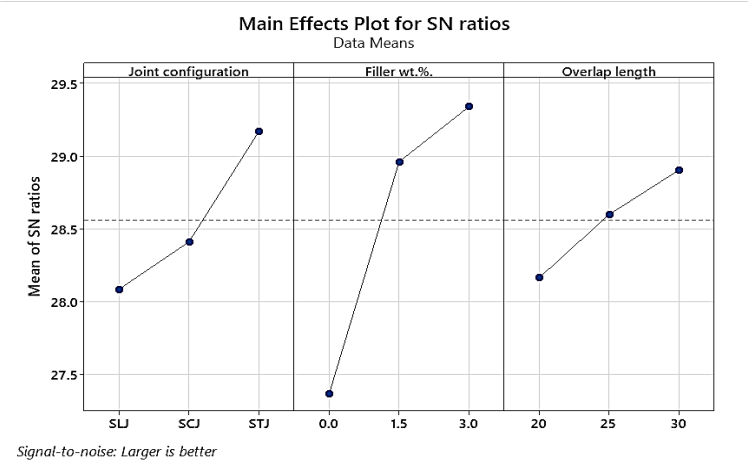

Figure 4. 18 The main effect plot for the SN ratio of tensile strength in adhesive joint

4.7.1.1 Analysis of variance for tensile strength of the composite adhesive joint

The optimum values for maximum joint tensile strength are joint configuration with STJ, SiC filler at 3 wt.%, and overlap length at 30mm. Based on these optimal values of the adhesively joined composite material, the analysis of variance for the S/N ratio of the tensile strength was obtained and given in Table 4.35. The maximum contribution % of 70.4788 % was achieved by filler wt.%, 19.9675% by joint configuration, and 8.9130 % by overlap length. The obtained results are in line with the work carried out earlier by (Basavarajappa et al., 2021).

Table 4. 34 Analysis of Variance for S/N ratio of the tensile strength

Source	DOF	Seq SS	Adj SS	Adj MS	F-value	P-value	Cont. %
Joint conf.	2	1.867	1.867	0.933	31.16	0.031	19.97
Filler wt.%.	2	6.588	6.588	3.294	109.98	0.009	70.48
Overlap length	2	0.833	0.833	0.417	13.91	0.067	8.91
Residual Error	2	0.060	0.060	0.030			0.64
Total	8	9.348					100
S = 0.1731, R-Sq = 99.36%, R-Sq(adj) = 97.44%							

Designation: Cont.%- percentage of contribution, Joint conf.- joint configuration

Table 4.34 discusses the percentage error between the actual and predicted values. The predicted joint tensile strength tested under the optimum value is 32.1981. The level of optimum parameters did not coincide with the experimental trial in the orthogonal array. The actual tensile strength value was not available in the experimental tests conducted using the designed L_9 orthogonal array. It was obtained after testing based on the new process parameters and 33.04 MPa of tensile strength was achieved.

Table 4. 35 Calculation of the percentage error value for tensile strength

Optimum parameter		Tensile strength actual	Tensile strength predicted	Error %
Joint configuration	STL	33.04	32.1981	2.54
Filler wt.%.	3%			
Overlap length	30			

4.7.2 Optimization of process parameters for flexural strength

The joint configuration, wt.% of SiC filler, and overlap lengths were optimized for tensile strength by employing the experimental result to identify the optimal parameter combinations that maximize the flexural strength of the joint.

4.7.2.1 Taguchi analysis using signal-to-noise ratio for flexural strength

The experimental results and SNR values are given in Table 4.36.

Table 4. 36 Flexural strength and S/N of the adhesive joints

Specimens	Joint configuration	Wt.% of SiC filler	Overlap length	S/N ratio (dB)
1	SLJ	0.0	20	34.9239
2	SLJ	1.5	25	35.8066
3	SLJ	3.0	30	36.6446
4	SCJ	0.0	25	36.2534
5	SCJ	1.5	30	36.9749
6	SCJ	3.0	20	37.6952
7	STJ	0.0	30	36.4899
8	STJ	1.5	20	37.1952
9	STJ	3.0	25	37.9782

The response Table for S/N ratios of joint flexural strength displayed in Table 4.36 shows filler wt.% (a 1.55 delta value) was the highest contributor to the adhesive joint strength of the composite materials developed from polyester matrix reinforced with sisal fiber, E-glass fiber, and SiC filler. Joint configuration (a 1.43 delta value) was the second-ranked parameter that affected the joint strength and finally, overlap length (a 0.1 delta value) was the third-ranked. These results show that the effect of filler materials was high for the joint strength of the composite.

Table 4. 37 S/N ratios response Table for joint flexural strength

Level	Joint configuration	Filler wt.%.	Overlap length
1	35.79	35.89	36.60
2	36.97	36.66	36.68
3	37.22	37.44	36.70
Delta	1.43	1.55	0.10
Rank	2	1	3

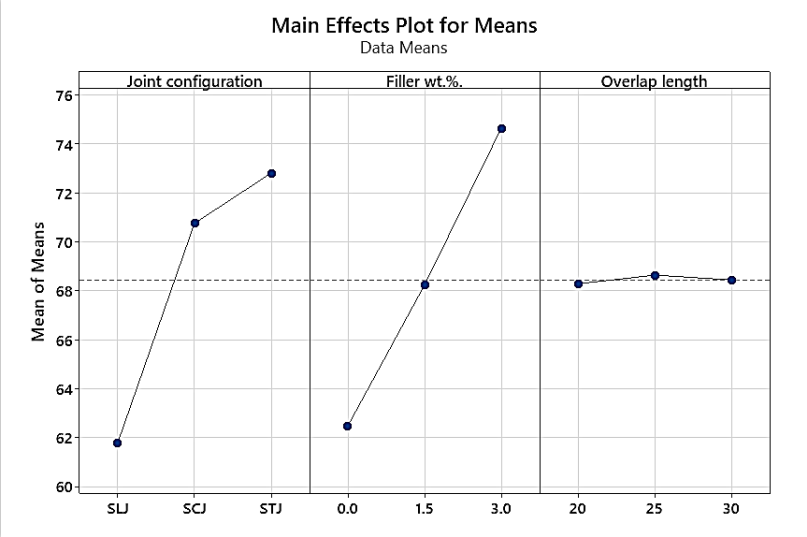

Figure 4. 19 The main effect plot for the SN ratio of flexural strength in adhesive joint

The main effect plot for the SNR of joint flexural strength displayed in Figure 4.19 shows the optimal parameter combinations for the increased joint flexural strength observed at the optimum SNR of STJ joint configuration in level 3, 3 wt.% SiC filler in level 3, and an overlap length of 25mm in level 2. Therefore, the optimum parameter combination for SNR of tensile strength was A3B3C2.

4.7.2.2 Analysis of variance for flexural strength of the composite adhesive joint

The optimum parameter combination for the SNR of joint flexural strength was A3B3C2. That means the optimal parameters for maximum joint flexural strength are joint configuration with STJ, SiC filler at 3 wt.%, and overlap length at 25mm. Table 4.39 displays the analysis of variance for the S/N ratio of the joint flexural strength. Filler wt.%. contributes a maximum contribution percentage of 50.55 % and Joint configuration contributes 49.1169%. The minimum contribution percentage of 0.2218 % was achieved by overlap length. The obtained results are in line with the work carried out earlier by (Mottaghian & Taheri, 2023).

Table 4. 38 Analysis of Variance for S/N ratio of the joint flexural strength

Source	DOF	Seq SS	Adj SS	Adj MS	F-value	P-value	Cont. %
Joint conf.	2	3.503	3.503	1.751	448.65	0.002	49.12
Filler wt.%.	2	3.605	3.605	1.803	461.76	0.002	50.55
Overlap length	2	0.016	0.016	0.008	2.03	0.330	0.22
Residual Error	2	0.008	0.008	0.004	-	-	0.11
Total	8	7.132	-	-	-	-	100
S = 0.0625, R-Sq = 99.89%, R-Sq(adj) = 99.56%							

Table 4. 39 Calculation of the percentage error value for joint flexural strength

Optimum parameter		Flexural strength actual	Flexural strength predicted	Error %
Joint configuration	STJ	79.23	79.16	0.09
SiC filler	3 wt.%			
overlap length	25mm			

The optimum parameters combination of the joint flexural strength were an STJ joint configuration, 3wt.% of SiC nanoparticle filler, and 25 mm of an overlap length. The predicted joint flexural strength was 79.16 and the actual flexural strength was 79.23. The calculated percentage error was 0.09, which was less than 5%. Therefore, the observed error was acceptable.

4.7.3 GRA for multi-response analysis of the adhesive joint strength

In this analysis, the joint mechanical properties (Joint tensile and flexural strengths) were converted into single results using GRA analysis to obtain the optimal joint process parameters. Joint tensile and flexural strengths need to be maximized, and hence larger the better case was selected throughout the responses.

Response values and S/N ratios for all experimental results of the output responses(joint tensile and joint flexural strength was) calculated and given in Table 4.40. The response values were the data obtained after the experimentation of each sample.

Table 4. 40 Response values and S/N ratios for all experimental results

Samples	Experimental results		Signal-to-noise ratios	
	TS	FS	TS	FS
1	26.4540	55.74	9.3964	34.9239
2	28.4682	61.71	15.8198	35.8066
3	29.3344	67.96	18.7101	36.6446
4	27.3794	64.96	19.3976	36.2534
5	29.1172	70.59	21.0076	36.9749
6	28.7381	76.69	19.0945	37.6952
7	28.2660	66.76	17.1828	36.4899
8	29.3007	72.40	17.1104	37.1952
9	29.9506	79.23	18.5782	37.9782

The normalized values and deviation sequences were calculated using Eq.3.19 and 3.21 respectively using Excel software. Grey relational coefficient and grey relational grade were calculated using Eq. 3.22 and 3.23 respectively. The values are given in Table 4.41. The ranks were identified using Excel, based on the maximum GRG.

Table 4. 41 Determination of the normalized values, deviation sequence of normalized S/N ratio, calculated GRC, GRG, and rank

Samples	Normalized values		Deviation sequence		Calculated GRC		GRG	Rank
	JTS	JFS	JTS	JFS	JTS	JFS		
1	0	0	1	1	0.3333	0.3333	0.1667	9
2	0.5532	0.2890	0.4468	0.7110	0.5281	0.4129	0.2352	8
3	0.8021	0.5634	0.1979	0.4366	0.7165	0.5338	0.3126	6
4	0.8613	0.4353	0.1387	0.5647	0.7829	0.4696	0.3131	5
5	1	0.6715	0	0.3285	1	0.6035	0.4009	2
6	0.8352	0.9073	0.1648	0.0927	0.7521	0.8437	0.3990	3
7	0.6706	0.5127	0.3294	0.4873	0.6028	0.5064	0.2773	7
8	0.6644	0.7436	0.3356	0.2564	0.5983	0.6611	0.3149	4
9	0.7908	1	0.2092	0	0.7050	1	0.4262	1

4.7.4 Analysis of mean for GRG

Table 4. 42 Response Table for a GRG (Larger is better)

Level	Joint configuration	Filler wt.%	Overlap length
1	0.2382	0.2524	0.2935
2	0.3710	0.3170	0.3249
3	0.3395	0.3793	0.3303
Delta	0.1328	0.1269	0.0368
Rank	1	2	3

The maximum effect on the mean from Table 4.42 was Joint configuration with a 0.1328 delta value ranked 1, Filler wt.% is ranked second with a 0.1269 delta value, and Overlap length was ranked third with a 0.0368 delta value.

Opm = A2 + B3 + C3 – 2m = 0.3710 + 0.3793 + 0.3303 – 2(0.3162) = 0.4482 is the actual value. Where m is the average performance mean value for GRG (i.e.: m = 0.3162)

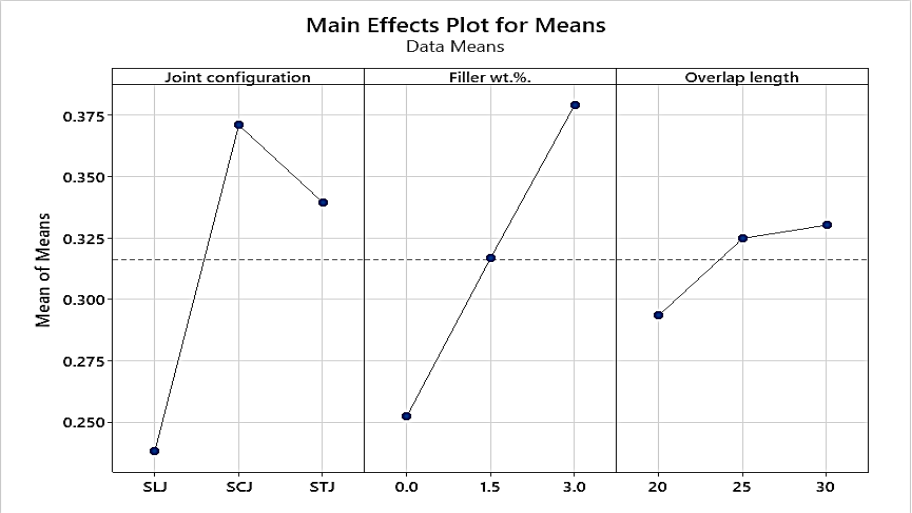

Figure 4. 20 The main effect plot for f GRG in the adhesive joint

4.7.5 Determining optimum condition for GRG of the composite adhesive joint

The optimum prediction condition for SNR in which, the GRG response result of the material was obtained with the terms set was shown in Table 4.43. The selected optimum parameters were A2B3C3.

Table 4. 43 The predicted optimal value of GRG

Factors	Levels	Values of levels	Rank	Predicted S/N ratio	Values mean
Joint conf.	2	SCJ	1	-6.26456	0.4481
SiC filler	3	3 wt.%	2		
overlap length	3	30mm	3		

Table 4. 44 Calculation of the percentage error value for GRG

Optimum parameter		GRG actual	GRG predicted	Error %
Joint conf.	SCJ	0.4482	0.4481	**0.022**
SiC filler	3 wt.%			
overlap length	30mm			

The calculated percentage error was 0.022, which was less than 5%. Therefore, the observed error was acceptable. The utilized model was also valid.

4.7.6 Analysis of variance for GRG of the composite adhesive joint

Table 4. 45 Analysis of Variance for GRG (mean)

Source	DOF	Seq SS	Adj SS	Adj MS	F-value	P-value	Cont. %
Joint conf.	2	0.0289	0.0289	0.0144	24.90	0.039	51.08
Filler wt.%.	2	0.0242	0.0242	0.0121	20.81	0.046	42.69
Overlap length	2	0.0024	0.0024	0.0012	2.04	0.329	4.18
Residual Error	2	0.0012	0.0012	0.0006	-	-	2.05
Total	8	0.0566	-	-	-	-	100

For the combined effects of responses, the joint configuration contributed 51.08 %, Filler 42.69 %, and overlap length 4.18 %. The joint configuration was highly influenced and filler wt.% holds the second effect, an overlap length shared minimum effects. These results are due to the high-stress distribution more evenly across the interface by joint configurations and SiC filler, leading to enhanced joint strength. The obtained investigation was in line with the work carried out earlier by (Hanumantharaya et al., 2019; Mottaghian & Taheri, 2023).

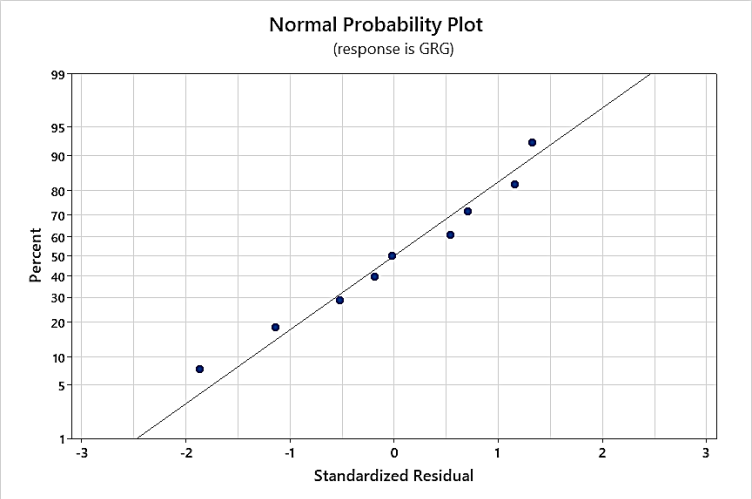

Figure 4. 21 Normal probability plot for GRG

The normal probability plot is given in Figure 4.21 and shows the data set closely follows the normal distribution.

4.8 Confirmation test for joint strength

After determining the optimal process parameters and their respective levels, the next step was to confirm if the predicted results disagreed with the experimental data. If the combination of optimal process parameters level matches any experimental trial in the orthogonal array, it will not be necessary to conduct a confirmation test. Unless it is appropriate to do experimentation at that new level. In this study, the predicted optimal process parameter combination was A2B3C3, and this predicted result did not coincide with the experimental results of sample nine. Therefore, the confirmation tests were conducted per optimal process parameters to confirm the standard quality for adhesively joined as suggested by experimental results for each response. The response values obtained from confirmation tests are a joint tensile strength of 32.63 MPa and a joint flexural strength of 90.15 MPa. Therefore, it can be concluded that the hybrid Taguchi and GRA combined gives an excellent result in predicting the joint tensile and flexural strengths in the adhesive joining of composite adherents fabricated from polyester resin matrix reinforced with sisal fiber, E-glass, and SiC filler.

Table 4. 46 Confirmation experiments for an optimized parameter combination determined by GRA

Exp. no.	**Input parameters**			**Outputs**	
	Joint configuration	Filler (wt.%)	Overlap length (mm)	Tensile strength (MPa)	Flexural strength(MPa)
1	SCJ	3wt.%SiC	30	32.63	90.15

4.8.1 SEM analysis for the developed composite

SEM analysis was done for the selected best composite having good mechanical properties after obtaining the result of GRA analysis for the developed composite. Therefore, samples 9, 6, 5, 3, and 1 were selected for SEM analysis. The morphology analysis was undertaken at a magnification of 20 μm for samples 9,6,5 and 3, and 100 μm for sample 1. The obtained results are discussed in Figure 4.49 respectively. SEM analysis was employed to examine the interfacial characteristics of the composite.

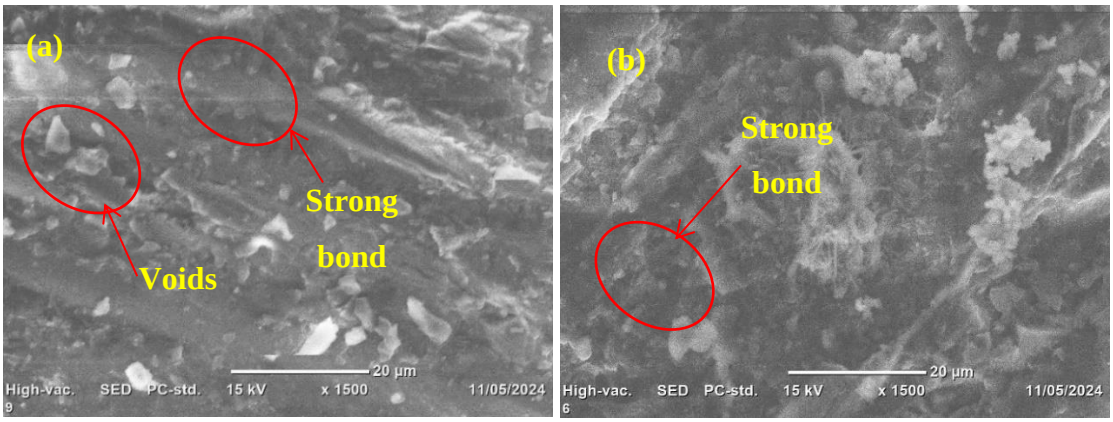

(a) Sample-9 (b) Sample-6

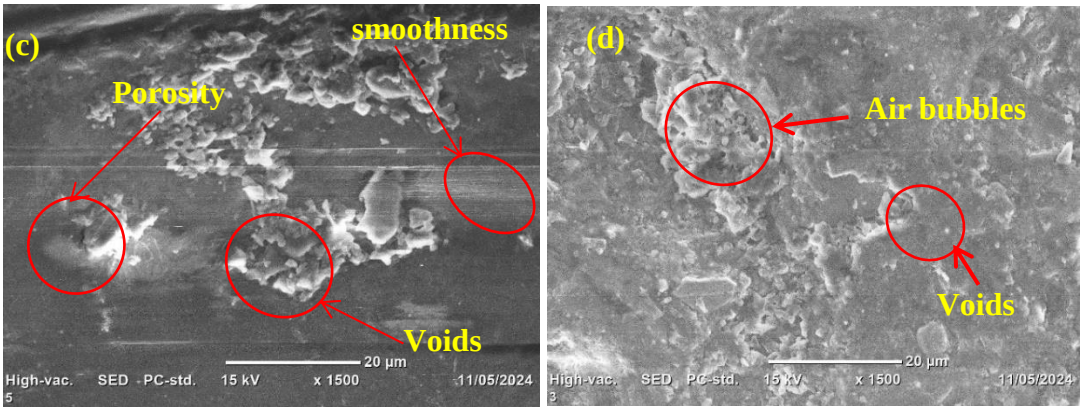

(c) Sample-5 (d) Sample-3

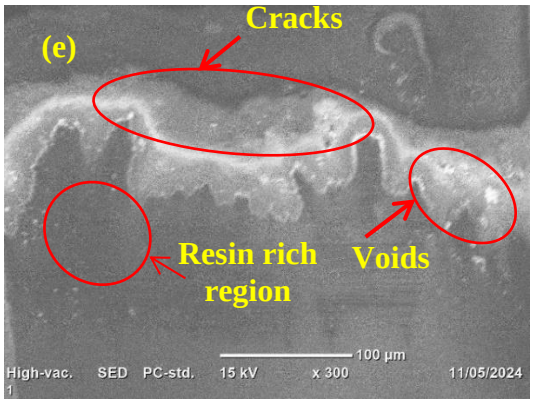

(e) Sample-1

Figure 4. 22 Image of SEM analysis.

As seen from the SEM images of the composite, Figure 4.22 (a), and (b) show the strong bond, which indicated better interaction of fibers and matrix, as a result, the mechanical properties were improved. Figure 4.22 (c) shows the voids and porosity in the laminate. Figure 4.22 (d) shows the voids in the laminate. Figure 4.22 (e) shows the resin-rich area and voids present in the laminate. In the resin-rich area, smoother surface cracking occurs. The proposed hybrid composite represents an excellent bond between fibers, filler material, and matrix when compared to composite with a minimum fibers as well as no fibers.

CHAPTER-5

CONCLUSION AND RECOMMENDATIONS

5.1 CONCLUSION

5.1.1 Composite fabrication, testing, and characterization

In this research paper, a hybrid polymer-based composite reinforced with sisal fiber, E-glass, and SiC filler was fabricated. The mechanical properties including tensile strength, flexural strength, impact strength, and Vickers hardness tests of the developed composites were investigated as per ASTM standards. SEM analysis was also investigated. The weight percentage of sisal fiber and E-glass fibers were optimized using Taguchi-based GRA. The obtained results provide valuable insights into the performance of the hybrid composite material, which can be useful for potential applications. Based on the accomplished investigation of the composite and its outcome, the following conclusions were drawn.

1. A maximum tensile strength result of 42.13 MPa was achieved for sample 9. The optimum SNR was achieved at A3B3. Therefore, the optimum fibers parameter combination of tensile strength was 15 wt.%. of E-glass fiber and 15 wt.%. of sisal fiber at level 3.
2. A maximum flexural strength result of 186.56 MPa was achieved for sample 6. The optimum parameter values for flexural strength were sisal fiber at 10 wt.% in level 2 and E-glass fiber at 10 wt.% in level 3.
3. A maximum impact strength result of 24.75 MPa was achieved for sample 9. The optimum parameter combination for SNR of impact strength was A3B3 with sisal fiber at 15 wt.% and E-glass fiber at 15 wt.% in level 3.
4. A maximum impact strength result of 97.93 MPa was achieved for sample 9. These optimum values for maximum Vickers hardness are sisal fiber at 15 wt.% and E-glass fiber at 15 wt.%.
5. From GRA analysis, the optimal combination ratio of fibers was achieved using 15 wt.% of sisal fiber and 15 wt.% of E-glass fiber. Therefore, the performance of the composites has been improved and a balancing effect is achieved by the hybridization of natural and synthetic fibers within the polyester resin matrix, and SiC.
6. Tensile strength, flexural strength, impact strength, and hardness were increased by increasing the weight percentage of fibers and SiC filler particles.

5.1.2 Composite adhesive bonding

Furthermore, the research focuses on optimizing the process parameters of the adhesive joined composite developed from a polyester matrix reinforced with sisal fiber, E-glass fiber, and SiC. The joint configuration, filler material (additive), and overlap length were considered as the process parameters, and the Taguchi-based GRA method was employed for the optimization process. Two-component araldite epoxy adhesives (Epoxy resin and epoxy hardener) were reinforced with silicon carbide nanoparticles. The nanocomposite adhesive was used to bond the composite material (adherends) developed from "a hybrid polymer-based composite reinforced with sisal fiber, E-glass, and SiC filler". The introduction of nano silicon carbide to the aforementioned two-component araldite epoxy adhesive led to an increase in the joint tensile and flexural strengths of the composite adherends. Based on the completed investigation the following conclusions were drawn.

1. The joint tensile and flexural strengths increased gradually from 21.02 to 29.29 MPa (with an increase of about 28.23 %), and 55.74 to 67.96 MPa (with an increase of about 17.98 %), respectively, by increasing the SiC contents from 0 to 3 wt.% and an overlap length from 20 to 30mm for SLJ. These could be attributed to the effective stress transfer that occurs between the araldite epoxy and the nanoparticles, which is crucial in enhancing the adhesion properties of adhesive bonds.
2. The joint tensile and flexural strengths increased gradually from 23.38 to 27.35 MPa (by 14.52 %), and 64.96 to 76.69 MPa (by 15.30 %), respectively, by increasing the SiC contents from 0 to 3 wt.% and varying overlap length of 20, 25, and 30mm with SCJ configuration.
3. Similarly, the joint tensile and flexural strengths enhanced from 25.90 to 31.44 (by 17.6 %), and 66.76 to 79.23 (by 15.74) respectively, by increasing the SiC contents from 0 to 3 wt.% and varying overlap length of 20, 25, and 30mm with STJ configuration.
4. The optimum process parameter values for maximum joint tensile strength are joint configuration with STJ, SiC filler at 3 wt.%, and overlap length at 30mm. It was obtained after testing based on the new level of the process parameters and 33.04 MPa of Tensile strength was achieved.
5. The optimal parameters for maximum joint flexural strength were joint configuration with STJ, SiC filler at 3 wt.%, and overlap length at 25mm. A 79.23 MPa of joint flexural strength was achieved.

6. The selected optimum process parameters for the composite joint strength obtained after GRA was **A2B3C3.** These were the joint configuration at level 2, SiC filler at level 3, and, overlap length at level 3. A 32.63 and 90.15 MPa of joint tensile and flexural strengths were obtained from a confirmation experiment for an optimized parameter combination determined by GRA. Therefore, SCT type joint configuration, 3 wt.% of SiC additive/filler, and 30 mm of overlap lengths were the optimum process parameters for effective adhesive joining of the adherends fabricated from a hybrid polymer-based composite reinforced with sisal fiber, E-glass, and SiC filler composite materials.

5.2 RECOMMENDATION

Based on the results and conclusions found in this study, the following recommendations were provided.

1. The addition of SiC filler with sisal and E-glass reinforcements has increased the hardness of the developed composite and using this composite material in applications requiring maximum hardness is recommended.
2. Sisal fiber has shown a potential effect in the hybridization with polyester, E-glass, and SiC filler, and can be used to replace the conventional reinforcements for various applications.
3. For an application requiring the maximum joint tensile strength, the joining parameters such as a joint configuration with STJ, SiC filler at 3 wt.%, and overlap length at 30mm are recommended.
4. Similarly, for an application requiring the maximum joint flexural strength, the joining parameters such as a joint configuration with STJ, SiC filler at 3 wt.%, and overlap length at 25mm are recommended.
5. The addition of SiC nanoparticles reinforces the adhesive matrix and increases the joint tensile and flexural strengths of the adhesively bonded composite joint. These are particularly beneficial in applications where high-strength bondings are required including the marine industry, automotive industry, energy source, and construction industry.

5.3 FUTURE WORK

This research work opens up several possibilities for future work. Some potential directions for future research include:

1. Fabrication of the composite using other fabrication methods like resin transfer molding.
2. Optimizing the process parameters considered in the research using other optimization techniques such as a Genetic algorithm (GA) and artificial neural network (ANN).
3. Assess the composite's resistance to environmental factors such as moisture, UV radiation, and temperature variation to ensure its suitability for real-world application.
4. Expand the study to include a broader range of adhesive joining parameters and optimize them. Consider the influence of factors such as adhesive type and the addition of other bio-nano filler materials into adhesives on the strength and reliability of the adhesive joints.
5. Explore the potential applications of the developed hybrid polymer composite in specific industries, such as automotive, aerospace, construction, or marine.

SPECIAL ACKNOWLEDGEMENT

This research work is funded by Adama Science and Technology University under the grant number ASTU/SM-R/1043/24, Adama, Ethiopia.

REFERENCES

Abas, A., Kader, E. I., & Abdulrahman, A. J. (2018). Synthesis of the Hybrid Polymer Matrix Composite Material by Using Hand Lay-Up Technique. 1, 102–108.

Abbasi, M., Ciardiello, R., & Goglio, L. (2023). Experimental Study on the Effect of Bonding Area Dimensions on the Mechanical Behavior of Composite Single-Lap Joint with Epoxy and Polyurethane Adhesives.. https://doi.org/10.3390/app13137683

Afendi, M., Teramoto, T., & Bakri, H. Bin. (2011). Strength prediction of epoxy adhesively bonded scarf joints of dissimilar adherends. International Journal of Adhesion and Adhesives, 31(6), 402–411. https://doi.org/10.1016/j.ijadhadh.2011.03.001

Ahmed, S. R., & Khanna, S. (2020). Investigation into features of fracture toughness of a transparent E-glass fiber reinforced polyester composites at extreme temperatures. Heliyon, 6(5), e03986. https://doi.org/10.1016/j.heliyon.2020.e03986

AİKHUELE, D. (2019). Evaluation of Adhesive Materials Used in Wind Turbine Blades. Erzincan Üniversitesi Fen Bilimleri Enstitüsü Dergisi, 12(3), 1189–1200. https://doi.org/10.18185/erzifbed.456945

Alemayehu, Z., Nallamothu, R. B., Liben, M., Nallamothu, S. K., & Nallamothu, A. K. (2020). Experimental investigation on characteristics of sisal fiber as composite material for light vehicle body applications. Materials Today: https://doi.org/10.1016/j.matpr.2020.07.386

Alves, D. L., Campilho, R. D. S. G., Moreira, R. D. F., Silva, F. J. G., & da Silva, L. F. M. (2018). Experimental and numerical analysis of hybrid adhesively-bonded scarf joints. International Journal of Adhesion and Adhesives. https://doi.org/10.1016/j.ijadhadh.2018.05.011

Anaç, N. (2023). The Effect of Organic Fillers on the Mechanical Strength of the.

Appadurai, M., Fantin Irudaya Raj, E., & LurthuPushparaj, T. (2022). Sisal fiber-reinforced polymer composite-based small horizontal axis wind turbine suited for urban applications—a numerical study. https://doi.org/10.1007/s42247-022-00375-x

Arpitha, G. R., Sanjay, M. R., Senthamaraikannan, P., & Barile, C. (2017). Hybridization Effect of Sisal / Glass / Epoxy / Filler Based Woven Fabric Reinforced Composites. 577–584. https://doi.org/10.1007/s40799-017-0203-4

Article, R., Ramesh, M., Rajeshkumar, L. N., Srinivasan, N., Kumar, D. V., & Balaji, D. (2022). Influence of filler material on properties of fiber - reinforced polymer composites : A review. 898–916.

Athawale, A. A., & Pandit, J. A. (2019). Unsaturated polyester resins, blends, interpenetrating polymer networks, composites, and nanocomposites: State of the art

and new challenges. In Unsaturated Polyester Resins: Fundamentals, Design, Fabrication, and Applications. Elsevier Inc. https://doi.org/10.1016/B978-0-12-816129-6.00001-6

Athith, D., Kittali, P., & Yogesha, B. (2021). Mechanical characterization of silicon carbide filled hybrid composites. Materials Today: https://doi.org/10.1016/j.matpr.2021.05.399

Atmakuri, A., Palevicius, A., Kolli, L., Vilkauskas, A., & Janusas, G. (2021). Development and analysis of mechanical properties of caryota and sisal natural fibers reinforced epoxy hybrid composites. Polymers,13(6),1–19. https://doi.org/10.3390/polym13060864

Banea, M. D., & Da Silva, L. F. M. (2009). Adhesively bonded joints in composite materials: An overview. Proceedings of the Institution of Mechanical Engineers, Part L: https://doi.org/10.1243/14644207JMDA219

Banea, M. D., Da Silva, L. F. M., Campilho, R. D. S. G., & Sato, C. (2014). Smart adhesive joints: An overview of recent developments. Journal of Adhesion, 90(1), 16–40. https://doi.org/10.1080/00218464.2013.785916

Banea, M. D., Rosioara, M., Carbas, R. J. C., & Silva, L. F. M. (2018). Multi-material adhesive joints for automotive industry. https://doi.org/10.1016/j.compositesb.2018.06.009

Barbosa, N. G. C., Campilho, R. D. S. G., Silva, F. J. G., & Moreira, R. D. F. (2018). Comparison of different adhesively-bonded joint types for mechanical structures. Applied Adhesion Science, 6(1), 1–19. https://doi.org/10.1186/s40563-018-0116-1

Begum, S., Fawzia, S., & Hashmi, M. S. J. (2020). Polymer matrix composite with natural and synthetic fibres. Advances in Materials and Processing Technologies, 6(3), 547–564. https://doi.org/10.1080/2374068X.2020.1728645

Bekele, A. E., Lemu, H. G., & Jiru, M. G. (2022). Exploration of Mechanical Properties of Enset–Sisal Hybrid Polymer Composite. Fibers, 10(2). https://doi.org/10.3390/fib10020014

Bichang'A, D. O., Aramide, F. O., Oladele, I. O., & Alabi, O. O. (2022). A Review on the Parameters Affecting the Mechanical, Physical, and Thermal Properties of Natural/Synthetic Fibre Hybrid Reinforced Polymer Composites. Advances in Materials Science and Engineering, 2022. https://doi.org/10.1155/2022/7024099

Brito, R. F. N., Campilho, R. D. S. G., Moreira, R. D. F., & Sánchez-Arce, I. J. (2020). Material and adhesive effect in adhesively-bonded composite stepped-lap joints. https://doi.org/10.1177/0954410020932014

Budhe, S., Banea, M. D., de Barros, S., & da Silva, L. F. M. (2017). An updated review of adhesively bonded joints in composite materials. International Journal of Adhesion and Adhesives, 72, 30–42. https://doi.org/10.1016/j.ijadhadh.2016.10.010

Campilho, R. D. S. G., Banea, M. D., Neto, J. A. B. P., & Da Silva, L. F. M. (2013). Modelling adhesive joints with cohesive zone models: Effect of the cohesive law shape of the adhesive layer. https://doi.org/10.1016/j.ijadhadh.2013.02.006.

Casas Pulido, A. F., Bohórquez, O., González-Estrada, O. A., Quiroga, J., & Pertuz, A. (2019). Adhesive joints for composite materials produced by additive manufacturing. Journal of Physics: https://doi.org/10.1088/1742-6596/1386/1/012005

Cavalcanti, D. K. K., Banea, M. D., Neto, J. S. S., Lima, R. A. A., da Silva, L. F. M., & Carbas, R. J. C. (2019a). Mechanical characterization of intralaminar natural fibre-reinforced hybrid composites. https://doi.org/10.1016/j.compositesb.2019.107149

Cavalcanti, D. K. K., Banea, M. D., Neto, J. S. S., Lima, R. A. A., da Silva, L. F. M., & Carbas, R. J. C. (2019b). Mechanical characterization of intralaminar natural fibre-reinforced hybrid composites. https://doi.org/10.1016/j.compositesb.2019.107149

Chaudhary, V., Rajput, A. K., & Bajpai, P. K. (2017). Effect of Particulate Filler on Mechanical Properties of Polyester based Composites. Materials Today: https://doi.org/10.1016/j.matpr.2017.06.289

Chavooshian, M., Kamali, R., Tutunchi, A., & Kianvash, A. (2017). Effect of silicon carbide nanoparticles on the adhesion strength of steel–epoxy composite joints bonded with acrylic adhesives.. https://doi.org/10.1080/01694243.2016.1215015

Chohan, J. S., Boparai, K. S., Singh, R., & Hashmi, M. S. J. (2022). Manufacturing techniques and applications of polymer matrix composites: a brief review. https://doi.org/10.1080/2374068X.2020.1835012

Chokshi, S., Parmar, K., & Gohil, P. (2017). Mechanical Characterization and Property Prediction of Sisal / Polyester Composite. 4, 1–7.

Choudhary, J., Kumar, B., & Gupta, A. (2020). Utilization of solid waste materials as alternative fillers in asphalt mixes: A review. https://doi.org/10.1016/j.conbuildmat.2019.117271

Dress, G. A., Woldemariam, M. H., & Redda, D. T. (2021). Influence of Fiber Orientation on Impact Resistance Behavior of Woven Sisal Fiber Reinforced Polyester Composite. https://doi.org/10.1155/2021/6669600

EL-Wazery, M. S., EL-Elamy, M. I., & Zoalfakar, S. H. (2017). Mechanical properties of glass fiber reinforced polyester composites. https://doi.org/10.6703/IJASE.2017.14(3).121

Fenta, E. W., & Tsegaw, A. A. (2023). Process Parameter Optimization of Single Lap-Adhesive Joint Date Palm Fiber Reinforced Polyester Composite Using ANN-Genetic Algorism BT- Springer Nature Switzerland.

Fiber, C., & Computational, A. A. (2022). The Mechanical Response of Epoxy – Sisal

Composites.

Ganesamoorthy, R., Suresh, G., Padmavathi, K. R., Rajaparthiban, J., Vezhavendhan, R., & Bharathiraja, G. (2022). Experimental Analysis and Mechanical Properties of Fly-ash Loaded E-Glass Fiber Reinforced IPN (Vinylester/polyurethane) Composite. https://doi.org/10.1007/s12221-022-4194-0

Gangil, B., Ranakoti, L., Verma, S., Singh, T., & Kumar, S. (2020). Natural and Synthetic Fibers for Hybrid Composites. Hybrid Fiber Composites, 1–15. https://doi.org/10.1002/9783527824571.ch1

Gopal Krishna, U. B., Srinivasa, C. S., Amara, N. S., & Gudoor, S. (2019). Processing, characterization and property evaluation of seashell and glass fibre added epoxy based polymer matrix composite. Materials Today: https://doi.org/10.1016/j.matpr.2020.02.818

Hanumantharaya, R., Sogalad, I., Basavarajappa, S., & Manjunath Patel, G. C. (2019). Modelling and optimisation of adhesive bonded joint strength of composites for aerospace applications. https://doi.org/10.1504/IJCMSSE.2019.104694

Hapuhinna, K., & Gunaratne, R. D. (2022). Thermal Mechanical Property Enhancement with Silicon. 721–730.

Hassan, A. D., Naeem, U. J., & Bachi, I. O. (2022). Processing and Evaluation of Ceramic Filler Reinforced Polymer Matrix Composites. Journal of Physics: Conference Series, 2361(1). https://doi.org/10.1088/1742-6596/2361/1/012009

Hatti, P. S., L., S. K., Somanakatti, A. B., & Rakshith, M. (2022). Investigation on tensile behavior of glass-fiber reinforced polymer matrix composite with varying orientations of fibers. Materials Today: https://doi.org/10.1016/j.matpr.2021.08.196

Hyeon-Seok, C., Byeong-Su, K., Seong-Min, P., Viet-Hoai, T., Young-Woo, N., & Jin-Hwe, K. (2020). Tensile strength of composite bonded scarf joint in various thermal environmental conditions. https://doi.org/10.1080/09243046.2019.1710679

Jaballi, S., Miraoui, I., & Hassis, H. (2017). Long-Unidirectional Palm and Sisal Fibers Reinforced Composite: An Experimental Investigation. Journal of Natural Fibers, 14(3), 368–378. https://doi.org/10.1080/15440478.2016.1212758

Jeevi, G., Nayak, S. K., & Abdul Kader, M. (2019). Review on adhesive joints and their application in hybrid composite structures. Journal of Adhesion Science and Technology, 33(14), 1497–1520. https://doi.org/10.1080/01694243.2018.1543528

Kadioglu, F., Avil, E., Ercan, M. E., & Aydogan, T. (2018). Effects of different overlap lengths and composite adherend thicknesses on the performance of adhesively-bonded joints under tensile and bending loadings. Materials Science and Engineering, 369(1). https://doi.org/10.1088/1757-899X/369/1/012034

Kadioglu, F., Demiral, M., & El Zaroug, M. (2019). Effects of overlap length on the strength of bolted, bonded and hybrid single lap joints with different adherend materials and thicknesses. https://doi.org/10.1080/01694243.2019.1623966

Karthi, N., Kumaresan, K., Sathish, S., Gokulkumar, S., Prabhu, L., & Vigneshkumar, N. (2019). An overview: Natural fiber reinforced hybrid composites, chemical treatments and application areas. Materials Today: https://doi.org/10.1016/j.matpr.2020.01.011

Khan, M. Z. R., Srivastava, S. K., & Gupta, M. K. (2018). Tensile and flexural properties of natural fiber-reinforced polymer composites: https://doi.org/10.1177/0731684418799528

Khashaba, U. A., Najjar, I. M. R., & Almitani, K. H. (2022). Failure analysis of scarf adhesive joints modified with SiC-nanoparticles under fatigue loading at room temperature. Composites Science and Technology, 221, 109301. https://doi.org/https://doi.org/10.1016/j.compscitech.2022.109301

Kumar Sharma, A., Bhandari, R., Sharma, C., Krishna Dhakad, S., & Pinca-Bretotean, C. (2022). Polymer matrix composites: https://doi.org/10.1016/j.matpr.2021.12.592

Kumaresan, M., Sathish, S., & Karthi, N. (2015). Effect of Fiber Orientation on Mechanical Properties of Sisal Fiber Reinforced Epoxy Composites. 18(3), 289–294. https://doi.org/10.6180/jase.2015.18.3.09

Li, M., Pu, Y., Thomas, V. M., Yoo, C. G., Ozcan, S., Deng, Y., Nelson, K., & Ragauskas, A. J. (2020). Recent advancements of plant-based natural fiber–reinforced composites and their applications. Composites Part B: Engineering, 200(February). https://doi.org/10.1016/j.compositesb.2020.108254

Lilly Mercy, J., Prakash, S., Krishnamoorthy, A., Ramesh, S., & Alex Anand, D. (2017). Multi-response optimisation of mechanical properties in self-healing glass fiber reinforced plastic using grey relational analysis. https://doi.org/10.1016/j.measurement.2017.07.013

Lokesh, P., Surya Kumari, T. S. A., Gopi, R., & Loganathan, G. B. (2020). A study on mechanical properties of bamboo fiber reinforced polymer composite. Materials Today: Proceedings, 22, 897–903. https://doi.org/10.1016/j.matpr.2019.11.100

Madhu Kumar, K. P., & Murthy, M. (2020). Studies on E-glass and S-glass Hybrid Polymer Matrix Composites. Materials Today: Proceedings, 24, 1064–1076. https://doi.org/10.1016/j.matpr.2020.04.420

Madhu, P., Girijappa, Y. G. T., & Pradeep, S. (2018). Studies on Mechanical Properties of Bamboo/Carbon Fiber Reinforced Epoxy Hybrid Composites Filled with SiC Particulates. International Journal Of Engineering Research and General Science, 6(5), 43–50.

Malekinejad, H., Carbas, R. J. C., Akhavan-Safar, A., Marques, E. A. S., Castro Sousa, F.,

& da Silva, L. F. M. (2023). Enhancing Fatigue Life and Strength of Adhesively Bonded Composite Joints: A Comprehensive Review. Materials, 16(19). https://doi.org/10.3390/ma16196468

Mbeche, S. M., Wambua, P. M., & Githinji, D. N. (2020). Mechanical Properties of Sisal / Cattail Hybrid-Reinforced Polyester Composites. 2020.

Mejbel, M. K., Allawi, M. K., & Oudah, M. H. (2019). Effects of WC, SiC, iron and glass fillers and their high percentage content on adhesive bond strength of an aluminium alloy butt joint: https://doi.org/10.26480/jmerd.05.2019.224.231

Melese, K. G., Naik, T. P., & Singh, I. (2021). Adhesive joining of sisal/jute/hybrid composites with drilled holes in lap area. Proceedings of the Institution of Mechanical Engineers. https://doi.org/10.1177/1464420720959808

Melese, K. G., & Tesfie, N. (2023). The adhesive joining of natural fiber-based polymer composites by FEM. January.

Melese, K. G., Tesfie, N., & Mekonnen, A. (2022). The adhesive joining of natural fiber-based polymer composites by FEM. II, 54–68.

Messler, R. W. (2004). Joining composite materials and structures: Some thought-provoking possibilities. Journal of Thermoplastic Composite Materials, 17(1), 51–75. https://doi.org/10.1177/0892705704033336

Mohamad, M. A., Jumahat, A., & Sapiai, N. (2023). 17 Flexural analysis of hemp, kenaf and glass fibre-reinforced polyester resin. https://doi.org/doi:10.1515/9783110769227-017

Mosisa, S., & Batu, T. (2021). Investigation of mechanical properties of bamboo/sisal fiber reinforced hybrid composite materials. https://doi.org/10.15406/mseij.2021.05.00152

Mosisa, S., & Sirhabizu, B. (2019). 100972-2169-0022-8-538.Pdf. 8(5).

Mottaghian, F., & Taheri, F. (2023). On the flexural response of nanoparticle-reinforced adhesively bonded joints mating 3D-Fiber Metal Laminates – A coupled numerical and experimental investigation. International Journal of Adhesion and Adhesives, 120, 103278. https://doi.org/https://doi.org/10.1016/j.ijadhadh.2022.103278

Mullaikodi, S. M., Shanmugasundaram, K., Rao, V. S., & Rengarajan, S. (2019). Synthesis, characterization and machinability studies on thin hybrid composites with SiC nano particles. Materials Research Express, 6(6). https://doi.org/10.1088/2053-1591/ab0ddc

Nagaraj, C., Mishra, D., & Reddy, J. D. P. (2020). Estimation of tensile properties of fabricated multi layered natural jute fiber reinforced e-glass composite material. Materials Today: Proceedings, 27(xxxx), 1443–1448. https://doi.org/10.1016/j.matpr.2020.02.864

Nagavally, R. R. (2016). Composite Materials - History, Types, Fabrication Techniques,

Advantages, and Applications. International Journal of Mechanical And Production Engineering, 2, 25–30.

Nascimento, H., dos Reis, M. O., Monteiro, E. C., & Ávila, A. F. (2021). An investigation on industrial adhesive nano-modified by graphene nanoplatelets under extreme environmental conditions. https://doi.org/10.1016/j.ijadhadh.2021.102982

Naveen.E, V. . and, & Maheswaran.N. (2015). Alkalichemical Treatment on the Surface of. International Journal of Innovative Research in Science, Engineering and Technology, 4(4), 172–178.

Naveen, J., Jawaid, M., Amuthakkannan, P., & Chandrasekar, M. (2018). Mechanical and physical properties of sisal and hybrid sisal fiber-reinforced polymer composites. Elsevier Ltd. https://doi.org/10.1016/B978-0-08-102292-4.00021-7

Neto, J., Queiroz, H., Aguiar, R., Lima, R., Cavalcanti, D., & Banea, M. D. (2022). A review of recent advances in hybrid natural fiber reinforced polymer composites. Journal of Renewable Materials, 10(3), 561–589. https://doi.org/10.32604/jrm.2022.017434

Njoku, R. E., Obayi, C. S., & Nnamchi, P. S. (2011). Hybrid effect on the mechanical properties of sisal fiber and e-glass fiber reinforced polyester composites.

Nurazzi, N. M., Asyraf, M. R. M., Fatimah Athiyah, S., Shazleen, S. S., Rafiqah, S. A., (2021). A review on mechanical performance of hybrid natural fiber polymer composites for structural applications. Polymers, 13(13), 1–47. https://doi.org/10.3390/polym13132170

Omairey, S., Jayasree, N., & Kazilas, M. (2021). Defects and uncertainties of adhesively bonded composite joints. SN Applied Sciences, 3(9). https://doi.org/10.1007/s42452-021-04753-8

Özer, H., & Erbayrak, E. (2018). The effects of curing temperature on fracture energy and cohesive parameters for the adhesive Araldite 2015. Journal of Adhesion Science and Technology, 32(12), 1287–1312. https://doi.org/10.1080/01694243.2017.1410080

Palanikumar, K., Ramesh, M., & Hemachandra Reddy, K. (2016). Experimental investigation on the mechanical properties of green hybrid sisal and glass fiber reinforced polymer composites. https://doi.org/10.1080/15440478.2015.1029192

Palle, R. R., Schuster, J., Shaik, Y. P., & Kazmi, M. (2022). Fabrication and Characterization of Glass Fiber with SiC Reinforced Polymer Composites. 16–29. https://doi.org/10.4236/ojcm.2022.121002

Pandya, V. J., & Rathod, P. P. (2020). Optimization of mechanical properties of green composites by gray relational analysis. Materials Today: Proceedings, 27(xxxx), 19–22. https://doi.org/10.1016/j.matpr.2019.08.166

Pereira, A. L., Banea, M. D., Neto, J. S. S., & Cavalcanti, D. K. K. (2020). Mechanical and thermal characterization of natural intralaminar hybrid composites based on sisal. Polymers, 12(4). https://doi.org/10.3390/POLYM12040866

Praveenkumara, J., Madhu, P., Yashas Gowda, T. G., Sanjay, M. R., & Siengchin, S. (2022). A comprehensive review on the effect of synthetic filler materials on fiber-reinforced hybrid polymer composites. https://doi.org/10.1080/00405000.2021.1920151

Radoor, S., Karayil, J., Rangappa, S. M., Siengchin, S., & Parameswaranpillai, J. (2020). A review on the extraction of pineapple, sisal and abaca fibers and their use as reinforcement in polymer matrix. https://doi.org/10.3144/expresspolymlett.2020.27

Rajak, D. K., Wagh, P. H., & Linul, E. (2022). A Review on Synthetic Fibers for Polymer Matrix Composites: Performance, Failure Modes and Applications. Materials, 15(14). https://doi.org/10.3390/ma15144790

Rajamahendran, S., Suresh, G., Srinivasan, T., Logesh, D., Yusuf, M. M., & Krishnan, L. M. (2021). An analysis on mechanical and sliding wear behavior of E-Glass fiber reinforced IPN composites. https://doi.org/10.1016/j.matpr.2020.07.072

Ramadan, N., Taha, I., Hammouda, R., & Abdellatif, M. H. (2017). Behaviour of hybrid SiC/jute epoxy composites manufactured by vacuum assisted resin infusion. Polymers and Polymer Composites, 25(5), 333–344. https://doi.org/10.1177/096739111702500503

Ramasubbu, R., & Madasamy, S. (2022). Fabrication of Automobile Component Using Hybrid Natural Fiber Reinforced Polymer Composite. Journal of Natural Fibers, 19(2), 736–746. https://doi.org/10.1080/15440478.2020.1761927

Rangaswamy, H., Sogalad, S., Acharya, S., & Manjunath Patel, G. C. (2020). Experimental analysis and prediction of strength of adhesive-bonded single-lap composite joints: Taguchi and ANN approaches. https://doi.org/10.1007/s42452-020-2851-8

Rasu, K., & Veerabathiran, A. (2023). No Title. Materials Testing, 65(4), 593–602. https://doi.org/doi:10.1515/mt-2022-0431

Ravi Raj, V., & Vijaya Ramnath, B. (2021). Mechanical, Thermal and Wear Behavior of SiC Particle Strengthening of PMMA-Toughened Glass-Epoxy Hybrid Composite. Silicon, 13(6), 1925–1932. https://doi.org/10.1007/s12633-020-00580-5

Saba, N., Jawaid, M., Alothman, O. Y., & Paridah, M. T. (2016). A review on dynamic mechanical properties of natural fibre reinforced polymer composites. Construction and Building Materials, 106, 149–159. https://doi.org/10.1016/j.conbuildmat.2015.12.075

Sadasivuni, K. K., Saha, P., Adhikari, J., Deshmukh, K., Ahamed, M. B., & Cabibihan, J. J. (2020). Recent advances in mechanical properties of biopolymer composites: a review.

Polymer Composites, 41(1), 32–59. https://doi.org/10.1002/pc.25356

Sahu, H. S., Kar, S., & Bhoi, S. (2021). Characteristic Study on Sisal Fibre Hybrid Composites Filled With Nano SiO2 and Marble Dust Particles. E3S Web of Conferences, 309. https://doi.org/10.1051/e3sconf/202130901223

Sanghvi, M. R., Tambare, O. H., & More, A. P. (2022). Performance of various fillers in adhesives applications: a review. In Polymer Bulletin (Vol. 79, Issue 12). Springer Berlin Heidelberg. https://doi.org/10.1007/s00289-021-04022-z

Sathish, S., Karthi, N., Prabhu, L., Gokulkumar, S., Balaji, D., Vigneshkumar, N., Ajeem Farhan, T. S., Akilkumar, A., & Dinesh, V. P. (2021). A review of natural fiber composites. https://doi.org/10.1016/j.matpr.2020.12.1105

Satyanarayana, K. G., Arizaga, G. G. C., & Wypych, F. (2009). Biodegradable composites based on lignocellulosic fibers-An overview. Progress in Polymer Science (Oxford), 34(9), 982–1021. https://doi.org/10.1016/j.progpolymsci.2008.12.002

Sayam, A., Rahman, & Faruque, M. O. (2022). A review on carbon fiber-reinforced hierarchical composites: mechanical performance, manufacturing process, structural applications and allied challenges. https://doi.org/10.1007/s42823-022-00358-2

Sen, D., Nayak, C., Sudhakar, K. G., & Birla, S. (2021). Mechanical properties of fabricated hybrid composites infused with Heat-Treated alkali sisal fiber and SiC particles: a quantitative analysis. Polymer Bulletin, 78(8), 4629–4648. https://doi.org/10.1007/s00289-020-03329-7

Shahinur, S., & Hasan, M. (2020). Jute/Coir/Banana Fiber Reinforced Bio-Composites: Critical Review of Design, Fabrication, Properties and Applications. Elsevier Ltd. https://doi.org/10.1016/B978-0-12-803581-8.10987-7

Shang, X., Marques, E. A. S., Machado, J. J. M., Carbas, R. J. C., Jiang, D., & da Silva, L. F. M. (2019). Review on techniques to improve the strength of adhesive joints with composite adherends. https://doi.org/10.1016/j.compositesb.2019.107363

Shang, X., Marques, E. A. S., Machado, J. J. M., Carbas, R. J. C., Jiang, D., & Silva, L. F. M. (2019). Review on techniques to improve the strength of adhesive joints with composite adherends. Composites Part B, 107363. https://doi.org/10.1016/j.compositesb.2019.107363

Sharma, H., Kumar, A., Rana, S., Sahoo, N. G., Jamil, M., Kumar, R., Sharma, S., Li, C., Kumar, A., Eldin, S. M., & Abbas, M. (2023). Critical review on advancements on the fiber-reinforced composites. https://doi.org/10.1016/j.jmrt.2023.08.036

Siddique, A., Iqbal, Z., Nawab, Y., & Shaker, K. (2023). A review of joining techniques for thermoplastic composite materials. https://doi.org/10.1177/08927057221096662

Sumesh, K. R., & Kanthavel, K. (2022). Grey relational optimization for factors influencing tensile, flexural, and impact properties of hybrid sisal banana fiber epoxy composites. Journal of Industrial Textiles, 51(3), 4441S-4459S. https://doi.org/10.1177/1528083720928501

Sumithra, G., Reddy, R. N., Dheeraj Kumar, G., Ojha, S., Jayachandra, G., & Raghavendra, G. (2023). Review on composite classification, manufacturing, and applications. Materials Today: https://doi.org/10.1016/j.matpr.2023.04.637

Suriani, M. J., Rapi, H. Z., Ilyas, R. A., Petrů, M., & Sapuan, S. M. (2021). Delamination and manufacturing defects in natural fiber-reinforced hybrid composite: A review. Polymers, 13(8), 1–24. https://doi.org/10.3390/polym13081323

Tesfay, A. G., & Kahsay, M. B. (2020). Effects of Chemical Treatment , Hybridization , and Hybrid Fiber Stacking Sequence and Orientation on Tensile and Impact Strength of Continuous Sisal Fiber Reinforced Polyester Composites. Journal of Natural Fibers, 00(00), 1–13. https://doi.org/10.1080/15440478.2020.1821283

Venkatesan, K., & Bhaskar, G. B. (2020). Evaluation and Comparison of Mechanical Properties of Natural Fiber Abaca-sisal Composite. https://doi.org/10.1007/s12221-020-9532-5

Venkateshwaran, N., ElayaPerumal, A., Alavudeen, A., & Thiruchitrambalam, M. (2011). Mechanical and water absorption behaviour of banana/sisal reinforced hybrid composites. https://doi.org/10.1016/j.matdes.2011.03.002

Venugopal, A., & Sudhagar P, E. (2024). Enhancing shear and flexural strength of single lap composite joints with a graphene nanoparticle-reinforced adhesive through a co-curing technique. https://doi.org/https://doi.org/10.1002/pc.28053

Worrall, C., & Vacogne, C. (2020). Joining of Fibre-Reinforced Polymer Composites.

Yan Li, Mai, Y., & Ye, L. (2000). Sisal fibre and its composites : a review of recent developments IM PA US AS DO ME US EX ON AS. Composites Science and Technology, 60(2000), 2037–2055.

Yogeshwaran, S., Natrayan, L., Rajaraman, S., Parthasarathi, S., & Nestro, S. (2020). Experimental investigation on mechanical properties of Epoxy/graphene/fish scale and fermented spinach hybrid bio composite by hand lay-up technique. https://doi.org/10.1016/j.matpr.2020.07.160

Yudhanto, A., Alfano, M., & Lubineau, G. (2021). Surface preparation strategies in secondary bonded thermoset-based composite materials: A review.. https://doi.org/10.1016/j.compositesa.2021.106443

APPENDIXES

Appendix-A: Experimental results of mechanical properties

Experimental results for tensile testing of composite

Samples		**S-1**	**S-2**	**S-3**	**S-4**	**S-5**	**S-6**	**S-7**	**S-8**	**S-9**
Tensile strength (MPa)	Trial-1	8.72	22.64	31.60	21.5	36.9	41.7	25.83	39.14	45.75
	Trial-2	11.6	28.8	33.12	23.6	34.7	36.64	23.34	33.4	40.64
	Trial-3	9.85	31.4	34.6	22.9	37.7	46.88	27.2	38.78	40.00
Av.Tensile strength(MPa)		10.06	27.61	33.11	22.67	36.43	41.74	25.46	37.11	42.13
Standard deviation		1.45	4.50	1.50	1.07	1.55	5.12	1.96	3.22	3.15

Experimental results for flexural testing of composite

Samples		**S-1**	**S-2**	**S-3**	**S-4**	**S-5**	**S-6**	**S-7**	**S-8**	**S-9**
Flexural strength (MPa)	Trial -1	11.72	82.06	93.78	64.48	162.02	187.57	99.65	117.23	158.26
	Trial -2	23.45	87.92	99.65	70.34	164.12	183.4	93.78	105.51	164.12
	Trial -3	41.03	58.62	98.47	71.8	165.29	185.7	82.06	134.82	152.4
Av.Flexural strength(MPa)		25.40	76.20	97.30	68.87	163.81	185.56	91.83	119.19	158.26
Standard deviation		14.7	15.5	3.10	3.87	1.7	2.1	9.0	14.8	5.86

Experimental results for Impact strength of composite

Samples		**S-1**	**S-2**	**S-3**	**S-4**	**S-5**	**S-6**	**S-7**	**S-8**	**S-9**
Impact strength (KJ)	Trial-1	4.5	6.5	9.25	10	11	12.5	18.5	22	25.5
	Trial-2	5	7	11.5	9.5	12	15	16.5	20	25
	Trial-3	4	6	10	9	11.5	13	16	21	23.75
Av. Impact (J)		4.5	6.5	10.25	9.5	11.5	13.5	17	21	24.75
Standard deviation		0.5	0.5	1.15	0.5	0.5	1.32	1.32	1	0.9

Experimental results for Vickers hardness testing of composite

Samples		**S-1**	**S-2**	**S-3**	**S-4**	**S-5**	**S-6**	**S-7**	**S-8**	**S-9**
Vickers hardness (MPa)	Trial-1	51.4	67.2	73.1	74.5	83.4	85.6	83.9	84.5	92.9
	Trial-2	58.9	69.5	77.1	89.2	77.1	91.1	96.0	90.4	95.2
	Trial-3	54.6	72.8	70.2	73.1	83.0	96.4	83.2	94.8	98.7
Av.hardness (HV)		58.3	69.83	73.47	78.93	81.17	91.03	87.7	89.9	97.93
Standard deviation		3.76	2.81	3.46	8.92	3.53	5.40	7.2	5.17	2.92

Experimental results for joint tensile strength testing of composite

Samples		**R-1**	**R-2**	**R-3**	**R-4**	**R-5**	**R-6**	**R-7**	**R-8**	**R-9**
Tensile strength (MPa)	Trial-1	20.92	26.04	29.87	23.96	29.67	25.66	25.64	30.48	30.35
	Trial-2	21.61	25.98	29.21	22.74	27.56	28.49	26.4	28.12	32.06
	Trial-3	20.54	27.51	28.79	23.46	28.47	27.89	25.66	28.93	31.92
Av.Tensile strength(MPa)		21.02	26.51	29.29	23.38	28.57	27.35	25.90	29.18	31.44
Standard deviation		0.54	0.87	0.54	0.61	1.06	1.49	0.43	1.2	0.95

Experimental results for joint flexural strength testing of composite

Samples		**R-1**	**R-2**	**R-3**	**R-4**	**R-5**	**R-6**	**R-7**	**R-8**	**R-9**
Flexural strength (MPa)	Trial -1	59.06	68.9	78.08	75.93	70.34	79.19	66.93	72.68	75.16
	Trial -2	60.93	56.77	64.4	58.6	71.28	72.05	67.57	73.23	76.42
	Trial -3	47.24	59.45	61.39	60.36	70.15	78.84	65.77	71.3	86.12
Av.Flexural strength(MPa)		55.74	61.71	67.96	64.96	70.59	76.69	66.76	72.40	79.23
Standard deviation		7.42	6.37	8.89	9.54	0.61	4.03	0.91	0.99	6.0

APPENDIX -B: Stress-elongation table and diagram

Stress – elongation table: Sample 9:trial 2

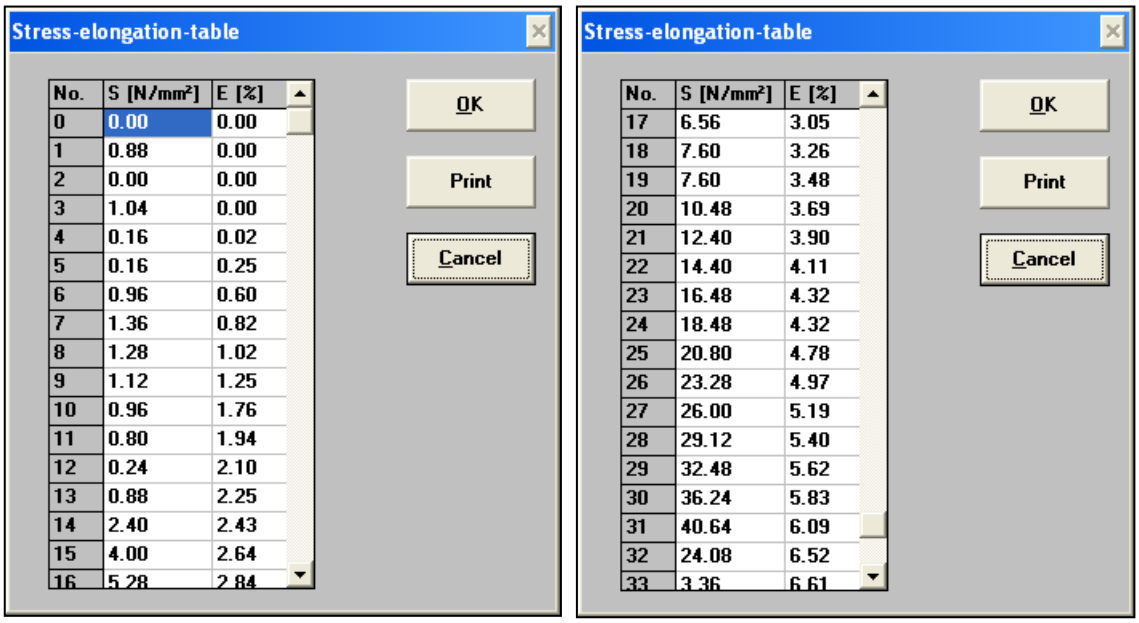

Stress (N/mm^2)– elongation (%) diagram: Sample 9:trial 2

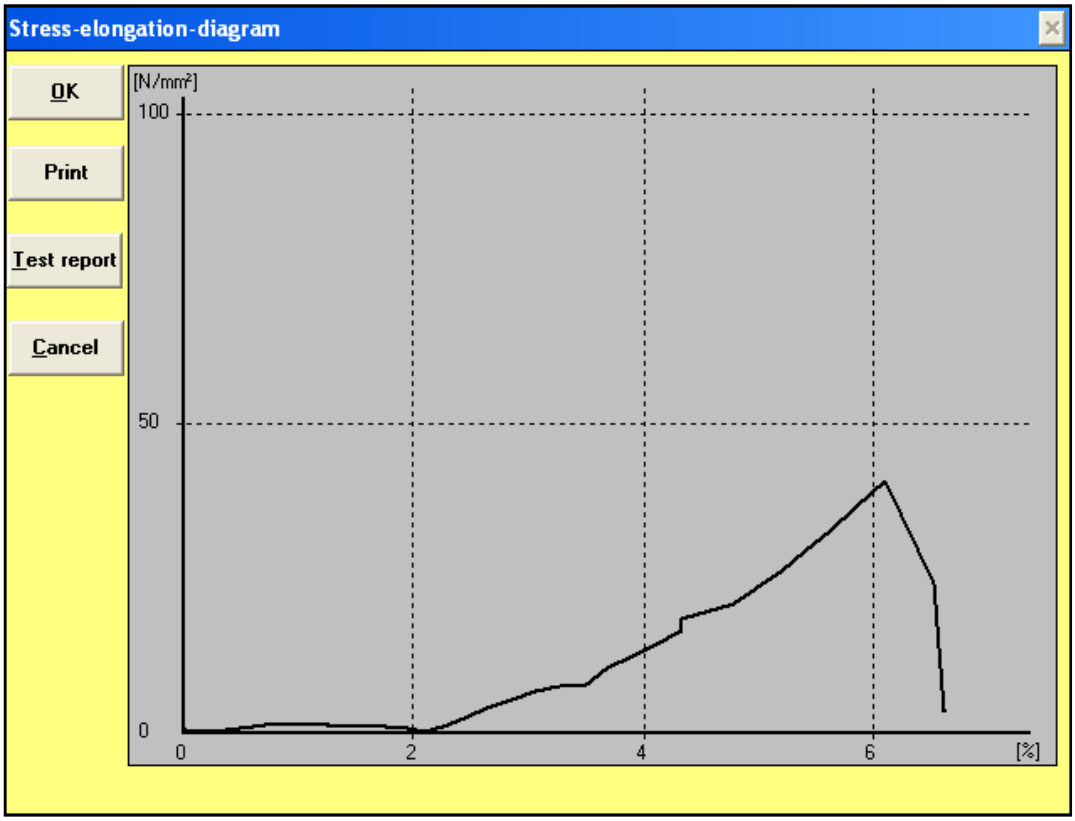

APPENDIX-C: Flexural bending test results

Flexural bending test loading for the composite and adhesive joint respectively

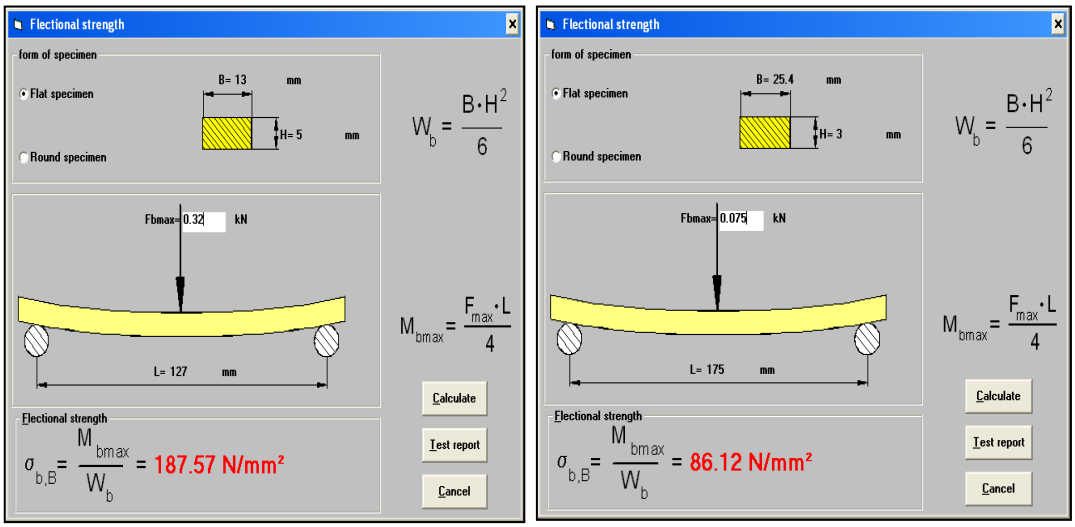

Flexural bending test for optimal parameters of the adhesive joint after confirmation test

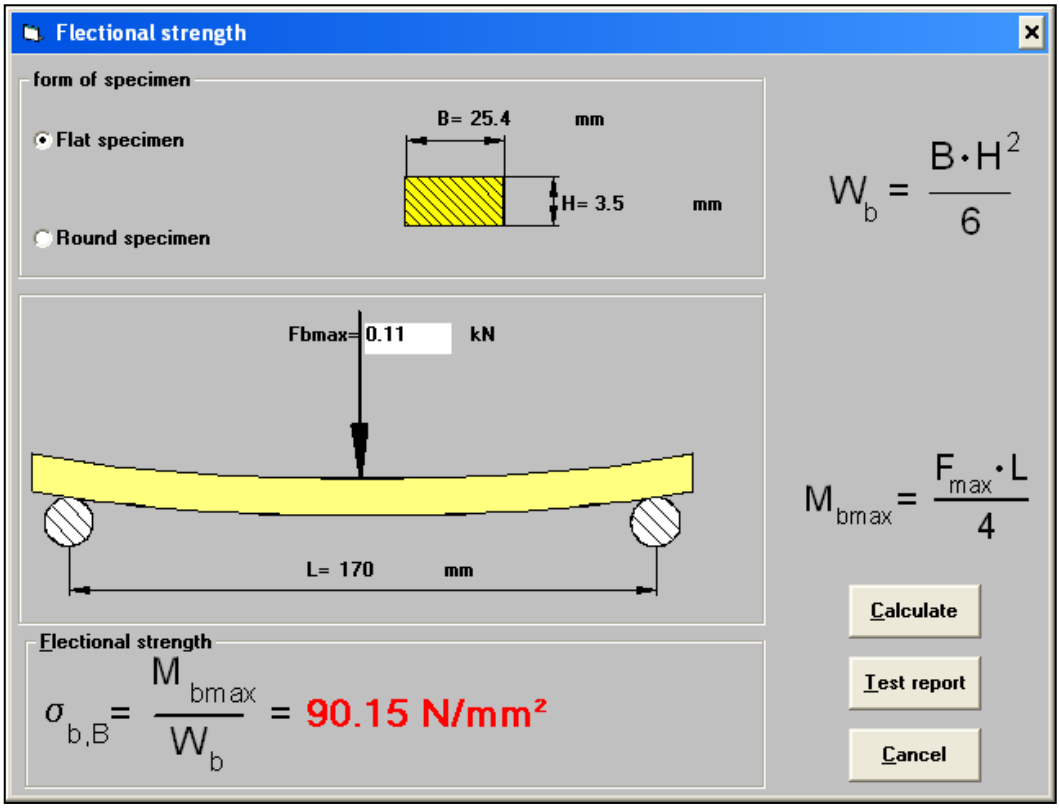

APPENDIX -D: Vickers hardness results

The result and image of vickers hardness for sample 6 and 9 respectively

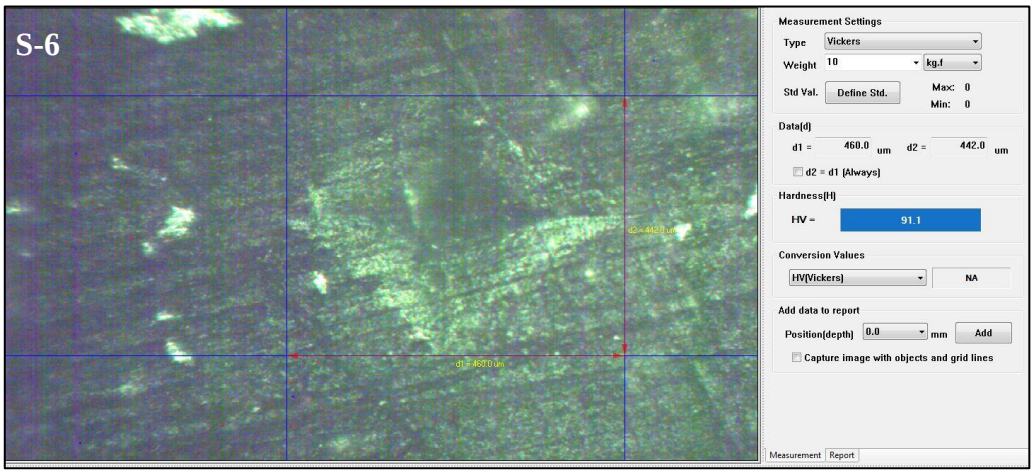

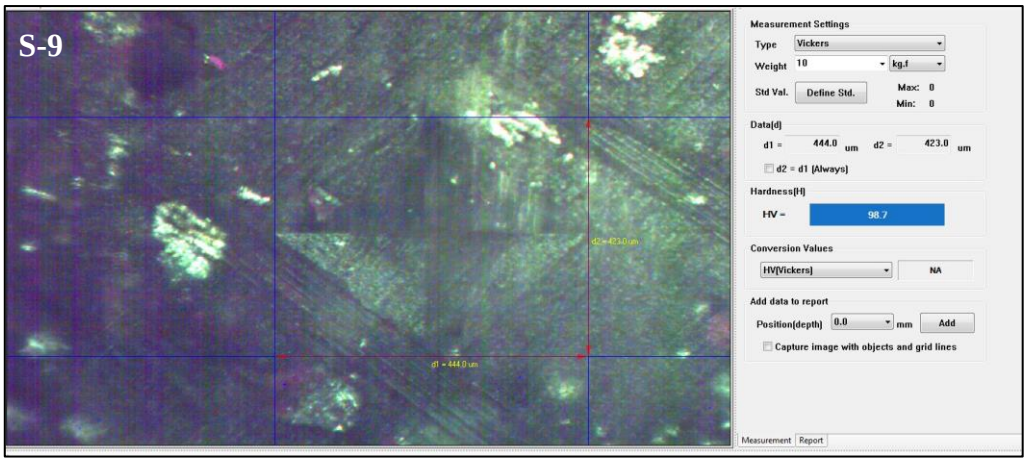

APPENDIX-E: Composite fabrication activities